2021

Assessment of Sex Differences in Basic Renal Mitochondrial Bioenergetics

Morgan J. Spicer
Medical University of South Carolina

Assessment of Sex Differences in Basic Renal Mitochondrial Bioenergetics

by

Morgan J. Spicer

A thesis submitted to the faculty of the Medical University of South Carolina in partial fulfillment of the requirements for the degree of Master of Science in Biomedical Sciences in the College of Graduate Studies

Department of Molecular and Cell Biology and Pathology

2021

Approved By:

Chairperson, Daria Ilatovskaya

Co-Chairperson, Kristine DeLeon-Pennell

Krisztian Stadler

Robin Muise-Helmericks

ACKNOWLEDGEMENTS

I would like to first begin by thanking my Mentor, Dr. Daria Ilatovskaya, for her abundance of guidance and willingness to share her knowledge with me during my graduate career. I have learned an inexplicable amount of information regarding not only science, but also about the academic community, while under her instruction. She has been very attentive to my career interests and goals, and has pushed me to a level of achievement that I would not have achieved on my own without her guidance, including my participation in several poster sessions, conferences, and talks. The other current and past members of the Ilatovskaya lab were also immensely helpful in my welcome and work during the course of my tenure, as well as in obtaining and analyzing data—I extend my gratitude to Ryan Schibalski, Mark Domondon, Regina Sultanova, Dr. Denisha Spires, Alexus Williams, Mikhail Fomin, and Callie Clarke. Ryan Schibalski and Mark Domondon in particular assisted with much of the establishment of protocols prior to my entry in the lab as well as in collecting data. I would also like to thank the various faculty at MUSC for my education, with special mentions of Dr. John Lemasters for his courses on mitochondrial bioenergetics, Dr. Kris Helke for her instruction in the basics of histopathology, and Dr. Hainan Lang for her warm introduction to the world of academic pathology. I would like to thank our collaborators in the Stadler lab at Pennington Biomedical Research Center for their expertise and assistance in running qPCR. The MCBP program Director, Dr. Robin Muise-Helmericks, and the MS program director, Dr. Laura Kasman, have provided much career guidance and program question assistance to me, for which I am grateful. I would like to thank the members of my Committee, Dr. DeLeon Pennell, Dr. Stadler, and Dr. Muise-Helmericks, for their mentorship and feedback on my work. I would also like to extend my most sincere thanks to my academic peers, friends, and family, especially my parents, Jamie and Stephen Spicer, for their extracurricular support throughout my tenure at MUSC. *This project was funded by NIH HL148114*.

TABLE OF CONTENTS

LIST OF FIGURES

	facilitate it, as well as the molecules coupled to sodium transport, along the nephron.
Figure 12	Summary of respirometry of isolated mitochondria from male and female renal cortex and medulla.
Figure 13	Oxygen consumption rate measurements of isolated renal mitochondria in male and female cortex and medulla.
Figure 14	Differential substrate feeding of isolated renal mitochondria from male and female cortex and medulla.
Figure 15	Respiratory gene mRNA expression.
Figure 16	Measurement of mitochondrial membrane potential from male and female cortex and medulla.
Figure 17	Western blots and analyses of fusion proteins MFN2 and OPA1.
Figure 18	A representative image set of male and female mitochondria from renal proximal tubules.
Figure 19	Electron microscopic analyses of isolated proximal tubular mitochondria in males and females.
Figure 20	Sites of ROS production by the electron transport chain.

LIST OF TABLES

LIST OF ABBREVIATIONS

ABBREVIATION	MEANING
Δψmito	Mitochondrial membrane potential
AKI	Acute kidney injury
ANOVA	Analysis of variance
ATP	Adenosine triphosphate
CKD	Chronic kidney disease
EGTA	Ethylene glycol tetraacetic acid
ETC	Electron transport chain
ERSD	End-stage renal disease
GFR	Glomerular filtration rate
GTP	Guanine triphosphate
IACUC	Institutional Animal Care and Use Committee
MFN	Mitofusin
mPTP	Mitochondrial permeability transition pore
NO	Nitric oxide
OXPHOS	Oxidative phosphorylation

PBS	Phosphate-buffered saline
RIPA	Radio-Immunoprecipitation Assay
ROS	Reactive oxygen species
SD	Sprague-Dawley (strain of rat)
SD^F	Female Sprague-Dawley
SD^M	Male Sprague-Dawley
SOD	Superoxide dismutase
TBST	Tris-buffered saline with 0.1% Tween® 20 Detergent

MORGAN J SPICER. Assessment of Sex Differences in Basic Renal Mitochondrial Bioenergetics. (Under the direction of DARIA ILATOVSKAYA).

Kidney diseases are closely linked with mitochondrial dysfunction, oxidative stress, and inflammation. Furthermore, it is established that sex plays an important role in the onset, development and severity of renal diseases. Recently, it has been revealed that sex hormones are implicated in mitochondrial bioenergetics. Despite information accumulated regarding the role of mitochondria in renal disease states, little is known about the bioenergetics of renal mitochondria in normal physiology, and no studies looked at sex differences pre-disease onset. We hypothesized that there are sex-related differences in renal mitochondrial bioenergetics in young, healthy rats. To test this hypothesis, we utilized renal tissue and live mitochondria isolated from healthy Sprague-Dawley rats 10-11 weeks of age. Assessment of oxygen consumption rates from male and female renal mitochondria revealed that female mitochondria have lower respiration vs male mitochondria in a pyruvate/malate containing buffer which stimulates ETC Complex I. Sex differences were de-accentuated in a succinate-based buffer which stimulates ETC Complex II. Next, female mitochondria displayed similar membrane potential in the cortex, but higher membrane potential in the medulla vs males. Analysis of renal cortical electron micrographs revealed lower density and number of female mitochondria in renal proximal tubules, as compared to males; however, female mitochondria were larger in size. Furthermore, female renal mitochondria displayed higher ROS levels and lower antioxidant capacity, while the activity of superoxide dismutase (SOD) was significantly higher in female renal cortex vs in male cortex. The link between mitochondrial ROS production and calcium handling prompted the quantification of mitochondrial calcium uptake and mitochondrial permeability transition pore (mPTP) opening. We observed that although male and female renal mitochondria have similar amounts of calcium uptake, the mPTP opens earlier in female mitochondria. Taken together, these data suggest that

female renal mitochondria are potentially more sensitive to oxidative stress, which allows for faster mPTP opening and elimination of dysfunctional mitochondria. Observed sex-related discrepancies in renal mitochondrial function prior to the onset of disease could be contributing to renoprotection generally observed in females pre-menopause.

CHAPTER 1 - Introduction and background

Kidney structure and function. Like all major organs, the kidneys are integral to the function of the body as a whole. They play a vital role in both the filtration of toxic metabolites and waste products from the blood, as well as in recapturing the nutrients from that filtrate in order to maintain homeostatic balance[1]. The physiological structure of the kidney is conducive to these filtration processes; each kidney is comprised of anywhere from 800,000 to 1,000,000 nephrons, the functional unit of the organ. Furthermore, the kidney contains two distinct regions, the cortex and the medulla, which are each responsible for different functions[1]. Blood flows into the kidney via the renal artery, where it is first filtered by the first portion of the nephron, the glomerulus. Filtrate flows through the glomerulus into the proximal tubule and the Loop of Henle, then into the thick ascending limb, the distal tubule, and the collecting duct. From here, the filtrate passes back into the renal medulla *via* a larger medullary tubule into a medullary collecting duct[1].

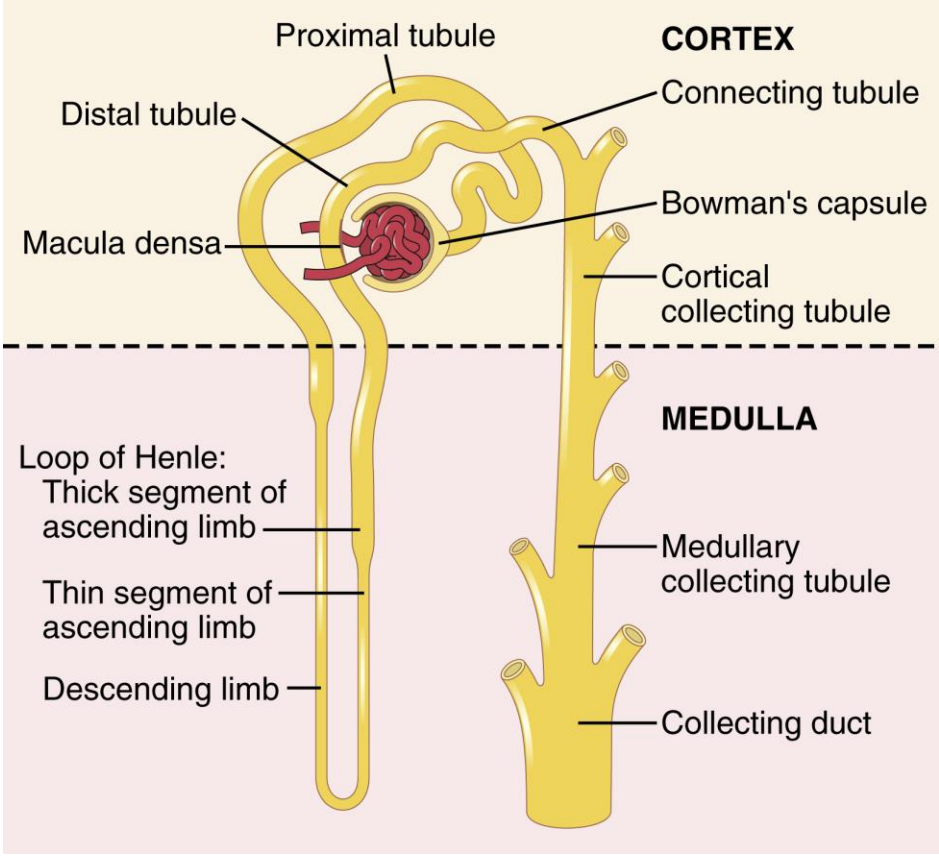

Figure 1. A schematic of the nephron, the functional unit of the kidney. Image used with permission from *Guyton and Hall Textbook of Medical Physiology*.

Prevalence of renal diseases and associated sexual dimorphisms. Given the complexity of kidney structure and the vast number of functions performed by the organs, it is not surprising that kidney disease is among the top causes of death in the United States as well as worldwide[2,3]. In fact, over 10% of the global population suffers from chronic kidney disease (**CKD**), and more than 15% of the adult population, or 1 in 7 adults, in the United States[4]. Notably, kidney diseases, including CKD, display sexual dimorphisms. Slightly fewer males present clinically with CKD (12% as opposed to 14% in females), but males undergo progression to end-stage renal disease (**ERSD**) more frequently[4], and suffer from higher pre-dialysis mortality rates than females[5]. In fact, female sex has been proposed as a protective factor against CKD-related hospitalization[6]. CKD is known to frequently transition from AKI, and indeed female sex has been found to also be protective against the extent of renal damage accumulated during acute kidney injury[6]. The renovascular disease hypertension is no exception to the trend of reduced severity in females; studies have shown that women present with slower rates of renal decline over time as compared to men[7,8]. Recently, a meta-analysis by Tejpal *et al.* has shown that female sex is protective against Covid-19-related renal outcomes, with women experiencing significantly less Covid-19-induced AKI than in men[9]. Even in the absence of renal disease, structural damage increases and glomerular filtration rate (**GFR**) decreases with age, but both more severely in males[10]. Some of the age- related renal protection observed in females has been to preservation of nitric oxide (**NO**) signaling, which is heightened by the presence of estrogens[10]. Even before age-related dimorphisms, sex-specific differences exist in the protein composition and function of kidneys. Female mice have been shown to excrete sodium loads earlier than mice, in part due to their heightened expression of transporters such as sodium/hydrogen ion exchangers, sodium/chloride cotransporters, and epithelial sodium channels[11]. Mice have also shown differences in sensitivity to the pressure-natriuresis relationship in response to the peptide hormone angiotensin II in both age and sex[12].

Important to note for these studies is the use of young females. In humans, the trend of female sex to be protective compared to age-matched males exists generally until menopause, where the sex discrepancies either cease to occur or display inversion of phenotype[5,13,14]. Administration of estrogen *via* hormone replacement therapy is shown to restore the sex-specific trends, however, clarifying that sex plays a role in renal function both in a normal physiological state as well as in disease[5]

Renal oxygenation and blood flow. Regardless of health status, the kidneys have a high metabolic load. Approximately 22% of the cardiac output is allocated to the kidneys, where blood flows from the renal artery into the interlobar arteries and subsequently the afferent arterioles which supply the glomerular capillaries[1]. This structure means that the cortex has an overall higher oxygenation level than the medulla, as it is more rapidly supplied by the oxygenated blood entering the kidney[15]. The medulla is supplied with oxygen via bundles of vessels called descending *vasa rectae,* which allows for the continuation of active transport in an otherwise poorly-oxygenated area[16,17]. Differences are thus to be expected in the bioenergetics of cortical and medullary mitochondria, as the regions have unique homeostatic balances. A schematic which illustrates renal blood flow and well as relative oxygenation rates across the nephron is shown in **Figure 2.**

The complexity of renal blood flow marks the kidney as a susceptible site for hypoxic damage. In fact, dysfunction in renal oxygenation is implicated in a number of kidney diseases. Acute kidney injury (**AKI**) is often caused by disruption to renal blood flow, resulting in ischemia-reperfusion injury[17]. These hypoxic renal vasculature functional alterations are also thought to be involved in chronic kidney disease (**CKD**)[18-20]. Dysfunctional oxygen handling and thus reduced oxygenation in the kidney have been shown to be associated with the progression of hypertension, as well[21]. In fact, the alteration of renal microvasculature caused by hypertension is a major causative factor

in the development of end-stage renal disease (**ERSD**)[21]. Renal hypo-oxygenation has also been linked to diabetic nephropathy, *via* hyperglycemia-induced dysregulation of nitric oxide availability, which subsequently alters renal oxygen homeostasis[22]. In summary, disruption to renal oxygenation is responsible for a large incidence of renal disease.

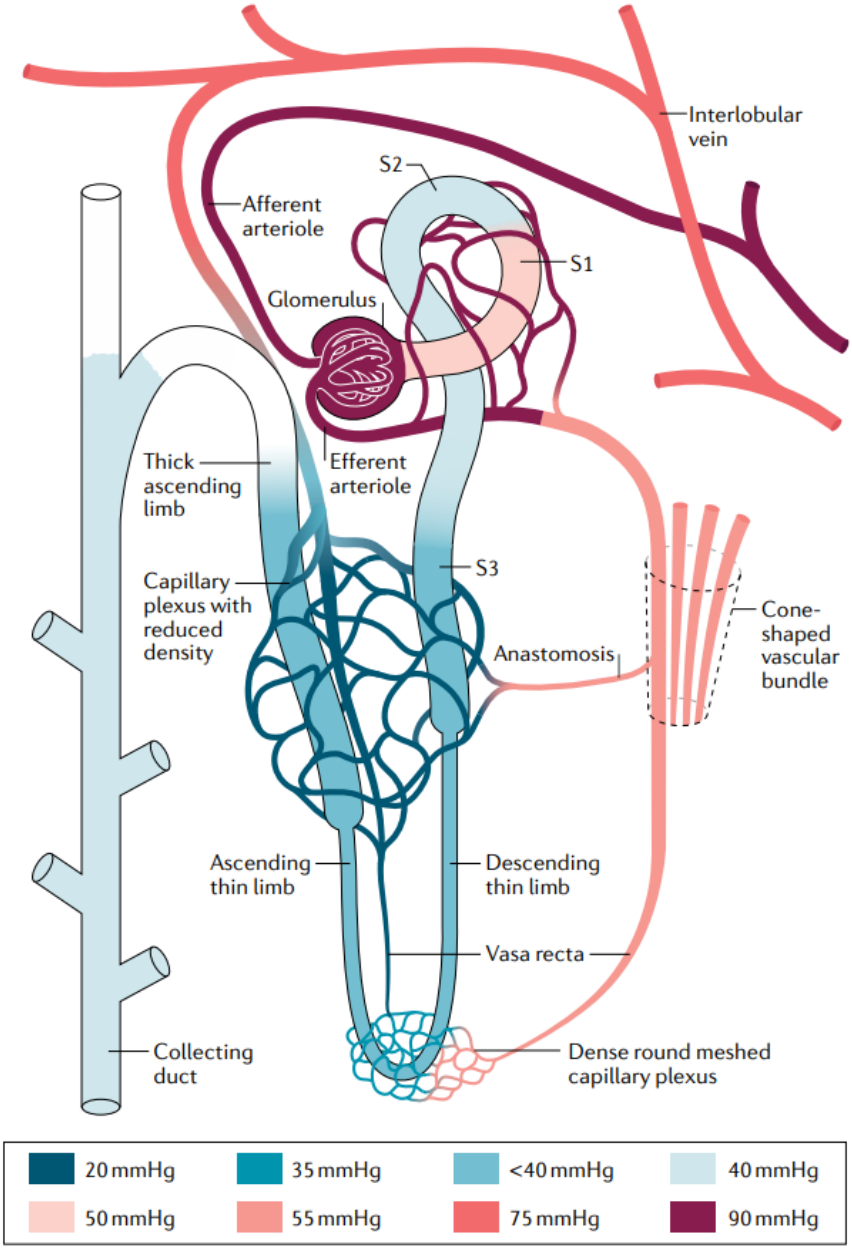

Figure 2. Schematic of renal blood supply and oxygenation. Figure used with permission from Scholz, H., Boivin, F.J., Schmidt-Ott, K.M. *et al.* Kidney physiology and susceptibility to acute kidney injury: implications for renoprotection. *Nat Rev Nephrol* 17, 335–349 (2021).

Even prior to the onset of renal disease, sexual dimorphism is seen in renal oxygenation and hemodynamics. Male and female kidneys have the same number of glomeruli, but there are differences in the hemostatic pressure of each due to

the larger amount of surface area in males; the glomerular vascular resistance is higher in females[23]. Males are known to have higher blood pressure, higher extracellular volume, and higher sensitivity to the blood pressure-regulating hormone angiotensin II. It is important to note that differences in tissue oxygenation have been shown to affect mitochondrial function[24,25]. The kidney displays sex differences in oxygenation, so it logically follows that sexual dimorphism exists in mitochondrial function.

Mitochondrial function across kidney disease and sex. In addition to the known link between tissue oxygenation and mitochondrial function, the number of renal pathologies linked with dysfunction in renal oxygenation suggest that perhaps the organelle primarily responsible in the consumption thereof may be involved. An emerging target that seems to be central to the origin of kidney pathologies is the mitochondrion. Mitochondrial dysfunction is implicated in glomerulosclerosis, whereby respiration is decreased, and gene expression of *Sod2* as well as other respiratory chain genes is suppressed[26]. Glomerulosclerosis is also linked with dysregulation of the pro-fibrotic TGF-β signaling, caused in part by an isoform of the protein IHG-1 which localizes to the mitochondria[27]. Diabetic nephropathy displays downregulation of the expression of the protein PGC1-α, the master regulator of mitochondrial biogenesis, in renal podocytes[28]. Reduction in mitochondrial reserve oxygen consumption capacity was also reported in diabetic nephropathy[29]. Downregulation of the mitochondrial inner membrane protein MPV17 has been shown to be linked with the development of diabetic nephropathy-induced glomerulosclerosis, despite the normal functions of the protein remaining unknown[30]. The cardiorenal disease salt-sensitive hypertension shows mitochondrial dysfunction in the forms of reduced mitochondrial membrane potential, ATP production, superoxide dismutase 2 activity, and oxygen consumption rates in the kidney[31,32]. Other renal pathologies have shown renal mitochondrial dysfunctions which range from alteration to mitochondrial bioenergetics, to

downregulation of mitochondrial biogenesis and upregulation of the fusion and/or fission processes[33-39].

Mitochondria are critical for all organ systems, so the question remains as to why it is that their dysfunction presents clinically with such a large number of renal pathologies. Mitochondrial function in renal disease is becoming well-defined, and renal disease has been well-demonstrated to possess sexual dimorphisms. Despite this, investigation of the sex discrepancies in renal mitochondrial function have yet to be defined in a normal physiological state.

Sex-related mitochondrial discrepancies have been studied in nearly all of the body's organ systems. It has been shown that sex is a factor for mitochondrial oxidative stress in cardiac cells, where female sex was shown to have lower expression of pro-apoptotic genes in rats of all ages, as well as higher expression of oxidative phosphorylation-related genes in older rats[40]. Cardiac mitochondria in males have displayed higher respiration rates as well as membrane potential compared to females, and even differences in response to cardiotoxicity. Mitochondria in the brain of female rats have been shown to accumulate less oxidative stress over time and maintain higher antioxidant capacity than their male counterparts[41]. Another similar study by Gaignard *et al.* claimed that these brain mitochondrial sex differences were ameliorated in females following ovariectomy[42]. Mitochondria isolated from the female liver generate less than half the amount of peroxides as compared to males, in addition to having higher levels of mitochondrial superoxide dismutase and glutathione peroxidase[43,44]. Liver mitochondria from females have also been demonstrated to be more differentiated than in males, as well as more efficient at making ATP[45]. In skeletal muscle, female mitochondria again displayed higher oxidative phosphorylation and antioxidant capabilities than in males, and also resisted dysfunction induced by a high-fat diet[46,47].

The mitochondria of both white and brown adipose tissues are no exception: female white adipose tissue contains more functional mitochondria than in males[48]. Furthermore, administration of estrogens on white adipocytes induced greater mitochondrial biogenesis and differentiation, while testosterone had the opposite effects[48]. Brown adipose tissue mitochondria displayed higher oxygen consumption as well as density, and more differentiation[49]. Notably, in a recent, comprehensive review of what is known about gender dimorphism in mitochondria, there is no mention of renal mitochondria[50]. In order to fill the existing gaps in knowledge regarding the sex differences in renal mitochondrial bioenergetics, it is key to assay the essential functions of these organelles.

Mitochondrial structure and functions. As displayed in **Figure 3**, the mitochondrion is an organelle composed of two dynamic membranes which surround its own set of DNA, and is frequently referred to as the "powerhouse of the cell" due to its function in producing energy in the form of ATP through a process known as oxidative phosphorylation or cellular respiration[51].

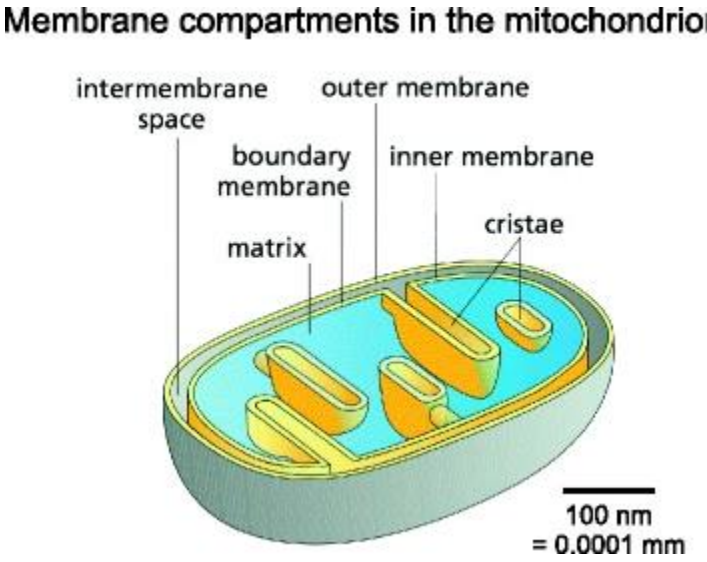

Figure 3. A diagram displaying the membrane compartments in the mitochondrion. Used under a Creative commons license from Kühlbrandt, W. Structure and function of mitochondrial membrane protein complexes. *BMC Biol* 13, 89 (2015). http://creativecommons.org/licenses/by/4.0/

Oxidative phosphorylation is the sum of a series of reactions involved in the consumption of oxygen to generate CO2, water, and energy in the form of ATP. These reactions occur *via* proteins in the electron transport chain, which is located in the mitochondrial inner membrane[51]. Electrons from NADH are transferred to Complex I, and those from FADH2 are transferred to Complex II. Electrons from both complexes are then shuttled through cytochrome *c* reductase, or Q. From here, electrons are transported to Complex III and then through cytochrome *c*. Following cytochrome *c*, electrons are shuttled to Complex IV, where they are then pumped into the mitochondrial matrix and used up in the generation of water from hydrogen and oxygen molecules. The energy from the electrons is used to generate a proton gradient in Complexes I, III, and IV, which summarily forms the mitochondrial membrane potential (**Δψmito**). Because of this higher concentration of protons in the mitochondrial intermembrane space, the gradient flows downwards through Complex V, where the proton movement powers the generation of ATP from ADP, as is shown in **Figure 4**[51].

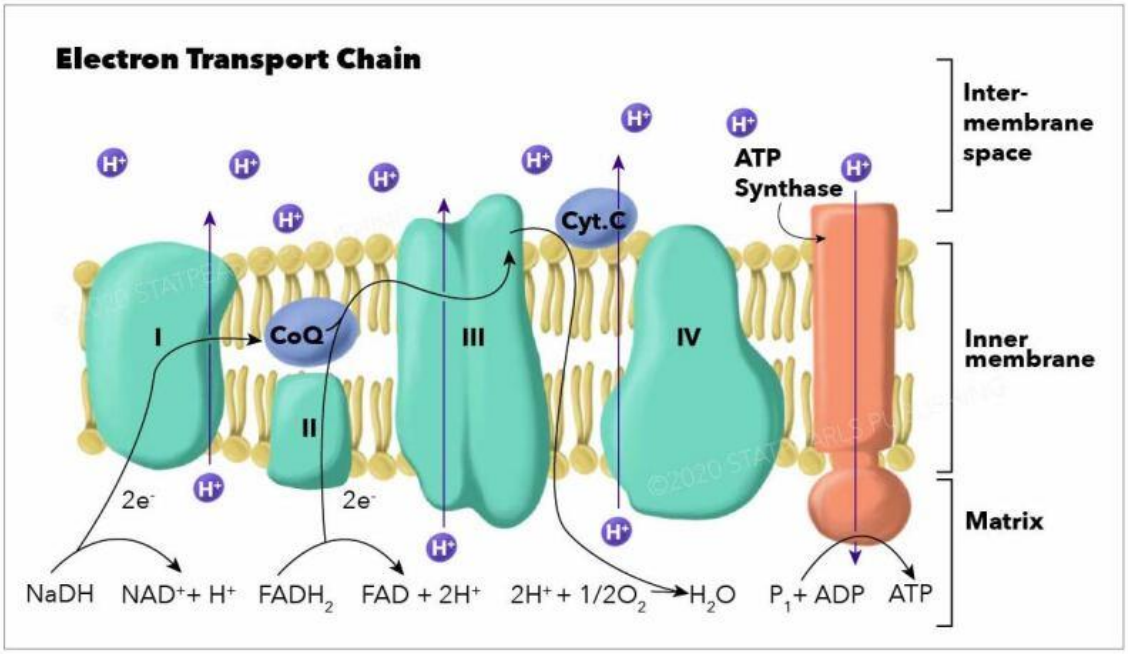

Figure 4. A schematic of the electron transport chain. Reprinted with permission from https://www.ncbi.nlm.nih.gov/books/NBK526105/ https://creativecommons.org/licenses/by/4.0/

Mitochondria are dynamic organelles that undergo a variety of shape-changing processes, mainly, the biogenesis of new mitochondria, as well as fission and fusion. The master regulator of mitochondrial biogenesis is the protein PCG1-α, which, when activated, stimulates the formation of new mitochondria *via* translocation from the cytoplasm to the nucleus and subsequent activation of nuclear genes[52]. Regarding dynamics, proteins such as mitofusins 1 and 2 (**MFN1** and **MFN2**) allow for the joining of two mitochondrial outer membranes together, and OPA1 allows for the fusion of the mitochondrial inner membrane[53]. Proteins responsible for mitochondrial fission include DRP1, which is involved in GTP-dependent fission of the mitochondrial outer membrane, and its receptors FIS1 and MFF, which are thought to be involved in the recruitment of DRP1 to the outer membrane[52,54]. Assessment of mitochondrial dynamics provides valuable information about mitochondrial bioenergetics: for instance, fusion is normally known to be coupled to respiration[55]. This is because the presence of GTP (and thus ATP) is required for the activation of OPA1, so levels of GTP are linked to levels of fusion [24970086].

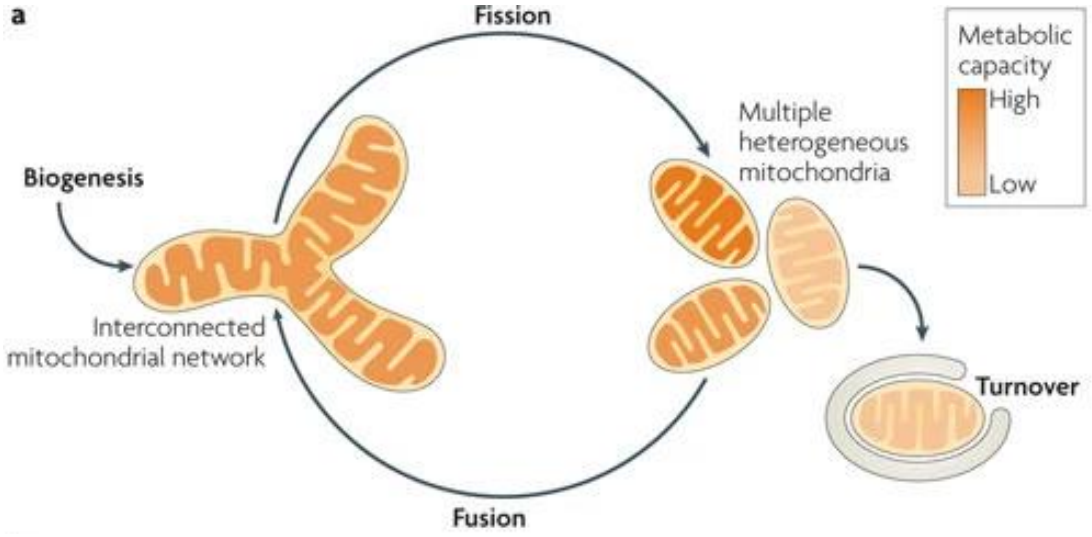

Figure 5. A schematic overview of the biogenesis, fission, and fusion processes mitochondria undergo. Used with permission from Westermann, B. Mitochondrial fusion and fission in cell life and death. *Nat Rev Mol Cell Biol* 11, 872–884 (2010)

Fission, conversely, is generally performed in order to mitigate damage; the separation of a damaged portion of mitochondria from a healthy one can salvage the damaged organelle and or induce healthy, regulated levels of mitophagy to degrade the nonfunctional portions of the organelles[52].

Mitochondria and energy metabolism in the kidney. Mitochondria are dynamic organelles, and in the kidney their distribution and activity are varied across segments of the nephron. For instance, the proximal tubule is the most abundant in mitochondria, due to the fact that a majority of the kidney's filtrate reabsorption and sodium handling occur there[56]. Proximal tubules primarily rely on aerobic respiration, mainly utilizing high ATP-yielding β-oxidation of fatty acids produce energy, and are also capable of gluconeogenesis[56,57]. In the passive transport environment of the glomerulus, there are significantly fewer mitochondria present. The distal tubules, however, primarily utilize glycolysis to produce ATP, and thus are relatively rich in mitochondria[56,57]. In fact, both the distal tubules and the thick ascending limb are also able to undergo anaerobic metabolism of glucose into lactate[56,57].

Mitochondria are known to be one of the largest sources of reactive oxygen species (**ROS**) production in the cell. ROS are known to be involved in the development of many diseases, such as hypertension, neurological diseases, cardiovascular injury, and cancer[58]. The kidney is no exception to ROS-mediated damage: ischemia-reperfusion AKI, CKD, diabetic nephropathy, and salt-sensitive hypertension all have strong correlations with high levels of oxidative stress[59-61]. Despite the number of disease states associated with excess ROS production, a normal physiological concentration of ROS (termed "mild oxidative stress by Frank *et al.*) causes degradation of damaged mitochondria *via* the process of mitophagy[62]. Removal of the damaged organelles helps to prevent buildup of oxidative stress and thus can keep the cell in a healthy

state. For this reason, there exists a delicate balance of ROS accumulation in the cell: small amounts can be beneficial, but excess lead to mitochondrial damage and subsequently target organ damage and disease[62].

In summary, the high metabolic load of the kidney means that a number of renal cell types in both the cortex and the medulla have high numbers of mitochondria, as well as many downstream processes such as filtrate reabsorption and ion transport which rely on the energy production and other functions of mitochondria. The sexually dimorphic nature of mitochondria in other organs paired with the observed sex-specific trends in renal disease onset and severity suggest that mitochondrial sex differences may a contributing factor. Given the involvement of mitochondria in the progression of a number of renal diseases, it is surprising that there is a lack of data regarding mitochondrial function in the healthy kidney or between sexes. Furthermore, many nephron segments are rich in mitochondria, a major source of ROS in cells. Although low levels can lead to protective mitophagy in cells, an excess of ROS are implicated in many renal diseases. In accordance with the observed reduction in severity and progression of renal diseases displayed in females, and presented with the fact that low levels of ROS are involved in a plethora of mitophagic signaling events prior to reaching disease-causing levels, we hypothesized that female renal mitochondria have higher sensitivity to oxidative stress.

CHAPTER 2 - Materials and methods

2.01 Animal model and experimental protocol

Male and female Sprague Dawley rats were originally obtained from Charles River Laboratories(Crl:CD(SD) stock # 001). Animals used for the experiments discussed henceforth were between 10 and 11 weeks of age (70-77 days), and experimental groups consisted of male and female renal cortices and medullae. They were placed on a 5v75 PicoLab diet (LabDiet Advanced Protocol, #0039980) with *ad libitum* food and water access, and all were exposed to the same 12hr day/night light cycle. This protocol was approved by IACUC (#2021-1044). In accordance with ARRIVE guidelines, the study design is outlined below in **Figure 6.** The number of rats used was based on *a priori* statistical analyses performed with the assistance of the MUSC biostatistics care, and *n* of animals is reported in each analysis that was performed. No exclusion criteria were set prior to the study. Animals used for the studies were randomized between litters, and confounding factors such as cage location were accounted for in the randomization.

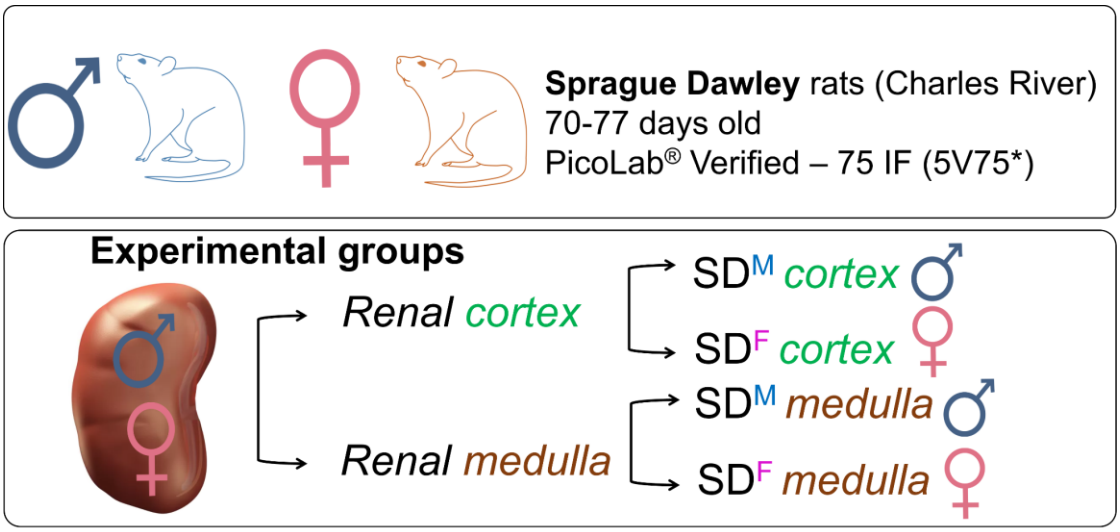

Figure 6. A depiction of the animal protocol and experimental groups used for the sets of experiments detailed in Sections 2.02-2.11. SD^F - female Sprague Dawley rat, SD^M - male Sprague Dawley rat.

2.02 Kidney flush procedure

At the respective endpoints of the experiment, rats underwent a kidney flush procedure. Animals were anesthetized with 5% isoflurane in the induction chamber and then 1.5-5% *via* the nose cone for the surgical procedure. An abdominal midline incision was made, and organs were moved to the side to then allow dissection of the abdominal aorta above the left kidney. The mesenteric and celiac arteries were then isolated, and loose ties using 4-0 silk threads were placed around those vessels. Then, below the left kidney in the abdominal region, the abdominal aorta is isolated and two loose ties with 4-0 silk are placed. The vessel was then clamped, and the lower tie was tightened. A hole was made in the aorta and the catheter was threaded in, with the upper tie used to hold the catheter in place. A schematic of the procedure is shown in **Figure 7**. The vessel clamp was removed, and blood was collected first into heparin-containing 1.7 mL tubes, followed by the kidneys being flushed at 3 mL/min until blanched with a solution of 40 mL of PBS and 200 ul of heparin to prevent clotting. Kidneys were subsequently removed and placed immediately into PBS on ice.

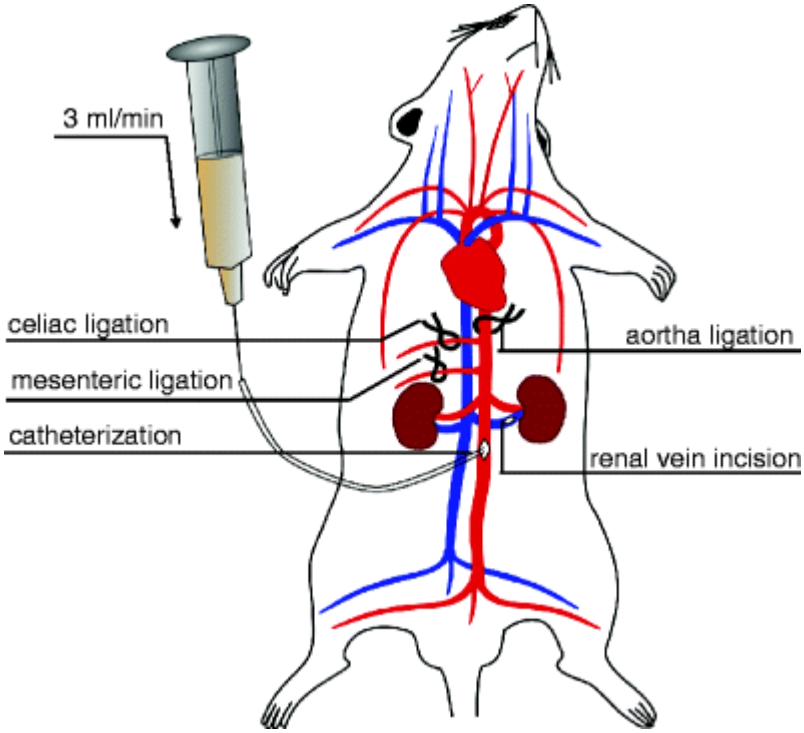

Figure 7. Schematic of the kidney flush procedure. Figure used with permission from Ilatovskaya, D. V., & Staruschenko, A. (2013). Single-channel analysis of TRPC channels in the podocytes of freshly isolated Glomeruli. *Methods in molecular biology (Clifton, N.J.)*, *998*, 355–369. https://doi.org/10.1007/978-1-62703-351-0_28

2.03 Isolation of renal mitochondria

Freshly harvested kidneys that underwent the flushing procedure as described above were first mechanically separated into cortex and medulla sections on ice. The following protocol was adapted from previously described methods by Frezza *et al*[63]. From here, tissue was minced briefly on ice with scissors and rinsed with chilled PBS, then minced more thoroughly using a razor blade in approximately 2 mL of ice-cold mitochondrial isolation buffer containing 200 mM sucrose, 10 mM Tris-MOPS, and 1 mM EGTA/Tris, pH 7.4. The minced tissue and buffer solution (approximately 3 mL) was poured into a 5 mL dounce and homogenized with 5 strokes of a Heidolph homogenizer at 1600 RPM. The cortex and medulla solutions were centrifuged at 1,000 x g at 4°C to remove debris, and the resulting supernatant was removed and placed into new 1.7 mL tubes. Again, the supernatant was centrifuged at 7,000 x g at 4°C, this time leaving pelleted mitochondria at the bottoms of the tubes. The supernatant was pulled off the pelleted mitochondria, which were then resuspended in 200 ul of isolation buffer and centrifuged again at 7,000 x g. The pelleted mitochondria were resuspended with 100µl of mitochondria isolation buffer. The final product was assessed for viability by loading a small aliquot of isolated mitochondria (approximately 10-15 ul) with 150 nM TMRM, and observation at 40x (Numerical Aperture: 0.75) under a fluorescence Nikon Eclipse Ti-2 microscope (objective: #OFN25) for detection of membrane potential. Isolated mitochondria were used immediately for functional experiments as described in **Figure 8** and Sections 2.05, 2,06, and 2.08. Samples that were to be stored for later use in experiments such as in Section 2.11 were snap-frozen with liquid nitrogen and stored at -80°C.

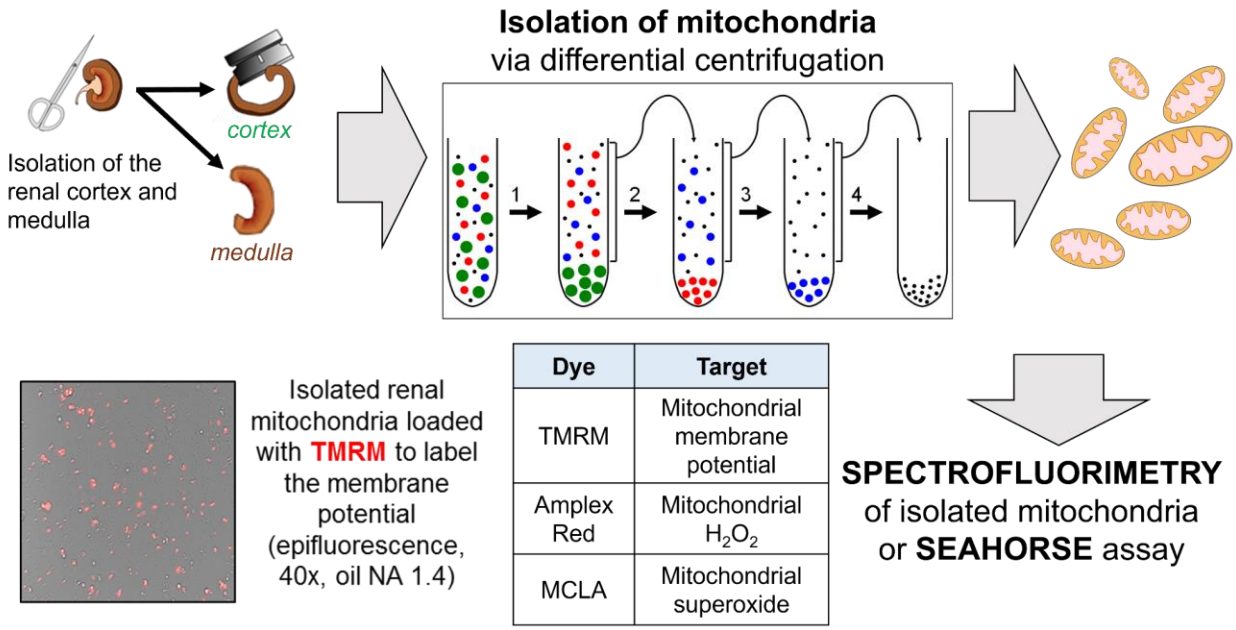

Figure 8. Illustration of the mitochondria isolation procedure. Excised renal cortex and medulla were minced, mitochondria were isolated *via* differential centrifugation. a small aliquot of the isolated mitochondria were loaded with TMRM to label membrane potential and viewed to assess viability. The remaining mitochondria were used as described in Sections 2.05, 2.06, and 2.07 for spectrofluorimetry or oxygen consumption rate experiments.

2.04 BCA assay for sample protein quantification

A Pierce BCA assay (ThermoFisher, IN) was used for Methods detailed in Sections 2.05, 2.07, and 2.11. In it, standards of 2000, 1500, 1000, 750, 500, 250, 125, 25, and 0 µg/mL are diluted from the supplied 1 mL ampule of Albumin Standard. Samples to be analyzed are diluted 1:20 in the supplied Working Reagent, and 100 µL of each standard and sample are pipetted in duplicate into a 96-well plate (Costar, #3916). After the Working Reagent was added, the plate was incubated at 37°C for 30 minutes, then absorbance was read at 562 nm in the Tecan reader.

Sample values were calculated by using a standard curve generated from the known concentrations of the standards, and then adjusting for dilution if necessary.

2.05 Oxygen consumption rate measurements in isolated mitochondria

Quantification of oxygen consumption rates using the Seahorse XF platform is an established, rigorous way to measure mitochondrial respiration[64-66]. For oxygen consumption rate (OCR) measurements, 2 to 10 ug of freshly isolated mitochondria from each experimental group were placed into a pH 7.2 buffer containing 70 mM sucrose, 200 mM mannitol, 10 mM KH_2PO_4, 5 mM $MgCl_2$, 2 mM HEPES, 0.2% BSA v/v, 1 mM EGTA 5 mM malate, 5 mM succinate, and 5 mM glutamate (MAS buffer) and loaded into Cell-Tak coated 96-well Seahorse XF96 plates (Agilent, CA; #102416-100) that were allowed to adsorb at RT for 20 minutes. The loaded plates were then spun at 1,000 x g for 1 minute to secure the mitochondria. Samples were plated and subsequently run on the Seahorse XF96 analyzer located in the MUSC Core Metabolomics Facility. Oxygen consumption rate (OCR) was measured at baseline for ten minutes and after the addition of 5ul of 10 mM of ADP, oligomycin, FCCP, and a rotenone+antimycin A cocktail, with the addition of each drug occurring in 15-minute intervals. An increase in observed OCR following the addition of adenosine diphosphate (ADP) is used to assess the viability of the mitochondria. Oligomycin is an ATP synthase (Complex V) inhibitor, and the addition quenches OCR below the basal level, which allows for calculation of ATP-linked respiration. FCCP is an uncoupling agent which disrupts the proton gradient, so the addition allows analysis of maximal respiration (beyond what would be observed physiologically). Finally, a cocktail of rotenone and antimycin A, which inhibit Complexes I and III, respectively, is added to quench all mitochondrial respiration in the sample. By subtracting this value from the basal rate, the non-mitochondrial oxygen consumption can be calculated. A graphical summary of the added drugs, their effects, and what pieces of data can be measured is depicted in **Figure 9.**

2.06 Oxygen consumption rate measurements in isolated renal mitochondria with different substrates

The experimental conditions follow those described in Section 2.05, however instead of the MAS buffer used in that protocol, one set of isolated mitochondria (male and female, cortex and medulla) was placed in a solution ideal for mitochondrial function containing 70 mM sucrose, 200 mM mannitol, 10 mM KH_2PO_4, 5 mM $MgCl_2$, 2 mM HEPES, 0.2% BSA v/v, 1 mM EGTA 5 mM malate, and 5mM pyruvate, to stimulate ETC Complex I; the other set was placed in a nearly identical buffer which omitted the malate and pyruvate, and instead contained only 5 mM succinate as substrate, to instead stimulate Complex II. Data were normalized to the protein concentration in each sample as calculated from a BCA assay as described in Section 2.04.

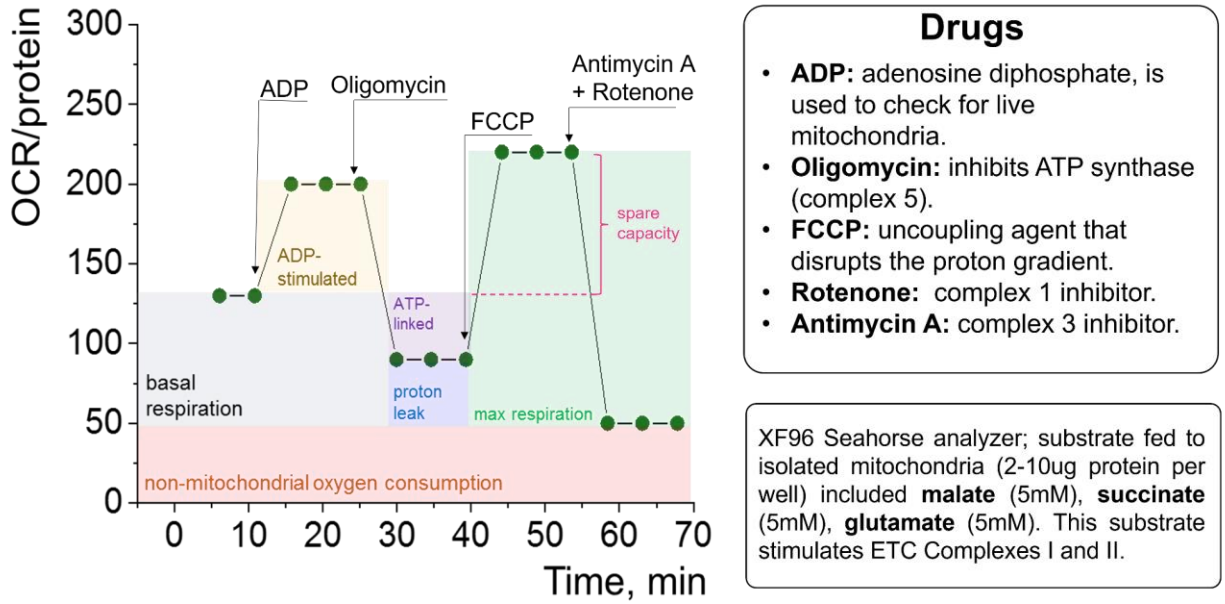

Figure 9. Oxygen Consumption Rate Measurement Schematic. The mitochondrial respirometry parameters that can be calculated after the addition of each drug are shown.

2.07 Polymerase chain reaction quantification of respiratory genes in renal mitochondria

Renal mitochondria were isolated as previously described[32], and TRIzol Reagent from Life Technologies was used per the manufacturer's instructions for the subsequent purification of RNA. Isolated RNA was reverse transcribed using the High-Capacity cDNA Reverse Transcription Kit with RNase inhibitor from Applied Biosystems. This kit utilizes a 20 µl mix consisting of 10 µl each of Master Mix and isolated RNA. Primer pairs were designed using Primer Express Software v3.0 (Applied Biosystems), in order to complement the sequences of the target genes obtained from the Ensembl genome browser. Synthesis of the designed primers was performed by Integrated DNA Technologies (Coralville, IA), and primers were reconstituted to a 10 µM working solution before use. The epMotion 5075 Liquid Handling Robot from Eppendorf was used to plate the reactions into a 384-well plate (Applied Biosystems), with 2 ng of cDNA being used per reaction. The reactions were carried out with default settings in the 7900HT Sequence Detection System (Applied Biosystems) for 40 cycles, and non-template (water) controls were used in conjunction with triplicate repeats for each reaction, as described previously[32].

2.08 Spectrofluorimetry of isolated renal mitochondria

Isolated mitochondria from Section 2.03 were placed in a 1:10 ratio into chilled buffer pH 7.5 containing 120 mM KCl, 10 mM sucrose, 2 mM KH2PO4, 2 mM MgCl2, 10 mM HEPES, 5 mM glutamate, and 5 mM malate (**KCl buffer**). For membrane potential measurements, 1 ul of 15 µM TMRM was added per 500 ul of mitochondria and KCl buffer. For hydrogen peroxide measurements, 2 µl of 10 mM Amplex Red and 1µl of HRP enzyme was added immediately before pipetting to the mitochondria and KCl buffer solution. For MCLA, 1 µl of 10 mM MCLA dye was added per 500 ul of mitochondria and KCl buffer. Then, 100 µl of the solution was immediately pipetted into an average of 8 wells of a black-bottom 96-well plate (Costar, #3916) and run in a

plate reader for fluorescence or luminescence, where appropriate. TMRM samples were read for ten minutes at an excitation of 560 nm and an emission of 600 nm. Amplex Red samples were read for 20 minutes, with an excitation 571 nm of and an emission of 585 nm. Both TMRM and Amplex Red experiments were run on the Tecan Infinite 200 Pro reader. MCLA is a luminescent dye, and luminescence was read on the Synergy H1 reader. TMRM and MCLA assays collected data for ten minutes, and Amplex Red assay collected data for 20 minutes, with data points being collected continuously. Data were normalized to total protein per sample as calculated by the BCA assay in **Section 2.04** for all three dyes. For Amplex Red, which forms an enzymatic curve instead of linear, data were integrated using Origin 2019 software, and the area under the curve was used for statistical analyses.

2.09 Analysis of superoxide dismutase activity in isolated renal mitochondria

Samples weighing approximately 25 mg each of male and female renal cortex and medulla were homogenized in a cold, pH 7.2, 20 mM HEPES buffer containing 1 mM EGTA and 210 mM mannitol, and 70 mM sucrose per gram of tissue, then centrifuged at 1500 x g at 4°C for five minutes to remove cellular debris. The supernatant, stored on ice, was then pipetted in 10 µL volumes into a clear 96-well plate. To this, 200 µL of the Radical Detector (Cayman Chem, MI) was added, and samples were briefly mixed. To initiate the reaction, 20 µL of xanthine oxidase (Cayman Chem, MI) was added to each well, and the plate was allowed to incubate on an orbital platform shaker for 30 minutes before the absorbance was read at 450 nm by a Tecan plate reader. Data were analyzed using the included standards of 0.000, 0.005, 0.010, 0.020, 0.030, 0.040, and 0.050 in combination with the equation $SOD\ (U/ml) = [(\{sample\ linear\ rate - b\} \div slope) \times (0.23 \div 0.01)] \times sample\ dilution$ to linearize the enzymatic curve and calculate sample values. A linearized rate is calculated by graphing the known concentrations of the standards, from which the y-intercept of the graph is subtracted. This value, $(Linear\ rate - y - intercept)$,

is then divided by the slope. To account for the 10 ul added to the 230 ul volume of the plate wells, it is multiplied by the fraction 0.23/0.01. Finally, this number is multiplied by the dilution of each individual sample to give the SOD activity in calculated Units/mL (U/mL). Data were analyzed with two-way ANOVA and Holm-Sidak post-hoc tests.

2.10 Proximal tubule electron microscopy and image analysis

Freshly isolated 1 mm^3 samples of male and female cortices were fixed with 2.5% glutaraldehyde in a phosphate buffer overnight. Then, they were rinsed in a 2x buffer for fifteen minutes, incubated in 2% osmium tetroxide on a rocking platform shaker for 1hr, and placed through an ethanol dehydration series up to 100%. When dehydration was complete, samples were placed into propylene oxide to allow penetration of the reagent Embed 812 (Electron Microscopy Sciences, #14120) in subsequent ratios of 1:2, 2:2, and 3:1 for 1 hour each. Samples were placed into pure plastic overnight on a rocking platform shaker, then placed into molds and allowed to polymerize in the oven overnight. Hardened blocks were sectioned at 0.5 um slices, mounted on glass, and stained with 1% toluidine blue. The sections were then observed for determination of appropriate areas to slice, and the block was trimmed accordingly. The new sections were placed on a 200-mesh cu grid and stained for 10 minutes with uranyl acetate, followed by a rinse step and subsequent stain with lead citrate. Final sections were imaged on a JEOL 1010 transmission electron microscope set to 80 kV. Images at 20000x magnification (pixel to nm ratio set to 1:0.145) were analyzed using FIJI software as distributed by NIH[67]; analysis parameters included mean gray value (density), area, number of mitochondria per field, and health scores from 1-5, with a score of 1 representing a perfectly healthy mitochondrion and a score of 5 representing a severely damaged mitochondrion. To prevent bias in mitochondria analysis, all analyses were carried out blinded to both sex and renal region of each image. Any mitochondria which were not completely visible in the image field were excluded from analysis. Mitochondria were selected manually using

the ROI freehand tool, and the measurement parameters in the FIJI software included Mean gray value, shape descriptors, and circularity. The brightness for each image in the software is within the range of 0 to 255. To convert the mean gray values into the density that is used for analysis, the mean gray value is first subtracted from 255. For each image, a representative “background” selection is made, which is also subtracted from 255. From here, the background value is subtracted from each sample value to generate density. Data were analyzed with two-way ANOVA and Holm-Sidak post-hoc tests.

2.11 Renal mitochondrial Western blotting

Western blot samples consisted of a 1:10 ratio of snap-frozen mitochondria from male and female renal cortex and medulla in radio-immunoprecipitation assay (RIPA) buffer. Samples were run in 4-20% polyacrylamide gels (Bio-Rad, #5671095) for 5 minutes at 50v, then for 75 minutes at 120v. Proteins were transferred to nitrocellulose membranes using a 2.5A, up to 25v, 7 minute transfermode on the TransBlot system from Biorad, Inc. Membranes were stained with Pierce stain (Thermo Scientific, IN; #786576) to detect total protein of the samples before blocking in 5% skim milk in Tris-buffered saline with Tween 20 (TBST: 20mM Tris, 150mM NaCl, 0.1% Tween 20, w/v, pH 7.4) for one hour. After blocking, membranes were incubated in primary antibodies overnight at 4°C. Primary antibody was then decanted, and a wash step consisting of three 5-minute washes in TBST on a low speed orbital platform shaker was performed. Secondary antibody was then added and allowed to incubate at room temperature on a low speed orbital platform shaker for one hour, followed by an additional wash step consisting of three 5-minute washes in TBST. Proteins were detected using SuperSignal West Pico PLUS reagent (Thermo Scientific, IN) and imaged with a Li-Cor Odyssey XF system to detect chemiluminescence of the HRP conjugate on the secondary antibody to the target protein. The catalog numbers and dilutions of the antibodies used can be found in **Table 1**.

Abbreviation	Target Protein Name	Vendor, Catalog Number	Species	Dilution
MFN2	Mitofusin 2	Proteintech, #12186-1-AP	rabbit	1:1000
OPA1	Mitochondrial dynamin-like GTPase	Fisher, #PA5-79771	rabbit	1:1000
SOD2	Superoxide dismutase 2	SCBT, #SC-137254	rabbit	1:500
HRP	Anti-rabbit (conjugated with a luminescent horseradish peroxidase tag)	Fisher, #31460	goat anti-rabbit	1:5000

Table 1. List of antibodies used for Western blots.

2.12 Renal mitochondrial calcium uptake measurements

Freshly isolated live mitochondria from male and female cortex and medulla were plated in a 96-well plate in wells containing 1 µl of 5 µM membrane-impermeable Calcium Green dye (Thermo Scientific, C3737), and a buffer of pH 7.5 containing 120 mM KCl, 10 mM sucrose, 2 mM KH_2PO_4, 2 mM $MgCl_2$, 10 mM HEPES, 5 mM glutamate, and 5 mM malate (**KCl buffer**). Using the injection feature on the Tecan Infinite 200 Pro plate reader, 5 ul of 250 uM $CaCl_2$ solution was injected into each well, and fluorescence reads were taken at 520 nm. $CaCl_2$ injections occurred sequentially

every 15 read cycles, and the end point of the experiment occurred after 11 injections. A schematic of this procedure is displayed in **Figure 10**. Fluorescence data were normalized to the total protein of each sample as calculated by BCA assay. To confirm that the observed decreases in Ca Green fluorescence are due to mitochondrial uptake, the drug Ru360, an inhibitor of mitochondrial calcium uptake, is used as a control by adding 5 µl of 500 mM stock to the mitochondria and buffer. Data were plotted, and the area under the curve for injection numbers 4 and 5 was integrated using Origin 2019b software. Following this, 2-way ANOVA with Holm-Sidak post-hoc tests were utilized on the integrated data to determine significance.

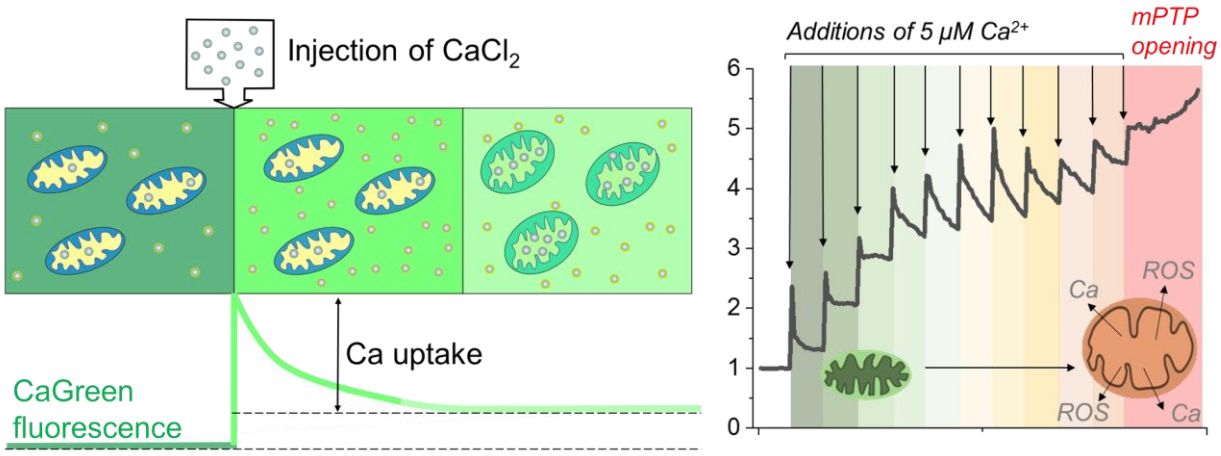

Figure 10. Schematic of the mitochondrial calcium uptake assay. Calcium green dye fluoresces when bound to calcium ions, causing increases in fluorescence when calcium chloride solution is added. As mitochondria absorb the calcium, it the ions dissociate from the membrane-impermeable Ca Green dye, which causes fluorescence readings to decrease and stabilize. He opening of the mPTP can be visualized at the point where fluorescence readings continually increase. Data were analyzed with two-way ANOVA and the Holm-Sidak post-hoc test.

2.13 Quantification of renal antioxidant capacity

An Antioxidant Assay kit from Cayman Chemical (709001) was utilized for the measurement of total antioxidant capacity of renal tissues. Approximately 10-15 mg of cortical or medullary tissue from male or female kidney for each sample was homogenized *via* sonication over ice. Following this, homogenate was centrifuged at 10,000 x *g* for 15 minutes at 4°C to pellet debris. The resulting supernatant was then diluted in a 1:50 ratio for use. Each well on the plate contained 10 µl of sample or standard, 10 µl of metmyoglobin, 150 µl of Chromogen, and 40 µl of Hydrogen Peroxide Working Solution for a total of 210 µl per well, with all samples and standards run in duplicate. Standards of Trolox in concentrations of 0.0, 0.068, 0.165, 0.203, 0.270, 0.338, and 0.495 were plated and used later to generate a standard curve. Absorbance was measured at 750 nm on a Tecan Infinite 200 Pro plate reader following a 5 minute shaking incubation at room temperature. A linear regression was performed using Standard values, and sample antioxidant concentrations were calculated using the equation $Antioxidant\ (mM) = [\{sample\ average\ absorbance\ -\ b\} \div slope] \times dilution.$

2.14 Statistical analyses

Data were analyzed using one-, two- or three-way ANOVA and the Holm-Sidak post-hoc test, where appropriate for each dataset. Statistical test information is also located in the figure legend of each section. Data are displayed as box-and-whisker plots, with the box representing standard error, the whiskers as 1x standard deviation, and the line as the median. Statistical significance was designated as values with $p < 0.05$. Outliers were tested for using the Grubbs test, and removed if $p < 0.01$, where applicable. These box plots and values were generated by Origin 2019b software. N and *n* values are displayed on graphs, where N represents the number of animals used (biological replicates), and *n* represents the number of technical replicates.

CHAPTER 3 - Characterization of basal bioenergetic profiles in male and female renal mitochondria

Introduction

Oxidative phosphorylation in the kidney.

The kidney is among the body's most metabolically active organs, with an energy expenditure similar to that of the heart in a resting state in healthy adults[68]. The kidney's demand for energy arises from its functions in filtering blood to remove waste products, maintaining electrolyte homeostasis, regulating acid-base balance, reabsorbing nutrients, and regulating blood pressure. The energy needed for these processes is supplied largely from the process of oxidative phosphorylation performed by mitochondria, and indeed the kidney is the second-highest organ in both oxygen consumption and also total mitochondrial content, following the heart[69,70].

Mitochondria supply the energy for renal functions directly, as ATP is the universal currency of energy in the cell, and also by providing ATP for the plethora of Na+/K+ ATPases found in the basement membranes of epithelial cells of the renal tubules[71]. These ATPases facilitate the development of a sodium ion gradient which is greater in the lumen than in the cell and intracellular space. Other transport proteins such as sodium glucose transporters (SGLTs), sodium phosphate transporters (NPTs), sodium bicarbonate exchangers (NBCs), sodium chloride cotransporters (NCCs), sodium channels such as ENaC (Epithelial Sodium Channel), and others couple non-sodium molecules to the sodium gradient to allow for reabsorption into the cell and thus into the body, as displayed in **Figure 11[71]**.

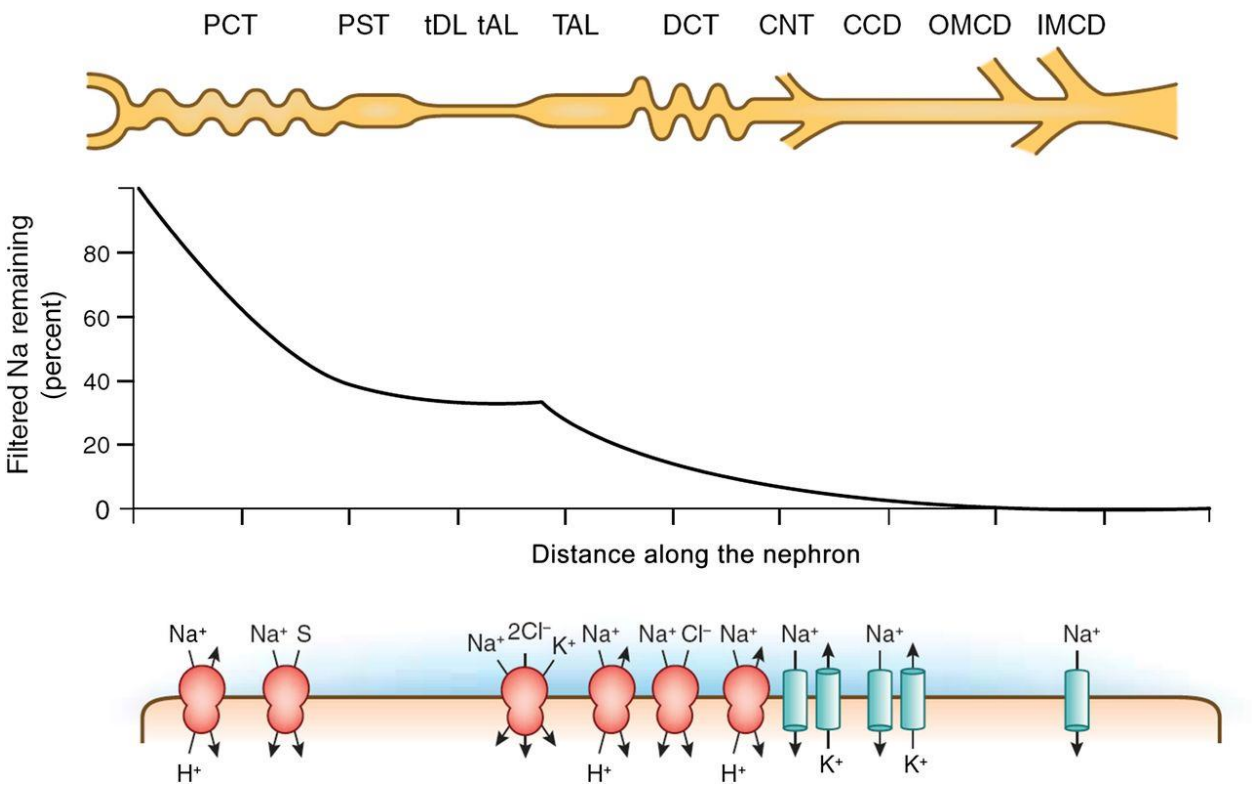

Figure 11. A schematic displaying a summary of sodium transport and the various proteins which facilitate it, as well as the molecules coupled to sodium transport, along the nephron. Reprinted with permission from CJASN.

As stated previously, kidney cells have both an extremely high energy demand and a high number of mitochondria to meet that demand[69,70]. Because of the fluctuating metabolic needs of the kidney, it is important for the mitochondria to have a high degree of plasticity to adjust to the changing energy requirements[52]. Therefore, it is very important for the kidney cells that mitochondria have ways of adjusting their energy output to maintain a homeostatic balance; one method is by the alteration of biogenesis and dynamics, that is, fission and fusion[52].

Many renal and cardiorenal disease states are linked to mitochondrial dysfunction, for example, salt-sensitive hypertension[31,32], glomerulosclerosis[26,27], diabetic nephropathy[28-30], tubulopathies such as Fanconi syndrome[72], and a number of other renal disease states[37-39]. Not only do renal diseases often display mitochondrial dysfunction, but they also present clinically in a sexually dimorphic manner. Female sex has been found to be protective against AKI and hypertension, and against the progression of CKD[6,7].

Despite this disease presentation, as well as sexual dimorphisms in normal kidney function, little is known about the differences in renal mitochondrial function in males and females. What is known includes that both estrogens and androgens do have effects on mitochondrial function: estrogens have been shown to attenuate tubular damage via altering the oxidative state of mitochondria[73], and female mice and rats are able to retain some forms of respiration in the presence of nephrotoxins compared to their male counterparts[74]. Androgenic effects on renal function have also been reported. For example, low doses of testosterone have been demonstrated to attenuate damage in renal ischemia-reperfusion injury[75]. These data oppose another study by Peng *et al.* which showed that administration of testosterone induced apoptosis and necrosis in tubular epithelial cells[76]. Interestingly, it has been shown that androgen receptors localize to mitochondria in other organs such as skeletal muscle and sperm cells[77,78]. Estrogen receptors have also displayed this nonclassical localization[78,79], but the question of whether this occurs in the kidney has not been answered yet.

In order to help fill this gap in knowledge regarding the sexual dimorphisms of renal mitochondria, we designed experiments to test the bioenergetic capacity of these organelles in renal male and female samples. First, we measured respiration rates of isolated renal mitochondria from male and female cortex and medulla, and then refined our baseline respirometry experiments to include

differential substrate feeding as well. From here, we examined expression of the ETC-related genes which are involved in mitochondrial respiration, and assessed mitochondrial membrane potential. Next, we investigated mitochondrial dynamics by analyzing both expression of dynamics-related proteins MFN2 and OPA1, as well as electron micrographs of proximal tubular mitochondria. These experiments helped to establish bioenergetic profiles of the mitochondria in male and female cortex and medulla.

Results

Comparison of the oxygen consumption rates of isolated male and female renal mitochondria.

One of the primary functions of the mitochondrion is the production of energy in the form of ATP through a process called cellular respiration[80]. The rates of respiration, which can be measured by examining the oxygen consumption rate of isolated mitochondria, are often tied to the health of the mitochondria[81]. In order to determine discrepancies in mitochondrial respiration the oxygen consumption rates were measured in the isolated mitochondria from each experimental group as defined in **Protocol 2.01**: male and female renal cortex and medulla. This allowed us to collect vital information about the bioenergetics from each group as displayed in **Figure 12**. The oxygen consumption rate (OCR) was measured by the Seahorse XF96 analyzer, the method of which is displayed in **Figure 9**. All data shown below are in experimental groups according to **Protocol 2.01**. The male mitochondria from both cortex and medulla have overall higher rates of respiration than both groups of female mitochondria, as seen in **Figure 12**. Male groups displayed higher **basal OCR** (Units shown are pmol/min/mg protein. Male cortex = 39.45 ± 1.12; female cortex = 26.57 ± 0.88; male medulla = 30.56 ± 0.74; female medulla = 21.69 ± 0.57), **ADP-stimulated OCR** (male cortex = 15.82 ± 0.79; female cortex = 12.79 ± 0.51; male medulla = 17.32 ± 0.80; female medulla = 11.85 ± 0.47), **ATP-linked OCR** (male cortex = 30.15 ± 1.07; female cortex =

24.60 ± 0.63; male medulla = 23.65 ± = 1.22; female medulla = 21.02 ± 0.47), **Leak OCR** (male cortex = 16.56 ± 0.63; female cortex = 11.01 ± 0.47; male medulla = 12.86 ± 0.43; female medulla = 8.59 ± 0.24), **Max OCR** (male cortex = 52.05 ± 2.33; female cortex = 32.56 ± 1.24; male medulla = 40.29 ± 1.23; female medulla = 25.05 ± 0.77), and **spare capacity** (male cortex = 14.34 ± 1.29; female cortex = 5.86 ± 0.58; male medulla = 11.64 ± 0.74; female medulla = 4.86 ± 0.57) than female cortex and medulla groups, as are shown in **Figures 12 and 13**. We report that cortical respiration was higher than medullary respiration for basal OCR, ATP-linked OCR, leak OCR, and max OCR in both male and female mitochondria (numerical data displayed above).

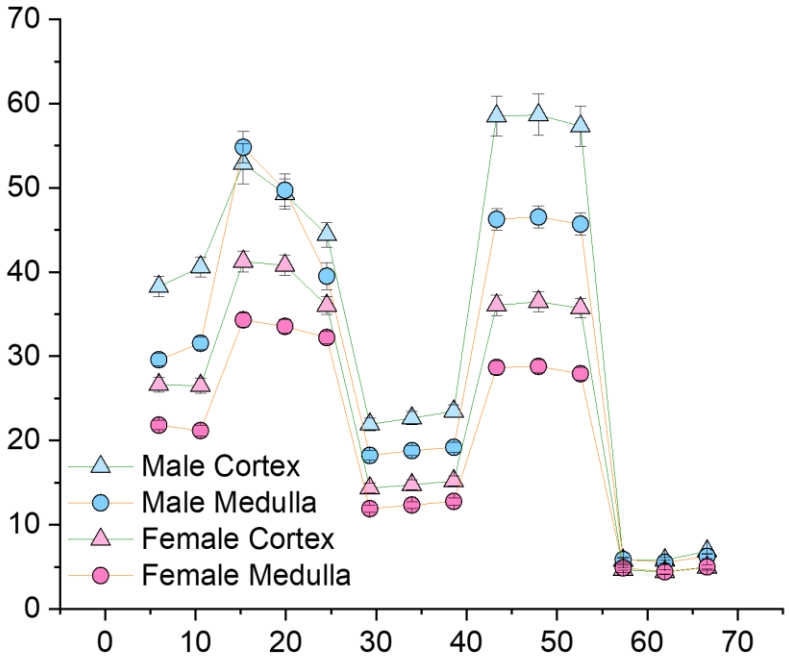

Figure 12. Summary of respirometry of isolated mitochondria from male and female renal cortex and medulla. Isolated renal mitochondria from males from both cortex and medulla displayed higher oxygen consumption over females for each measured parameter. Biological and technical replicates displayed on individual graphs in **Figure 13.**

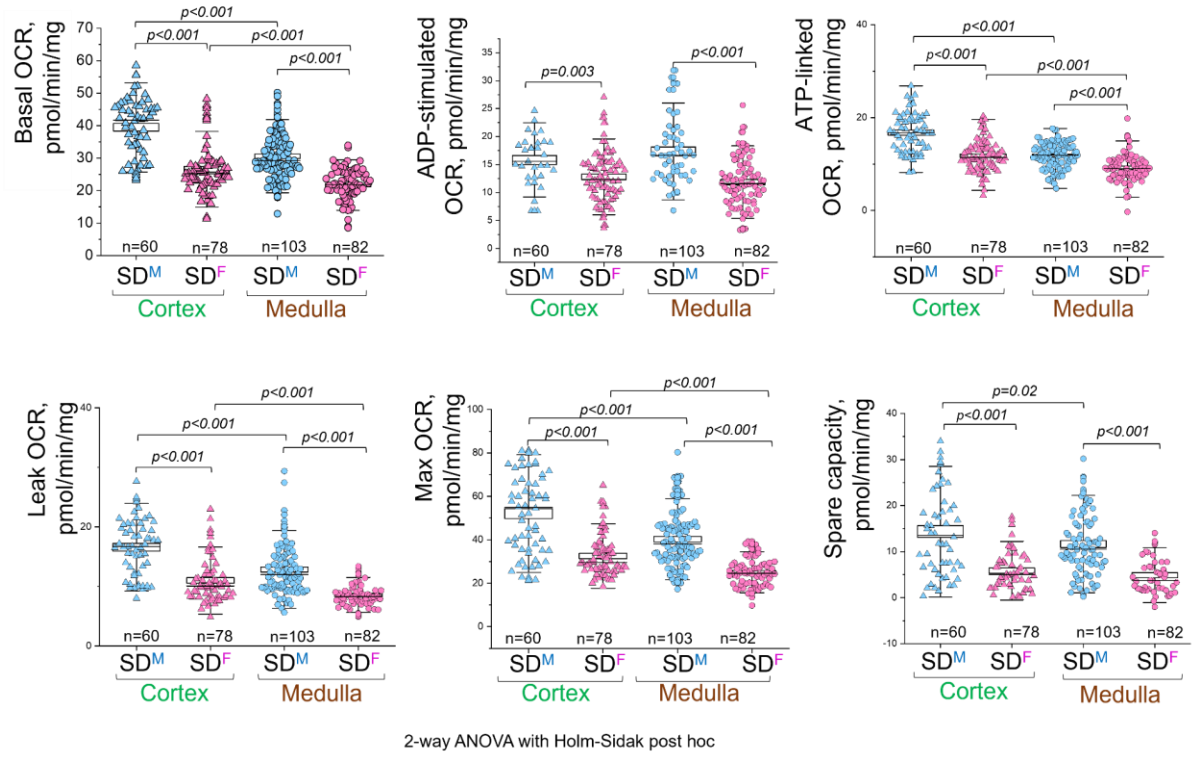

Figure 13. Oxygen consumption rate measurements of isolated renal mitochondria in male and female cortex and medulla. N value represents the number of biological replicates, and is 5 for each group shown. The *n*-values shown on the graph represent technical replicates. Analysis was 2-way ANOVA with the Holm-Sidak post-hoc test. .

The ETC is a multiprotein system where numerous factors, from expression to activity of each protein, could be potential driving factors of the observed discrepancies in respiration by sex. Respirometry can be tailored to observe differences in ETC function by complex. To assess the ETC complex dependency of mitochondria in male and female cortex and medulla, an additional experiment measuring OCR was performed. The experimental groups remained the same as in **Figures 12 and 13**, but were split into two groups with mitochondrial substrates which would independently stimulate unique complexes of the ETC, thus allowing for more mechanistic insight to the altered levels of oxygen consumption. As described in **Protocol 2.06** The first solution

contained malate and pyruvate sugars to stimulate respiration through Complex I, and the second solution contained only succinate to stimulate respiration through Complex II. **Figure 14** shows that, in malate/pyruvate buffer, male mitochondria followed the previous trends and had significantly higher basal OCR compared to the female mitochondrial groups (Units shown are pmol/min/mg protein. Male cortex = 15.63 ± 0.90; female cortex = 10.91 ± 0.57; male medulla = 16.09 ± 1.12; female medulla = 10.20 ± 0.45), max OCR (male cortex = 43.39 ± 2.23; female cortex = 44.34 ± 2.93; male medulla = 51.23 ± 2.57; female medulla = 43.85 ± 2.20), and leak OCR (male cortex = 12.03 ± 1.03; female cortex = 9.76 ± 0.58; male medulla = 14.23 ± 1.14; female medulla = 9.44 ± 0.64). Interestingly, when fresh isolated renal mitochondria were placed into the succinate buffer, significant sex-related discrepancies in respiration were absent.

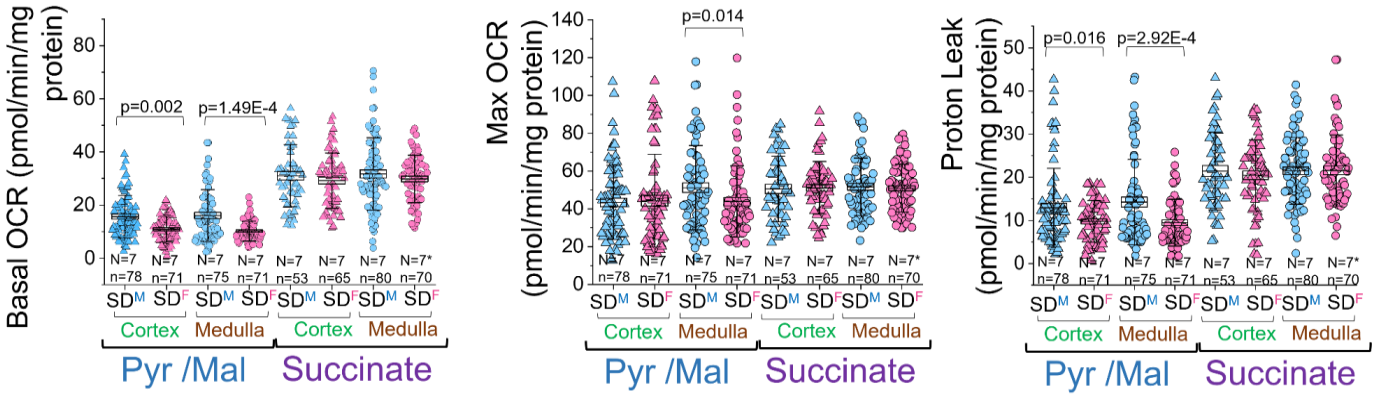

Figure 14. Differential substrate feeding of isolated renal mitochondria from male and female cortex and medulla. N values represent the number of biological replicates. The *n*-value represents technical replicates. *P*-values with statistical significance are displayed. Data were analyzed with 3-way ANOVA and the Holm-Sidak post-hoc test.

Differentiation of the expression of respiration-linked genes in male and female renal mitochondria.

There are a plethora of proteins which make up the ETC and contribute to the process of oxidative phosphorylation. Through respirometry, we were able to stimulate complexes I and II, but needed to further investigate the ETC to identify other segments which could be contributing to the observed sex-related discrepancies in respiration. To accomplish this, qPCR was performed as described in **Protocol 2.07** to analyze the mRNA levels of the proteins produced by the genes *Atp5f1a,* which codes for ATP synthase or complex V in the ETC, as well as *Cox4i1* and *Cycs,* which encode for complex IV and cytochrome *c*, respectively, and data are displayed in **Figure 15.** Cytochrome C is an essential protein for the function of the electron transport chain, given its role in shuttling electrons from complex III to complex IV, and Pgc1-α affects respiration by increasing the number of mitochondria available to perform the function[52]. No significant differences were observed in the mRNA levels from the *Atp5f1a*, *Cox4i1,* or *Ppargc1a* genes, however, the expression level of the transcripts from the *Cycs* gene were significantly higher in both the cortex and medulla of males as compared to females (Units displayed as fold change/male average. Male cortex = 1.0 ± 0.24; female cortex = 0.40 ± 0.09; male medulla = 1 ± 0.15; female medulla = 0.40 ± 0.11).

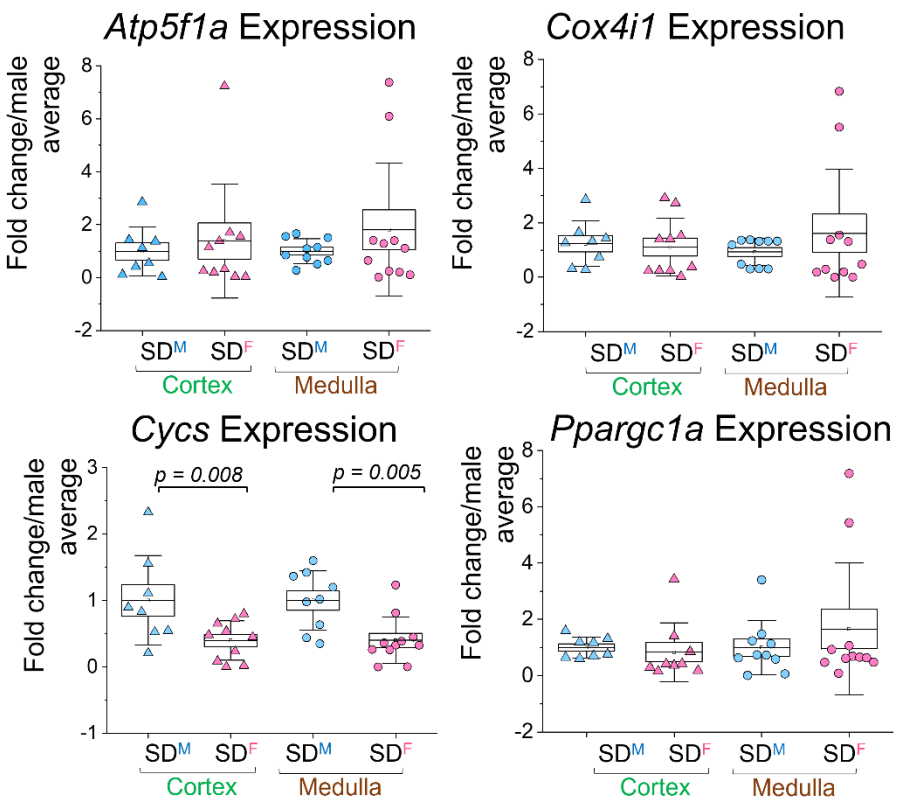

Figure 15. Respiratory gene mRNA expression. qPCR was performed on genes *Atp5f1a*, *Cox4i1, Cycs, and PparGc1a.* Data points each represent one biological replicate. Data were analyzed with 2-way ANOVA and the Holm-Sidak post-hoc test.

Quantification of mitochondrial membrane potential and reactive oxygen species production in isolated renal mitochondria.

The ETC has obvious functions in the generation of ATP for the cell, but one byproduct of this process is the generation of a proton gradient between mitochondrial membranes. This gradient gives each mitochondrion a membrane potential, or Δψmito[51], therefore all live, healthy mitochondria have a Δψmito value, which can be measured using the fluorescent dye TMRM. The proton gradient, and thus membrane potential, is responsible for the generation of ADP from ATP by Complex V; for this reason, discrepancies in Δψmito can be indicative of differences in mitochondrial bioenergetics[52]. We observed that the isolated mitochondria from renal medullae displayed overall higher levels of Δψmito than did cortices in both males and females (Units

displayed as au/mg protein. Male cortex = 92.87 ± 3.80; female cortex = 102.76 ± 5.51; male medulla = 162.02 ± 8.77; female medulla = 238.05 ± 12.38), as displayed in **Figure 16**. Female medullary mitochondria also displayed significantly higher Δψmito compared to the male medullary mitochondria.

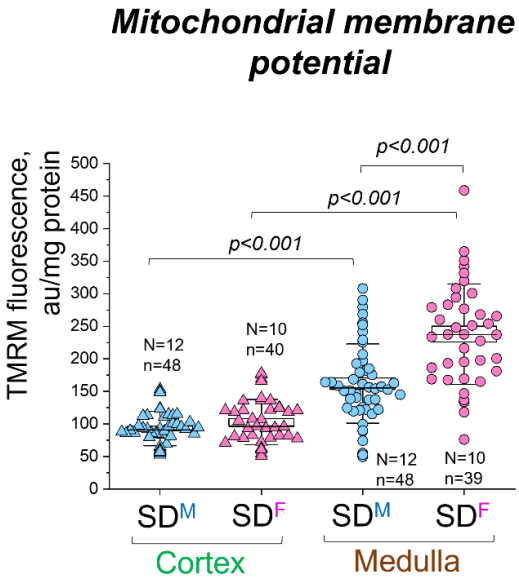

Figure 16. Measurement of mitochondrial membrane potential from male and female cortex and medulla. N represents the number of biological replicates, and *n* represents the number of technical replicates. Data were analyzed with 2-way ANOVA and the Holm-Sidak post-hoc test.

Assessment of mitochondrial respiration and dynamics-related proteins via Western blot in isolated renal mitochondria.

Mitochondrial fusion state often correlates with respiration[52]. In order to determine whether the upregulation in male mitochondrial oxygen consumption we observed was due to fusion levels, Western blots were performed to measure the expression of the proteins MFN2 and OPA1, both of which are integral for the mitochondrial fusion process. MFN2 expression was higher in male isolated mitochondria from both cortex and medulla regions, compared to the expressions in females (Units displayed as au/mg protein. Male cortex = 92.87 ± 3.80; female cortex = 102.76 ± 5.51; male medulla = 162.02 ± 8.77; female medulla = 238.05 ± 12.38), as shown in **Figure 17**. OPA1 expression in the cortex and medulla of males was not significantly different than in the mitochondria isolated from female kidney regions; however, the OPA1 expression in female

cortex groups was much lower than in female medulla groups (Units displayed as au/mg protein. Female cortex = 0.93 ± 0.07; female medulla 0.73 ± 0.05).

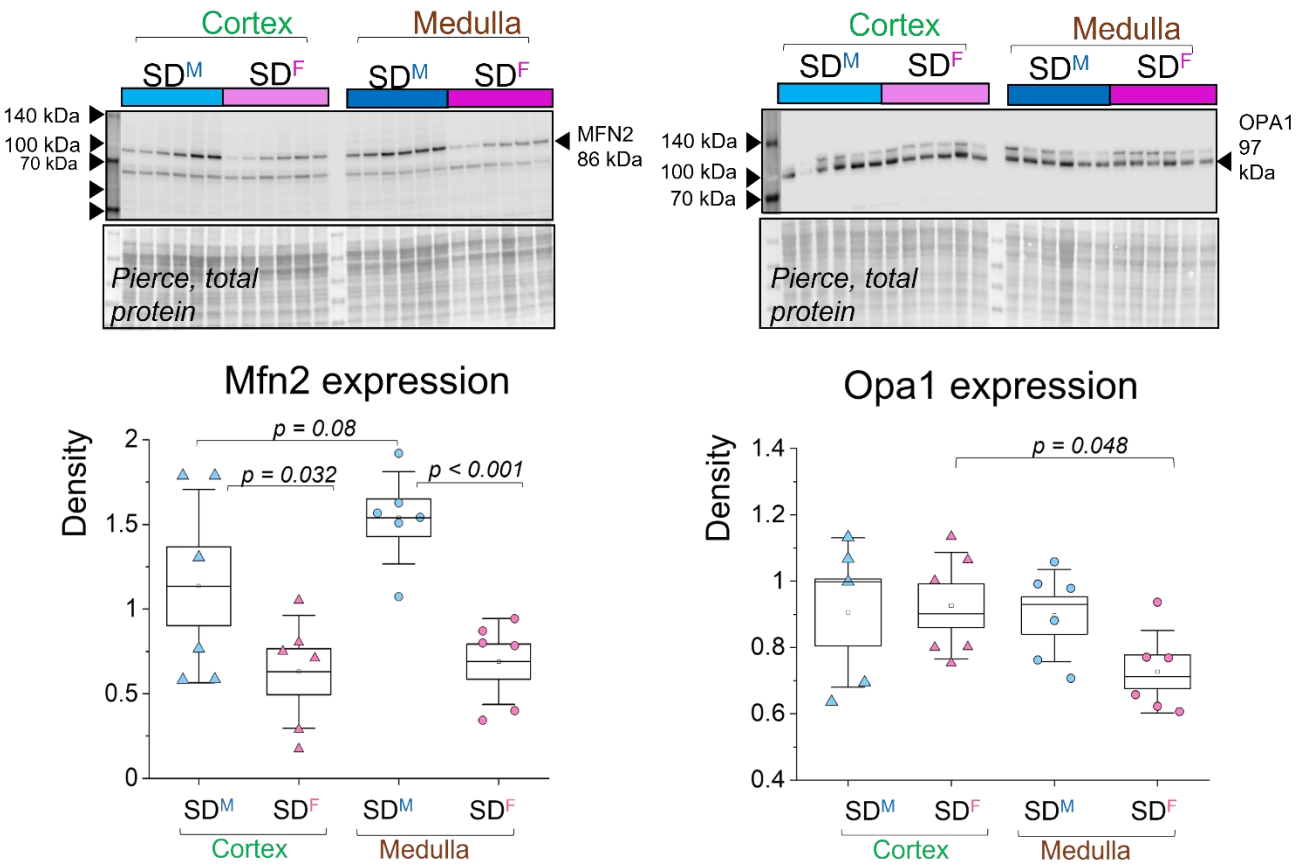

Figure 17. Western blots and analyses of fusion proteins MFN2 and OPA1. Images were obtained with a Li-Cor Odyssey XF system, and densitometry was performed using FIJI software. Data points each represent one biological replicate. Data were analyzed with 2-way ANOVA and the Holm-Sidak post-hoc test.

Size, density, number, and health of isolated renal mitochondria.

We observed sexual dimorphisms in the expression levels of fusion protein Mfn2, thus the next logical experiment was to visualize and analyze mitochondria to further elucidate whether

changes in fusion state were responsible for differences in respiration. This was done using transmission electron microscopy. Proximal tubule cells were used for analysis to represent the cortical fraction of the kidney as they comprise the largest portion of the renal cortex [28804120]. Analysis of density, being used as a crude indicator of mitochondrial health, revealed that male mitochondria were significantly more dense than the female group (male = 42.58 au ± 0.57; female = 39.30 au ± .05) . Male mitochondria were also smaller in area (male mean = 0.29 μm^2 ± .01; female = 0.38 μm^2 ± 0.01) and more numerous per field (male = 44.36 mitochondria/field ± 1.91; female = 34.94 mitochondria/field ± 1.93) . Notably, despite differences in morphology, both male and female mitochondria displayed nearly identical health scores. Representative images are shown in **Figure 18**, and quantitative analyses of the identified parameters are displayed in **Figure 19.**

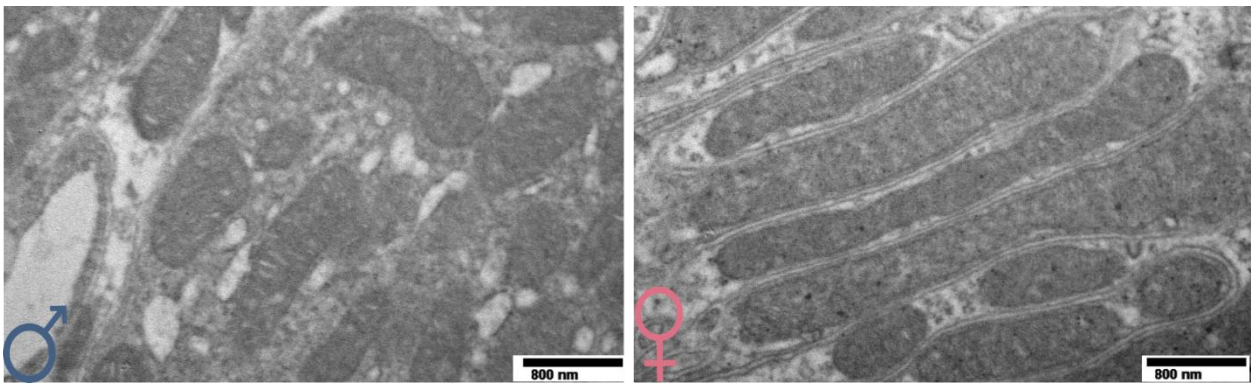

Figure 18. A representative image set of male and female mitochondria from renal proximal tubules. Images were obtained with a JEOL 1010 transmission electron microscope set to 80 kV. Images are displayed at 20000x magnification.

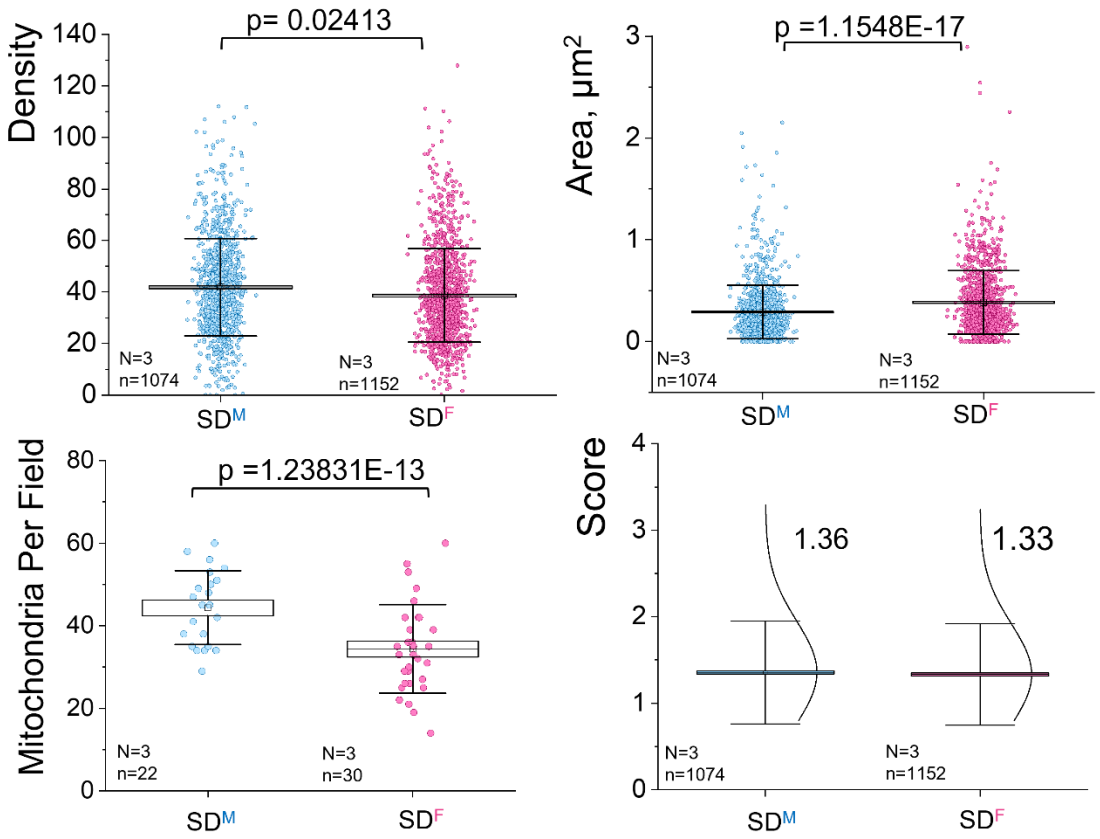

Figure 19. Electron microscopic analyses of isolated proximal tubular mitochondria in males and females. Data were analyzed with 1-way ANOVA and the Holm-Sidak post-hoc test. N represents the number of animals analyzed. The *n*-value represents the number of mitochondria analyzed for density, area, and score; *n*-value represents the number of fields of view analyzed for number of mitochondria.

Discussion for Chapter 3

Overall, the results obtained in Chapter 3 showed that male mitochondria had higher overall respiration compared to female mitochondria. These differences were apparent in a Complex I-

stimulating buffer, but ameliorated in a Complex II-stimulating buffer. qPCR showed that the expression level of cytochrome *c* was altered between sexes, being higher in males in both cortex and medulla. Membrane potential was interestingly higher in females than in males, particularly in the medulla. When the expression of fusion proteins MFN2 and OPA1 was measured, MFN2 displayed higher expression in males. Electron microscopy analysis showed that male mitochondria were in fact smaller and more numerous, which could point to a less fused phenotype than in the females. The relative health scores as determined by electron microscopy were nearly identical between sexes.

In our hands, isolated male renal mitochondria displayed overall higher levels of respiration. The trend for most other organs in the body is for male mitochondria to display lower levels of respiration[50], which is the opposite trend. It is important to note that the kidney, unlike other organs, has metabolic rates that are directly influenced by the rate of renal blood flow[82]. The cortex has a much higher oxygenation level than the medulla, which likely accounts for the higher overall levels of respiration in cortical mitochondria compared to those that are medullary[15,16]. This could also be one explaining factor for the sex-related discrepancy in observed mitochondrial bioenergetics, and could also account for the trend of female renal mitochondria having higher levels of membrane potential and ROS production, which appear to be unique to the kidney - males have a higher metabolic load, which could account for their increases in respiration[83]. This could be further tested by matching GFR from males and females to isolated mitochondria and respirometry results as a future experiment.

Regarding oxygen consumption, the fact that sex-related discrepancies only appear in the Complex I-stimulating malate/pyruvate substrate buffer and not the Complex II-stimulating succinate substrate buffer suggests that the observed sex-related discrepancies in oxygen

consumption may arise from Complex I. This suggests that regardless of the contributions of Complex I to respiratory efficiency, there are other factors both in and outside the ETC which could account for the discrepancy in disease incidence and severity between sexes.

Other studies which examined the energetics in renal mitochondria have shown reduction in the renal expression of ETC Complexes in diseases such as diabetic nephropathy and acute kidney injury[84-86]. Our previous studies in salt-sensitive hypertension showed that the respiration rates of glomerular mitochondria were depressed in rats fed a HS diet, which develop profound renal damage[32]. Doe *et al.* found reductions in OXPHOS activity in the mitochondria of skeletal muscles of mice afflicted by CKD, though interestingly no measurements of renal mitochondrial OXPHOS activity were made[87]. Smith *et al.* measured the activity of OXPHOS components in patients with CKD, and reported that Complex IV activity was significantly reduced, though once again the isolated mitochondria did not come from the kidney, and instead came from peripheral blood mononuclear cells[60]. Notably, in the same study the authors observed that although Complex IV activity was lower in CKD patients, the protein expression for the same Complex was significantly higher, likely indicative of a compensatory mechanism[60]. This poses future directions for our experiments: it would be beneficial to measure the expression of genes and proteins involved in OXPHOS, as well as the activities of each Complex to see if the trend holds true in the kidney: the next step would be to test whether higher expression levels correlate with reduced activity in disease states, and, if so, whether this holds true in healthy states and across sexes.

Our studies did address the key pieces of this puzzle by examining the expression of several respiratory genes involved with the ETC. For instance, there were no differences observed in the expression of the *Atp5f1a* or *Cox4i1* genes, but it is important to note that levels of gene expression do not necessarily correlate directly with levels of protein expression[88] or activity, as noted above. Furthermore, *Atp5f1a* or *Cox4i1* comprise a small section of the number of genes

which are code for all the ETC complexes, so they do not represent the entire picture[51]. The mRNA expression level of cytochrome *c*, which is critical in shuttling electrons from Complex III to Complex IV in the ETC[51], was shown to be higher in males. As reported previously, we found that OCR levels were also higher in male renal mitochondria, and higher expression of *Cycs* may partially explain this phenomenon. Released cytochrome *c* is also used as a way to measure apoptosis; it has recently been suggested that measurement of plasma or urinary levels of cytochrome *c* could be used to assess renal damage[89,90]. This allows us to speculate that the increase in *Cycs* gene expression in males could be used as an early indicator for the severity of renal disease observed later in life, and more studies measuring the protein expression as well as the urinary and plasma levels of cytochrome *c* need to be performed in order to assess this intriguing correlation. This experiment, in addition to the measurements of OXPHOS protein expression and activity in the kidney proposed above, would provide a clearer picture of how mitochondrial respiratory chain function *in the kidney* relates to disease, and would expand upon the limited knowledge of the dimorphisms in function between males and females in a healthy state.

Our analysis of Western blots for fusion protein expression posed a seemingly contradictory point to the respiratory data: generally, fusion state is correlated with respiration[55,91]. And, despite increases in MFN2 protein level in males, the analysis of our electron micrographs, show the opposite of what the expression would indicate: shorter, rounder mitochondria belonging to the males, and the females displaying the more fused phenotype. This could be due to a number of factors, the first being that protein expression does not necessarily correlate with protein activity[92,93]. There are also a variety of other factors which influence mitochondrial dynamics, such as the proteins DRP1, the prime regulator of mitochondrial fission[94], and PGC1-α[52]. DRP1 has been shown to be upregulated in the kidney in renal disease states such as AKI[86,95] and diabetic

nephropathy[96]. These alterations are concurrent with downregulation of both PGC1-α and the fusion protein MFN2[86,97,98]. Our studies showed no changes in gene expression level of *Ppargc1a*, but electron micrograph analysis did show significantly higher numbers of mitochondria in males, which allows us to speculate that biogenesis is being upregulated.

Changes in dynamics are also associated with renal disease. Notably, a low fusion state caused by loss of either mitofusins 1 or 2, or OPA1 causes mitochondrial dysfunction[99], and is seen in renal disease states such as diabetic nephropathy, and AKI[86,100,101]. Our data showed lower expression of OPA1 in females, which is interesting to note as it appears to contradict the phenotype of the mitochondria analyzed *via* electron microscopy as well as the respirometry data. It should be noted that though fusion state can be indicative of respiratory efficiency, there are many cases in disease states where mitochondrial dynamics contraindicate this: long, highly fused mitochondria can be senescent, and have significantly reduced membrane potential over smaller but more active mitochondria[102]**,** and both abundance and lack of fission is seen in multiple disease states[103-105]. Smith *et al.* showed higher levels of OPA1 protein expression in a human tubular cell model of CKD as compared to healthy ones[106], additionally highlighting the dichotomy of mitochondrial dynamic states with disease. Further studies regarding mitochondrial dynamics and bioenergetics are needed to contextualize our data. Experiments such as measuring the protein expression of MFN1, PGC1-α, and DRP1, quantifying mitochondrial biogenesis, and analyzing electron micrographs from other cortical cell types such as glomeruli, as well as medullary regions, are needed to elucidate the discrepancies observed between sexes and clarify whether these changes are contributing to the sexual dimorphism observed in renal disease.

CHAPTER 4 - Oxidative stress and calcium uptake in renal mitochondria

Introduction

The primary product thought about in regard to oxidative phosphorylation is ATP; however, there are many other byproducts of this reaction which are of high importance to the function of the mitochondrion, the cell, and the organism in general. One key group of molecules that is generated during oxidative phosphorylation is reactive oxygen species (ROS). Molecules that constitute ROS can range from harmful to beneficial, and include superoxide, hydrogen peroxide, singlet oxygens, hydroxyl radicals, alkoxyl radicals, ozone, nitric oxide, and others[107]. When electrons are shuttled during various steps of the ETC, electrons leak through the mitochondrial inner membrane from donor centers within the Complexes themselves (such as 2-oxoacid dehydrogenase complexes located in Complex I) as well as from other molecules such as ubiquinone and ubiquinol[108,109]. A schematic displaying ROS production is shown in **Figure 20.** ROS are produced as a byproduct during routine function of the ETC, so naturally, their production rate increases during times of increased respiration in the body, such as exercise[109,110].

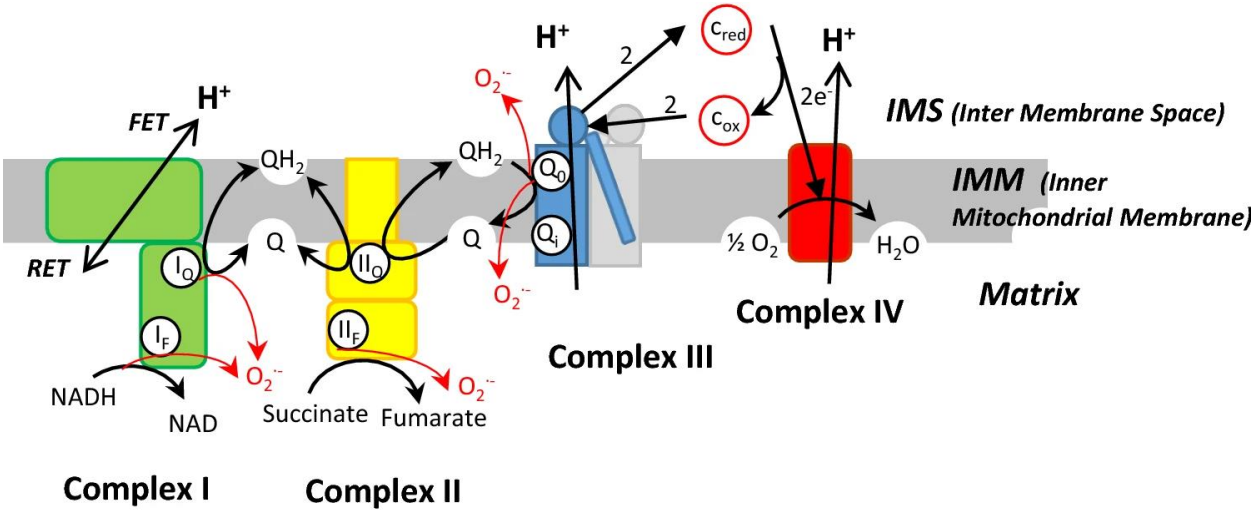

Figure 20. Sites of ROS production by the electron transport chain. Used with permission from Mazat, JP., Devin, A. & Ransac, S. Modelling mitochondrial ROS production by the respiratory chain. Cell. Mol. Life Sci. 77, 455–465 (2020). https://doi.org/10.1007/s00018-019-03381-1

Low levels of ROS are necessary for a plethora of biological signaling processes. These range from cell-signaling functions such as proliferation, immune functions, including both host defense as well as termination of inflammatory processes, to regulatory functions in nutrient-sensing and aging pathways[58,111]. Despite many known and yet to be discovered roles in normal physiology, ROS have also been implicated in a number of disease states: renal, neurological and cardiovascular diseases as well as cancers have been shown to have ROS involvement [58,111]. These links with disease are caused by the ability of ROS to interact with a variety of biological molecules such as DNA, lipids, and proteins, and usually occur when ROS are produced in aberrant, high levels. The cell has many systems in place to process ROS and reduce the negative effects thereof; these include antioxidant enzymes such as superoxide dismutases and glutathione peroxidases[61].

The kidney, due to its high energetic demand, has some of the highest concentrations of mitochondria in the body[52]. Similarly, the proximal tubules have the highest mitochondrial content in the kidney, and thus are particularly susceptible to mitochondrial-induced oxidative stress[52,112,113]. Various renal diseases are associated with excess production of ROS, including CKD, diabetic nephropathy, AKI, and salt-sensitive hypertension[60,61,114-117]. ROS-related damage is caused both directly by free radicals, as well as by alterations of biological molecules such as proteins, which are susceptible to oxidation and thus differentiation of structure or function[61]. Some pathways, such as nitric oxide synthase signaling, are pathologically downregulated in the presence of high levels of oxidative stress, as is seen in salt-sensitive hypertension[116,117]

.

Oxidative stress is linked with the ETC function of the mitochondria; however, the ETC is not the only link between mitochondria and ROS. One major cellular signaling pathway involved with ROS is calcium handling. Calcium levels in the cell are critical for a variety of signaling cascades,

making the calcium ion one of the most important messaging molecules in the cell[118]. Calcium signaling is involved in the modification of proteins; binding of calcium to proteins can cause conformational changes and thus activation or inhibition of function[118]. Changes in cellular calcium concentration are also involved in the contraction of muscles, secretion of hormones, initiation of apoptosis, and other functions[118,119]. Mitochondria are an important mediator in calcium signaling. The MCU protein complex allows mitochondria to selectively uptake calcium in an electrogenic fashion, which occurs generally as the cytosolic concentration of calcium increases, in order to maintain a homeostatic balance[118]. Mechanistically, involvement with ROS comes in part *via* excess of mitochondrial calcium uptake; disruption to cellular and mitochondrial calcium handling can cause opening of the mPTP, thus releasing ROS and calcium and inducing mPTP opening in adjacent mitochondria--this is termed ROS-induced ROS release[120-123].

When calcium homeostasis is disrupted and the intramitochondrial concentration of calcium becomes excessive, the mitochondrial permeability transition pore (mPTP) opens, which leads to an efflux of both calcium and ROS[124,125]. The mPTP is a nonspecific protein with an as-of-yet undetermined structure. The only confirmed component is cyclophilin D, which sensitizes the pore complex to inhibition *via* cyclosporin A[126,127]. Many other components are still being debated, though there is evidence for the voltage-gated anion channel, adenine nucleotide translocator, and a mitochondrial phosphate carrier as parts of the mPTP[124,128,129]. Despite the gaps in knowledge regarding its structure, the mPTP has a variety of defined functions, primarily regarding damage and apoptosis[125,130]. In the kidney, mPTP opening can be used to reduce the mitochondrial membrane potential, which increases oxygen consumption and therefore reduces ROS generation[131]. In excess, however, renal mPTP opening is linked with the activation of apoptotic pathways, initiation of calcium crystallization, and the transition from AKI to CKD[61,125] .

There is a strong correlation between calcium overload and ROS generation, due to its discussed roles in mPTP opening. Quantification of both ROS levels and mitochondrial calcium would help elucidate the mechanism by which mitochondrial dysfunction, and thus renal damage, occurs. Since many renal diseases are linked with excess oxidative stress, the experiments in this chapter were designed to provide insight into whether the observed sexual dimorphisms in renal disease are caused by dysfunction in mitochondrial ROS handling, especially in relation to mitochondrial calcium-induced ROS production.

Chapter 4 Results

Quantification of reactive oxygen species in isolated renal mitochondria.

One of the main forms of reactive oxygen species (ROS) produced in mitochondria is mitochondrial superoxide, which is formed from the leak of electrons from the ETC. The physiological half-life of superoxide is relatively short, however, as the enzyme superoxide dismutase rapidly converts it to hydrogen peroxide. We observed that the levels of hydrogen peroxide produced in female mitochondria from both cortex and medulla regions were significantly higher than those produced by the males for each region (Units displayed as au/mg protein. Male cortex = 69.94E3 ± 1.71E3; female cortex = 99.44E3 ± 3.06E3; male medulla = 60.61E3 ± 2.30E3; female medulla = 113.37E3 ± 5.43E3). Additionally, hydrogen peroxide levels were higher in the medulla than in the cortex for females (numerical values displayed above). Graphical representations of these data are shown below in **Figure 21.**

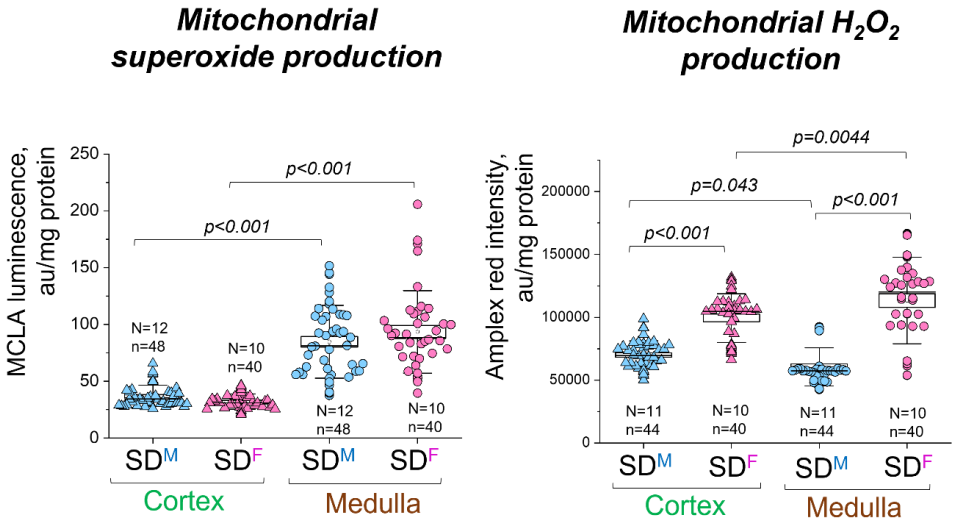

Figure 21. Mitochondrial superoxide and hydrogen peroxide production in isolated renal mitochondria from male and female cortex and medulla. N represents the number of animals used. The *n*-values represent technical replicates. Data were analyzed with two-way ANOVA and the Holm-Sidak post-hoc test.

Measurement of antioxidant capacity in male and female renal tissues.

Antioxidant systems are one of the cell's main defenses against oxidative stress. In order to examine the ROS-handling capabilities of male and female renal mitochondria, an antioxidant capacity assay as described in **Protocol 2.13** was performed. Here, male medulla showed a significantly higher level of antioxidant capacity over female medulla (Units displayed as mM/mg tissue. Male cortex = 0.21 ± 0.03 ; female cortex = 0.16 ± 0.02; male medulla = 0.20 ± 0.04; female medulla = 0.08 ± 0.02). Though not significant, the cortex shows a similar trend of males having increased antioxidant capacity over females, and female cortex has increased capacity compared to female medulla (numerical data displayed above).

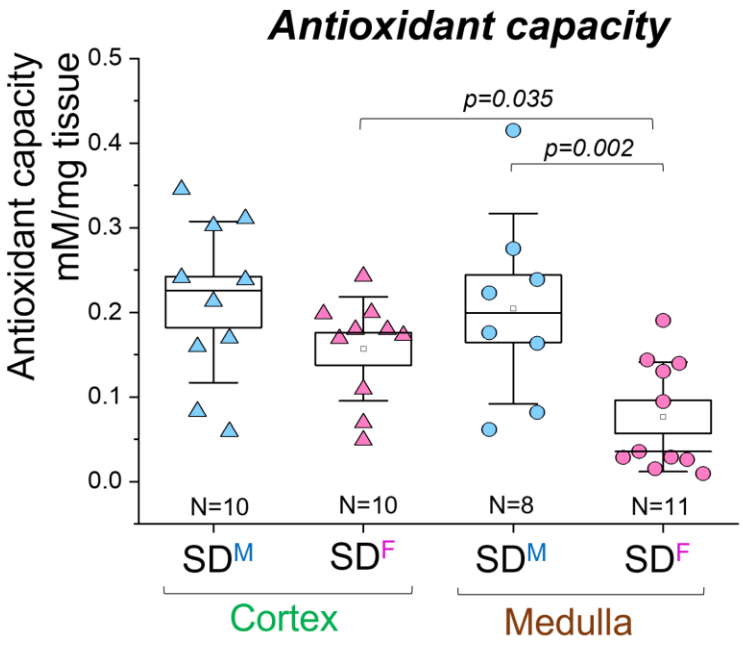

Figure 22. Antioxidant capacity in male and female kidneys. N represents the number of animals used (biological replicates). Data were analyzed with two-way ANOVA and the Holm-Sidak post-hoc test.

Activity of superoxide dismutase in isolated renal mitochondria.

To help elucidate why female mitochondria displayed higher levels of ROS, a functional assay was performed for superoxide dismutase (SOD), the enzyme responsible for converting superoxide into hydrogen peroxide. The total SOD activity (SODs 1, 2, and 3) was significantly higher in female cortices as compared to males (Units displayed as U/uL. Male cortex = 273.63 ± 36.14 ; female cortex = 422.04 ± 22.29), as displayed in **Figure 22**. There was no observed difference in mitochondria isolated from renal medullae (male medulla = 199.40 ± 38.53; female medulla = 169.65 ± 17.92).

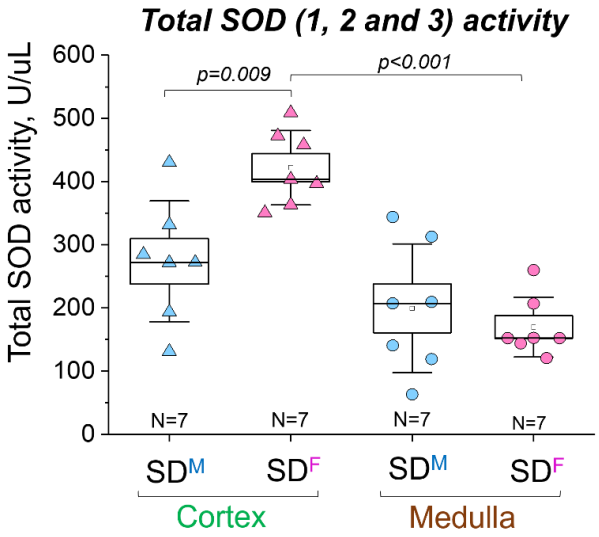

Figure 23. Total SOD activity of male and female renal tissues. Each data point represents one biological replicate. Data were analyzed with two-way ANOVA and the Holm-Sidak post-hoc test.

Calcium uptake of isolated renal mitochondria.

Calcium uptake and the subsequent opening of the mPTP and ROS efflux are implicated in a variety of renal dysfunctions such as AKI, CKD, salt-sensitive hypertension, and diabetic nephropathy[61]. As is the case with most of the other mitochondrial functions, little is known regarding the sexual dimorphism of calcium handling in the kidney. In order to elucidate the trends in healthy individuals, we performed a series of experiments designed to measure the uptake of calcium in renal mitochondria, as well as the opening of the mPTP. Freshly isolated renal mitochondria from male and female cortex and medulla were loaded with Calcium Green dye. Fluorescence was measured at baseline, and after serial injections of calcium chloride solution. As displayed in **Figure 24**, the amount of calcium taken up by the medullary mitochondria was significantly higher in both males and females (Units displayed as calcium uptake per mg tissue. Male cortex = 15.33 ± 0.83 ; female cortex =18.24 ± 1.20; male medulla = 26.21 ± 2.14; female

medulla = 26.32 ± 2.78) as compared to the cortical mitochondria. Notably, there was no significant difference in the amount of Ca uptake between males and females in either region of the kidney.

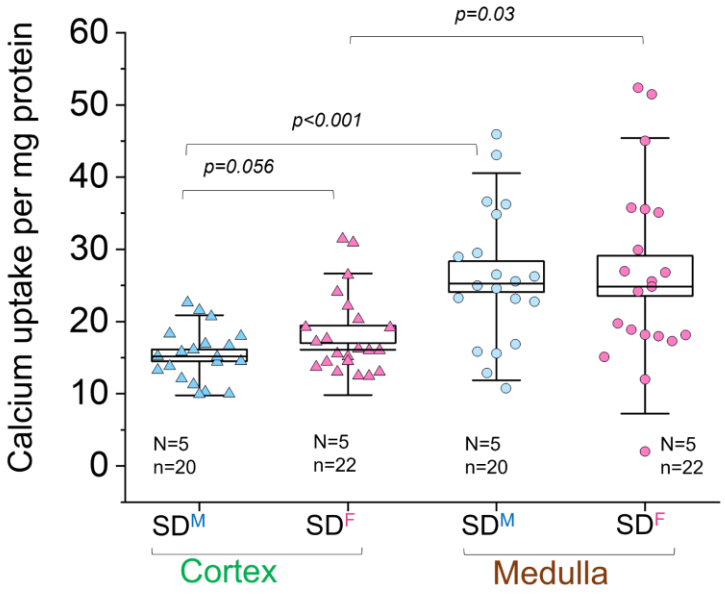

Figure 24. Calcium uptake in isolated mitochondria from male and female renal cortex and medulla. N value represents biological replicates. The *n*-values represent technical replicates. Data were analyzed with 2-way ANOVA and the Holm-Sidak post-hoc test.

As noted above, the amount of calcium uptake was not the only piece of quantifiable data which comes from this experiment. In each kidney region, the number of injections at which the mitochondrial permeability transition pore opens was also measured. Overall, medullary mitochondria had earlier mPTP openings in both males and females (Units displayed as calcium uptake per mg tissue. Male cortex = 15.33 ± 0.83 ; female cortex =18.24 ± 1.20; male medulla = 26.21 ± 2.14; female medulla = 26.32 ± 2.78). Female mitochondria, however, displayed a significantly earlier mPTP opening in both the cortex and medulla groups (Units displayed as injection number at which mPTP opened. Male cortex = 10.25 ± 0.21 ; female cortex = 9.05 ± 0.18; male medulla = 9.25 ± 0.35; female medulla = 8.18 ± 0.13), as can be seen in **Figure 25.**

Figure 25. Injection number at which mPTP opened in male and female cortical and medullary mitochondria. N-value represents biological replicates. The *n*-values represent technical replicates. Data were analyzed with 2-way ANOVA and the Holm-Sidak post-hoc test.

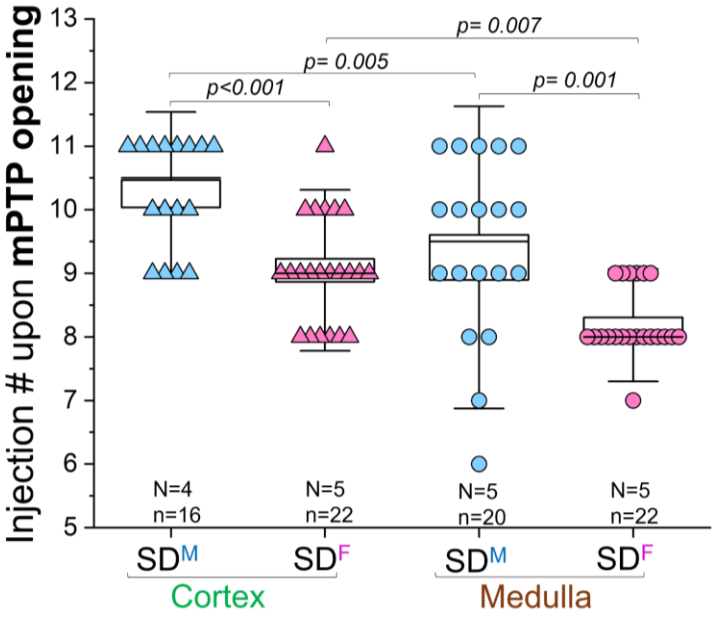

Discussion for Chapter 4

We report that female renal mitochondria had higher levels of ROS production in both cortex and medulla compared to those from males. In line with this, female kidneys also displayed lower levels of **total** antioxidant capacity in both the renal cortex and medulla. Surprisingly, SOD activity was higher in cortical tissues than in medullary, and higher from female cortical tissues than in those from the male cortex. No sexual dimorphisms were observed in SOD activity from medullary tissues, but expression of SOD2 in both cortical and medullary mitochondria could be analyzed to examine whether sex-related discrepancies exist solely in mitochondrial superoxide dismutase activity. Calcium uptake was higher in medullary mitochondria than in cortical, but no sex-specific trends were found. The opening of the mPTP was significantly earlier in female mitochondria as compared to males in both cortex and medulla, and earlier in medullary mitochondria as compared to cortical.

The higher levels of ROS observed in female renal mitochondria are contrary to the trends observed in most other organs in the body. For example, in the heart, brain, liver, and skeletal muscle, female mitochondria have been demonstrated to produce fewer ROS than in males[40,42-44,50,132]. This poses an interesting contradiction; high levels of oxidative stress are linked to many renal disease states such as ischemia-reperfusion AKI, CKD, salt-sensitive hypertension, and diabetic nephropathy[7,60,61,117,133-135], where females generally have better clinical prognoses[6,7,134,136]. Low levels of oxidative stress are known to activate protective mitophagic pathways[62], which allows us to speculate that the higher levels of ROS observed in female renal mitochondria may be enacting similar protective pathways, due to the lower incidence of renal disease observed in premenopausal women, as described above.

The cellular mechanisms which counteract oxidative stress are referred to as antioxidant systems. Female renal mitochondria displayed lower **total** antioxidant capacity as compared to males, which is in line with the ROS production data. An interesting discrepancy exists between these data and the elevated SOD activity shown in females. One experiment to help clarify non-SOD antioxidant system involvement in ROS handling between sexes and kidney regions would be to perform an enzymatic activity assay for glutathione peroxidase 4, a protein which catalyzes the reduction of peroxides and has been shown to have an anti-inflammatory role[137].

ROS levels have also been linked with the opening of the mPTP; high levels of intramitochondrial calcium can cause backwards transport of electrons, and opening of the mPTP to allow efflux of ROS and calcium restores the mitochondrial membrane potential and thus the forward flow of electrons through the ETC[130]. Mechanisms such as this prevent the formation of more ROS by

increasing consumption of oxygen, but depending on the amount of ROS released by the mPTP, the cell may undergo harmful or apoptotic pathways[52,125,130].

Our results show similar levels of calcium uptake in males and females, but significantly earlier opening of the mPTP in females. This is a key set of data which suggests that female renal mitochondria are more sensitive to oxidative stress. The unique oxygen metabolism caused by the complex architecture of the kidney, paired with the data we have collected so far allow us to speculate that perhaps renal mitochondria behave differently than in other areas of the body. If true, this could contribute to why the sex-specific trends in ROS levels we observed in renal mitochondria differ from the trends observed in many other organs[40,42-44,50,132]. Despite producing more ROS, which are generally considered pathogenic, perhaps the renal mitochondrial ROS levels are activating protective pathways earlier in females, as opposed to male mitochondria. Pathways known to be affected by ROS signaling which may be protective include activation of the HIF1-α pathway to help restore redox homeostasis, various PTEN cascades for cell growth, and NRF2-mediated antioxidant protein synthesis[138-142]. Experiments which could help clarify the downstream signaling events include the analysis of the pathways mentioned above in the young, healthy stage that our model represents. To further clarify the involvement of the mPTP, experiments to test the activation of apoptotic cascades, such as the cytochrome *c*-mediated activation of procaspase-9 and -3, to compare males and females could be performed[143]. Interestingly, not all cytosolic release of cytochrome *c* is guaranteed to induce apoptosis. Several studies suggest that some levels of released cytochrome *c* are responsible for vital cellular processes such as proliferation and differentiation[144-148]. Furthermore, analyzing the lipid peroxidation profiles of these renal cells would be beneficial in order to examine how much of the generated ROS may be pathological in nature; lipid peroxidation is considered a hallmark of the AKI-to-CKD transition, and is also linked with diabetic nephropathy and glomerulosclerosis[61,149].

Evaluation of the levels of endothelial nitric oxide synthase (eNOS) activity within male and female kidneys could also reveal a pathway by which ROS are helping or hindering--high levels of ROS are known to inhibit nitric oxide signaling, which is one of the mechanisms by which salt-sensitive hypertension develops[133,150]. Examination of nNOS activity or expression could also be beneficial, as nNOS has been shown to produce several ROS[151,152 153]. The measurement of NO levels in both the cortex and medulla could also be performed to contextualize results obtained from measuring ENOS activity Overall, more experiments are needed to determine whether the controversially high levels of ROS produced by female renal mitochondria are contributing to renoprotective mechanisms.

CHAPTER 5 - Final conclusions, discussion, and future directions

Given the large contributions of mitochondria to renal function[52], and the number of renal diseases linked with renal mitochondrial dysfunction[31-39,52], it is imperative to understand the baseline bioenergetic parameters of the organelles. The sex-specific trends observed in renal diseases further prompt investigation into the sexual dimorphisms of baseline renal mitochondrial functions, to observe is perhaps impaired mitochondrial function in males prior to the onset of diseases is in part responsible for the more severe clinical manifestations of renal pathology.

In Chapter 3, the process of oxidative phosphorylation as well as the respiratory rates of renal mitochondria were examined. This was done as a baseline measurement of mitochondrial function, as oxidative phosphorylation is perhaps the most impactful mitochondrial function across the body and in the kidney[51,52]. It was found that, contrary to what is seen in many other organ systems[50], female mitochondria exhibit lower rate of oxygen consumption, as well as lower expression of the *Cycs* gene, as compared to males. The differential substrate feeding respirometry results allowed us to speculate that ETC Complex I is at least partially responsible for the sex-related discrepancies in respiration. It is important to note, however, that overall levels of respiration were lower in males and females in the pyruvate/malate buffer as compared to the pyruvate/malate/succinate buffer. This suggests that although there is a sexual dimorphism in Complex I function, it is not the only portion of the ETC responsible for the differences we observed in respiration between sexes. Furthermore, it is important to take into consideration that isolated mitochondria used in our experiments lack the physiological context of the cellular milieu; methods for measuring respiratory flux using intact, permeable cells are routinely employed in cultured cells[154]. Using this method for respirometry in tissue homogenates or isolated nephron segments may give us more physiologically relevant data, as there are many cytosolic and

nuclear factors which interact with the mitochondrion to affect cellular signaling pathways, including those related to respiratory demand and regulating oxidative stress[155-159].

Mitochondria from the medullae of females displayed higher mitochondrial membrane potential, which was not necessarily expected given the fact that membrane potential is coupled with respiratory rate under normal physiological conditions, and female mitochondria in both renal regions displayed lower respiratory rates than males[52,160]. Both higher membrane potential in female mitochondria as well as lower respiration compared to males are contrary to what is seen in sex-specifc mitochondrial trends from most other organ systems, such as the heart, liver, and skeletal muscle[45,46,50,161]. Presented with this apparent controversy, it is necessary to go back to the distinct oxygenation and vascular architecture of the kidney. Unlike all other organs in the body, whereby metabolic rate determines blood flow and oxygen consumption, the kidney's metabolism and oxygen consumption are directly influenced by the blood flowing through the organ[1,68,82]. Given the unique metabolic microenvironment of renal mitochondria, it is not surprising that the bioenergetics of renal mitochondria would differ from that of other organ systems.

Electron micrograph analysis of proximal tubular mitochondria showed that female mitochondria were more elongated and larger, though less dense than in males. This falls in line with what has been observed in hepatocytes and cardiomyocytes[45,161], though interestingly is not what would be expected in concordance with the respirometry data: generally, more fusion is indicative of higher oxygen consumption[50,162]. It should be noted, however, that it is possible that elongated mitochondria are senescent and display significantly reduced levels of oxidative phosphorylation activity, and this is not something that would be able to be detected from the analysis of an electron micrograph[102]. Given the fact that the analyzed organelles were from young, healthy animals, however, large numbers of senescent mitochondria in females does not seem likely.

Notably, increases to mitochondrial fusion are often seen both in healthy states, such as in times of higher cellular energy demand[52,162]. To expand on the data provided in this set of experiments, further analysis of mitochondria from other nephron segments are required in order to fully reconcile our findings. Though the proximal tubules make up a large portion of the renal cortex, in EM we assayed mitochondria isolated from all the cortical renal tissue altogether, which is likely a contributing factor to the observed discrepancies as different tubular segments could exhibit different trends[1]. Furthermore, mitochondrial size and scores should be assessed in medullary renal segments as well.

In Chapter 4, we sought to examine levels of oxidative stress in male and female renal mitochondria. Given that high levels of oxidative stress are implicated in a variety of renal diseases[61], investigation of ROS emission and antioxidant capacities prior to the onset of disease may provide context for the renoprotection observed in females. Our experiments displayed that mitochondria from female medulla produce higher levels of superoxide, and that both cortical and medullary mitochondria displayed hydrogen peroxide than male renal mitochondria. This is in accordance with the membrane potential data discussed above, as ROS are formed during oxidative phosphorylation, so mitochondrial membrane potential should normally correlate with formation of ROS[61,163]. Generally, however, female mitochondria have been shown to produce less ROS than in males[50].

Many other studies also show that females have higher antioxidant capacities than males, in part due to higher expression or activity of mitochondrial superoxide dismutase or glutathione peroxidases[41,43,44]. Our data showed that females have reduced antioxidant capacity in the kidney as well as lower superoxide dismutase activity, both trends of which oppose what has been demonstrated in other organs. Of the superoxide dismutase family, three isoforms exist which contribute to the total SOD activity that we reported in Chapter 4. A clearer picture of which isoforms are contributing to the results may be obtained by the measurement of the expression

of mitochondrial SOD2, as well as the cytosolic forms SOD1 and SOD3. In particular, loss of SOD2 has been demonstrated to lead to many kinds of renal injury, and its presence has been suggested as protective against oxidative stress[164,165]. Examination of SOD expression levels, particularly of SOD2, could assist in reconciling the higher total SOD activity observed in female renal mitochondria with the elevated ROS levels seen. Furthermore, superoxide dismutase is not the only antioxidant system present in the cell. As briefly discussed above, the glutathione peroxidase family, in particular GPX4, is responsible for the reduction of reactive oxygen species[137]. Reduction in GPX4 is associated with increases in oxidative stress, inflammation, and renal tubular cell death *via* ferroptosis[137,166,167]. GPX4 has recently been suggested as protective against ischemia-reperfusion AKI as well as renal fibrosis[168,169]. For its antioxidant and renoprotective functions, the analysis of GPX4 activity in renal tissues would provide valuable insight on the antioxidant pathways being enacted in renal cells, and help to further contextualize our antioxidant capacity data. Notably, we assayed for total antioxidant capacity in tissue lysates. This analyzed the total antioxidant capacity of the renal cells, but did not assess the specific capacity of the mitochondria; the assay could be repeated on isolated mitochondrial samples in order to determine what portion of the cell's antioxidant capacity is conveyed by the mitochondria. In summary, we have obtained information about the total antioxidant state of the cell, but not of the specific pathways which cause the differences in male and female kidneys.

The data discussed so far, taken together, align with female renal mitochondria behaving in ways which embody the opposite bioenergetic trends than in what is known about other organ systems. This poses a controversy primarily because the sexual dimorphism of renal diseases is in accordance with other pathologies, such as in cardiac dysfunction, liver failure, and in neurological disease: pre-menopausal females display protection from many diseases in and outside of the renal system[6,10,14,170-175]. This brings up questions regarding what could be driving the

renoprotection in females: high ROS levels and low antioxidant capacity are thought to be driving factors in the development of renal diseases such as AKI, CKD, diabetic nephropathy, and salt-sensitive hypertension[60,61,117]. Like many biological systems, however, a single molecule can be responsible for a variety of signaling events. Excess oxidative stress is associated with the development and exacerbation of many disease states, but lower levels of ROS are associated with increases in mitophagic signaling[62]. These increases in mitophagy can result in removal of dysfunctional mitochondria from the cell, or termination of an unhealthy cell *via* apoptosis in a controlled manner, both of which can function to prevent target organ damage[62]. By extrapolating from this, we can speculate that renal cells may have a higher threshold for beneficial ROS signaling as opposed to other organs, or that the high metabolic rate of the kidneys facilitates a higher degree of mitochondrial damage, which requires elevated levels of mitophagy.

A comprehensive review by Mitchell *et al.* suggests that renal disease stems from a three-part axis that includes mitochondria, oxidative stress, and inflammation, as shown in **Figure 26.** A large expansion to our study could involve the investigation of the inflammatory portion of this disease axis, including a plethora of experimental methods. For one, analysis of the inflammatory profiles of the experimental groups, both in kidney regions as well as systemically, *via* the use of a comprehensive cytokine profiling assay would provide insight as to which inflammatory pathways are upregulated between sexes, which may provide context for the respirometry and ROS-related datasets.

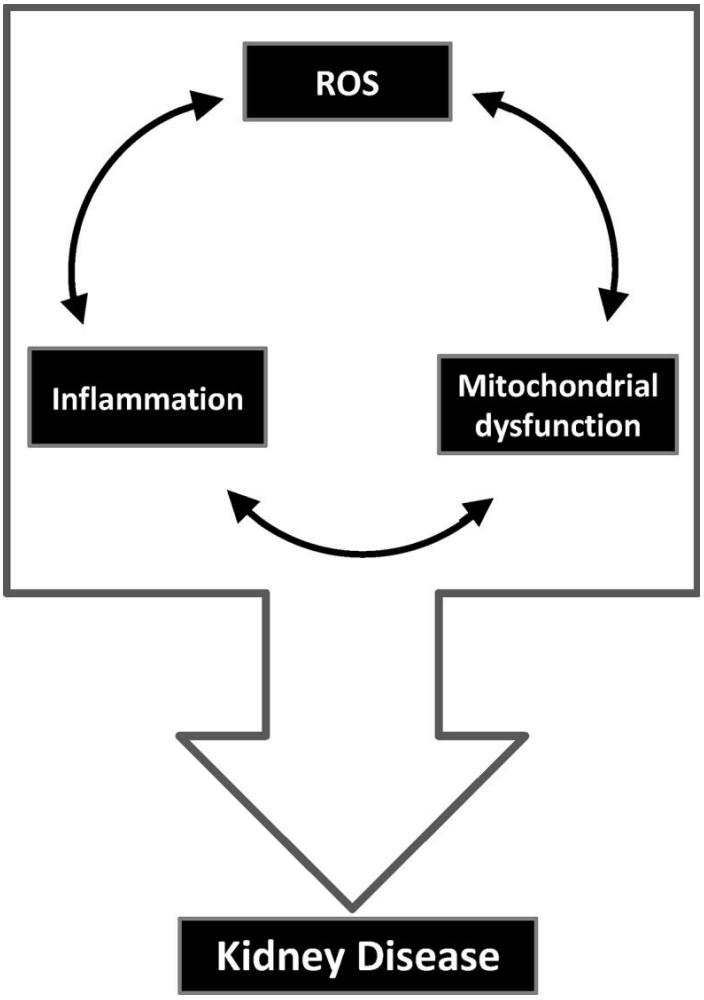

Figure 26. A schematic of the proposed causative axis which is responsible for the bulk of renal disease. Used with permission from Aranda-Rivera, A. K., Cruz-Gregorio, A., Aparicio-Trejo, O. E., & Pedraza-Chaverri, J. (2021). Mitochondrial Redox Signaling and Oxidative Stress in Kidney Diseases. http://creativecommons.org/licenses/by-nc-nd/4.0/

Additionally, several early markers of kidney disease such as N-acetylglutamine, N-acetylornithine, or acetyllysine could be examined both locally in the kidney as well as systemically in plasma *via* a metabolomics approach[176-178].

An important factor that must be taken into consideration in the case of disease markers such as those mentioned above is that their presence can often be counterintuitive. Molecules such as N-acetylglutamine, N-acetylornithine, or acetyllysine may be produced during the early phases of damage, but their presence often allows for early detection of damage (such as in clinical scenarios), or earlier signaling for damage remediation pathways[176-178]. This perspective on damage markers could also be applied to our ROS production datasets. It is known that ROS can be involved in protective signaling cascades involving both mitophagy as well as vital processes such as cellular proliferation and differentiation[144-148]. ROS are also tightly linked with cellular and

mitochondrial calcium signaling *via* the mPTP: excess mitochondrial calcium uptake, is implicated in the opening of the mPTP, which causes efflux of ROS into the cytosol[61,179].

The final experiment discussed in Chapter 4 is the renal mitochondrial calcium uptake assay, which measured not only the mitochondrial calcium uptake in male and female cortex and medulla, but also the amount of calcium that is sufficient to trigger the irreversible mPTP opening. In our hands, female mitochondria from both regions of the kidney displayed earlier mPTP opening than their male counterparts, while the amounts of calcium taken up by mitochondria were similar. The opening of the mPTP can trigger a variety of signaling events including ROS-induced ROS release, whereby other mitochondria in the cell release ROS. It has been proposed, however, that the mPTP opens in more states than the irreversible calcium-overloaded state. Evidence exists for mPTP "flickers" which briefly cause opening of the pore--this is thought to occur in order to restore the elevated mitochondrial membrane potential back to physiological levels and increase forward flow of electrons through the ETC, and can also result in efflux of ROS and calcium back into the cytosol without triggering any apoptotic cascades[130,180-182]. In this manner, mPTP opening can be beneficial in restoring mitochondrial function.

Taken further from this angle of a conservative mPTP opening, it is important to examine the other mechanisms by which mPTP-induced ROS efflux in female renal mitochondria could be affecting the observed renoprotection in females. As discussed in Chapter 4, ROS are involved in a number of signaling cascades. A major pathway involving mitochondrial ROS is the activation of molecular mechanisms which combat hypoxia: they are involved in HIF1-α cascades to mediate hypoxic damage[139,183-186]. Mitochondrial ROS have also been shown to have roles in the signaling of cellular differentiation, apoptosis, growth, proliferation, and metalloproteinase activity[183]. Cialó *et al.* further suggest that reverse transport of electrons, which is often paired with reduced activity in Complex I, produces ROS that are responsible for extension of lifespan in *Drosophila*[187]. In the

kidney, the dual functions of ROS are beginning to be explored: some ROS-induced post-translational modifications of proteins have been demonstrated to be protective against sepsis-AKI damage[188], while excess levels of ROS are implicated in the transition of AKI to CKD as well as in the development of salt-sensitive hypertension[59,133]. Our studies propose that, in the kidney, female mitochondria display a higher sensitivity to oxidative stress, and induce a conservative, protective mPTP opening which is responsible for our observed discrepancies in the bioenergetics and dynamics compared to males. The higher levels of ROS observed in females may be indicative of this phenomenon. A schematic summary of our hypothesis and findings is displayed below in **Figure 27.**

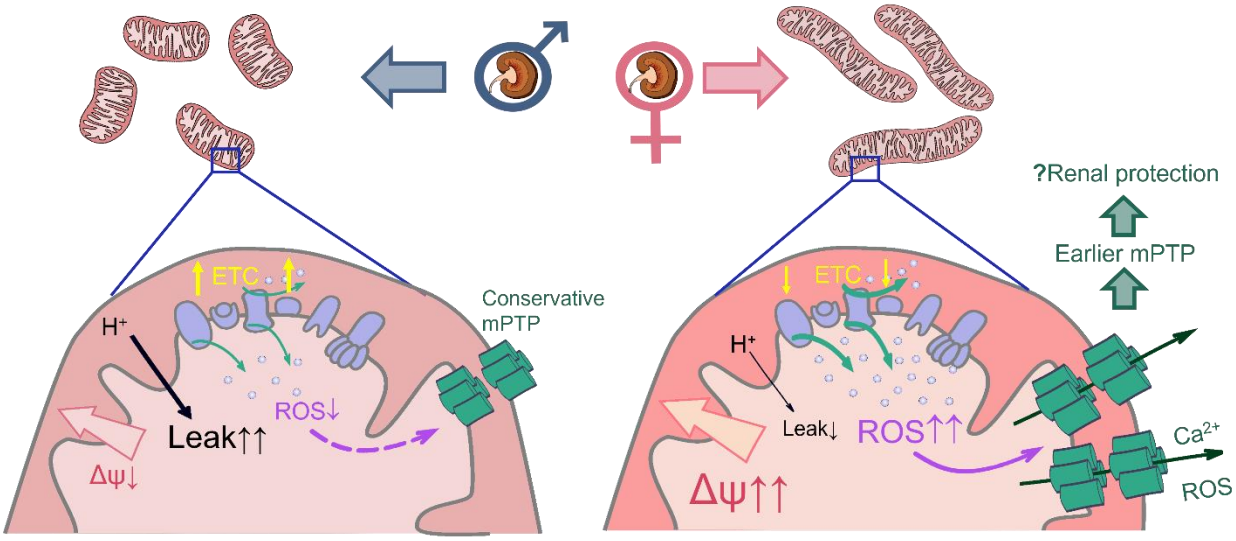

Figure 27. A schematic detailing a summary of our experimental conclusions and our current hypothesis regarding protective mPTP opening in female renal mitochondria.

Conclusions. Though mitochondria are implicated in a plethora of renal diseases, and these renal pathologies are known to be sexually dimorphic, little is known about renal mitochondrial

sex-specific discrepancies in a healthy physiological state. Though still in early phases of research, it is clear that renal mitochondrial bioenergetics displays profound sexual dimorphisms. We have hypothesized that female renal mitochondria display a higher sensitivity to oxidative stress, and proposed that this allows for earlier ROS-related signaling in females *via* the calcium uptake-mPTP-ROS axis. We believe that our studies have opened the way for exploration of mechanisms which may be responsible for the renoprotective effects observed in females. Furthermore, our breakthrough into a novel area of science has provided a scaffold for other studies to examine renal mitochondrial bioenergetics prior to the onset of disease.

Future Directions. This set of studies is, to our knowledge, the first which examines renal mitochondrial bioenergetics in males and females in a healthy physiological context. For this reason, there are a plethora of directions which need further exploration in order to fully characterize the sex-specific discrepancies observed in renal mitochondrial function in physiology *vs*. pathology. In order to fully define the roles that the respective sex hormones are playing, the experiments discussed in Chapters 3 and 4 could be performed again with groups of gonadectomized animals. In fact, Gaignard *et al.* performed gonadectomies on healthy mice, and reported amelioration of sex differences in brain mitochondrial respiration and ATP production[42]. Ovariectomized mice also displayed reduced recovery time from calcium-induced mitochondrial depolarization as compared to females[189]. To further expand on the roles sex hormones play in mitochondrial function, a set of similar experiments as described in Chapter 2 could be performed with a “rescue” group composed of gonadectomized animals with hormone replacement therapy for their respective sexes. Eliminating and subsequently replacing the hormones will elucidate any causal roles they have in the sex-specific differences noted in renal mitochondrial function, and perhaps in the trends observed in renal disease onset.

Other future experiments to expand upon these studies include the performance of more in-depth analyses of proteins involved in oxidative phosphorylation, as well as for each superoxide dismutase isoform and GPX4. Examination of the expressions and activities of other proteins involved in the bioenergetics and dynamics homeostasis of mitochondria would also serve to expand our set of studies: potential targets include mitochondrial uncoupling proteins UCP1 and UCP2, fission proteins PINK1 and Parkin[52]. This would help clarify which complexes other than Complex I could be contributing to the sex differences we observed in our respirometry experiments. This could be complemented by the performance of metabolomics, as suggested above. A metabolic profile of the substrates and products related to oxidative phosphorylation could reveal key differences in respiratory chain Complexes, contextualizing our respirometry data and investigating what TCA metabolites and other mitochondrial molecules could be influencing cellular signaling[155].

There are also additional methods to measure oxidative stress in the kidney; quantifying lipid peroxidation is one such method. Loosely ligated ("labile") iron is able to react with superoxide and/or hydrogen peroxide to form oxygen-centered radicals, which is then able to form a resonant structure with a hydrogen atom of a polyunsaturated fatty acid, and thus is able to react with molecular oxygen to form a lipid peroxyl radical in a process referred to as Fenton chemistry or the Fenton reaction[190,191]. Both the destruction of lipids which comprise membranes, as well as the high level of reactivity of lipid peroxyl radicals are harmful to cells; lipid peroxides are known to be involved with CKD and polycystic kidney disease, and are also suggested as early markers of renal disease prior even to decline in renal function[192,193]. Performance of electron paramagnetic resonance (**EPR**) would elucidate levels of lipid peroxidation in male and female renal tissues, which would allow interpretation as to whether the higher ROS levels observed in

females was to a pathogenic degree, further clarifying our hypothesis of the protective mPTP opening and subsequent ROS efflux in females.

Though we have measured ROS levels and other physiological parameters of renal mitochondria in males and females, we have yet to examine whether sex hormones are responsible for the dimorphisms we report. There are a number of emerging studies which place the mitochondrion in a prime position for investigation regarding sexual dimorphism of function: mitochondria have been shown to express sex hormone receptors. Studies from Solakidi *et al.* and Pronsato *et al.* found that testosterone receptors can localize to mitochondrial membranes in sperm cells, as well as in skeletal muscle, respectively[77,78]. Recent studies have also shown nonclassical localization of estrogen-β receptors to the outer mitochondrial membrane in breast and neural cancer cells[79,194]. Several of these directions would be beneficial in the expansion of our study: gonadectomized rat groups would allow for the observation of whether mitochondrial bioenergetics are sexually dimorphic in the lack of hormones, which would provide mechanistic insight regarding renal disease incidence and development, as well as providing context for the differences in renal disease phenotype observed in women pre- and post-menopause[5,13,14]. Furthermore, examining renal mitochondria for the presence of colocalized estrogen or androgen receptors would not only be novel, but would present a direct pathway by which sex hormones could be influencing mitochondrial function and thus progression or prevention of disease.

To summarize the above, extensive and detailed future studies aimed at exploring the function and expression of the network of proteins involved in mitochondrial bioenergetics, as well as the function and phenotypes of mitochondria in other renal cell types, are needed in order to expand upon the foundational studies we have performed. This will allow for a more robust understanding of the reasons behind the sex-specific discrepancies we have observed in mitochondrial

bioenergetics and ROS handling, and would open up an avenue for the discovery of the specific mitochondrial mechanisms which may be enacting renoprotection in females pre-menopause.

REFERENCES

1. Hall JE, Guyton AC. *Guyton and Hall textbook of medical physiology.* 12th ed. Philadelphia, Pa.: Saunders/Elsevier; 2011.
2. The top 10 causes of death. 2020; https://www.who.int/news-room/fact-sheets/detail/the-top-10-causes-of-death. Accessed 3 October 2021, 2021.
3. Leading Causes of Death. https://www.cdc.gov/nchs/fastats/leading-causes-of-death.htm.
4. Chronic Kidney Disease. https://www.worldkidneyday.org/facts/chronic-kidney-disease/, 2021.
5. Neugarten J, Golestaneh L. Female sex reduces the risk of hospital-associated acute kidney injury: a meta-analysis. *BMC Nephrol.* 2018;19(1):314.
6. Zhang J, Zhu J, Wei J, et al. New Mechanism for the Sex Differences in Salt-Sensitive Hypertension: The Role of Macula Densa NOS1beta-Mediated Tubuloglomerular Feedback. *Hypertension.* 2020;75(2):449-457.
7. Neugarten J, Acharya A, Silbiger SR. Effect of gender on the progression of nondiabetic renal disease: a meta-analysis. *J Am Soc Nephrol.* 2000;11(2):319-329.
8. Tejpal A, Gianos E, Cerise J, et al. Sex-Based Differences in COVID-19 Outcomes. *J Womens Health (Larchmt).* 2021;30(4):492-501.
9. Baylis C. Sexual dimorphism in the aging kidney: differences in the nitric oxide system. *Nat Rev Nephrol.* 2009;5(7):384-396.
10. Veiras LC, Girardi ACC, Curry J, et al. Sexual Dimorphic Pattern of Renal Transporters and Electrolyte Homeostasis. *J Am Soc Nephrol.* 2017;28(12):3504-3517.
11. Mirabito KM, Hilliard LM, Kett MM, et al. Sex- and age-related differences in the chronic pressure-natriuresis relationship: role of the angiotensin type 2 receptor. *Am J Physiol Renal Physiol.* 2014;307(8):F901-907.
12. Yu MK, Lyles CR, Bent-Shaw LA, Young BA, Pathways A. Risk factor, age and sex differences in chronic kidney disease prevalence in a diabetic cohort: the pathways study. *Am J Nephrol.* 2012;36(3):245-251.
13. Garovic VD, August P. Sex Differences and Renal Protection: Keeping in Touch with Your Feminine Side. *J Am Soc Nephrol.* 2016;27(10):2921-2924.
14. Stenvinkel P, Wanner C, Metzger T, et al. Inflammation and outcome in end-stage renal failure: does female gender constitute a survival advantage? *Kidney Int.* 2002;62(5):1791-1798.
15. Lee CJ, Gardiner BS, Evans RG, Smith DW. Analysis of the critical determinants of renal medullary oxygenation. *Am J Physiol Renal Physiol.* 2019;317(6):F1483-F1502.
16. Zhang W, Edwards A. Oxygen transport across vasa recta in the renal medulla. *Am J Physiol Heart Circ Physiol.* 2002;283(3):H1042-1055.
17. Scholz H, Boivin FJ, Schmidt-Ott KM, et al. Kidney physiology and susceptibility to acute kidney injury: implications for renoprotection. *Nat Rev Nephrol.* 2021;17(5):335-349.
18. Pruijm M, Milani B, Pivin E, et al. Reduced cortical oxygenation predicts a progressive decline of renal function in patients with chronic kidney disease. *Kidney Int.* 2018;93(4):932-940.
19. Sugiyama K, Inoue T, Kozawa E, et al. Reduced oxygenation but not fibrosis defined by functional magnetic resonance imaging predicts the long-term progression of chronic kidney disease. *Nephrol Dial Transplant.* 2020;35(6):964-970.

20. Zhou H, Yang M, Jiang Z, Ding J, Di J, Cui L. Renal Hypoxia: An Important Prognostic Marker in Patients with Chronic Kidney Disease. *Am J Nephrol.* 2018;48(1):46-55.
21. Bleyer AJ, Chen R, D'Agostino RB, Jr., Appel RG. Clinical correlates of hypertensive end-stage renal disease. *Am J Kidney Dis.* 1998;31(1):28-34.
22. Palm F. Intrarenal oxygen in diabetes and a possible link to diabetic nephropathy. *Clin Exp Pharmacol Physiol.* 2006;33(10):997-1001.
23. Munger K, Baylis C. Sex differences in renal hemodynamics in rats. *Am J Physiol.* 1988;254(2 Pt 2):F223-231.
24. Tiede LM, Cook EA, Morsey B, Fox HS. Oxygen matters: tissue culture oxygen levels affect mitochondrial function and structure as well as responses to HIV viroproteins. *Cell Death Dis.* 2011;2:e246.
25. Serebrovskaya TV, Nosar VI, Bratus LV, Gavenauskas BL, Mankovska IM. Tissue oxygenation and mitochondrial respiration under different modes of intermittent hypoxia. *High Alt Med Biol.* 2013;14(3):280-288.
26. Daehn I, Casalena G, Zhang T, et al. Endothelial mitochondrial oxidative stress determines podocyte depletion in segmental glomerulosclerosis. *J Clin Invest.* 2014;124(4):1608-1621.
27. Corcoran JB, McCarthy S, Griffin B, et al. IHG-1 must be localised to mitochondria to decrease Smad7 expression and amplify TGF-beta1-induced fibrotic responses. *Biochim Biophys Acta.* 2013;1833(8):1969-1978.
28. Long J, Badal SS, Ye Z, et al. Long noncoding RNA Tug1 regulates mitochondrial bioenergetics in diabetic nephropathy. *J Clin Invest.* 2016;126(11):4205-4218.
29. Qi H, Casalena G, Shi S, et al. Glomerular Endothelial Mitochondrial Dysfunction Is Essential and Characteristic of Diabetic Kidney Disease Susceptibility. *Diabetes.* 2017;66(3):763-778.
30. Casalena G, Krick S, Daehn I, et al. Mpv17 in mitochondria protects podocytes against mitochondrial dysfunction and apoptosis in vivo and in vitro. *Am J Physiol Renal Physiol.* 2014;306(11):F1372-1380.
31. Wang Z, Sun Q, Sun N, Liang M, Tian Z. Mitochondrial Dysfunction and Altered Renal Metabolism in Dahl Salt-Sensitive Rats. *Kidney Blood Press Res.* 2017;42(3):587-597.
32. Domondon M, Polina I, Nikiforova AB, et al. Renal Glomerular Mitochondria Function in Salt-Sensitive Hypertension. *Front Physiol.* 2019;10:1588.
33. Dugan LL, You YH, Ali SS, et al. AMPK dysregulation promotes diabetes-related reduction of superoxide and mitochondrial function. *J Clin Invest.* 2013;123(11):4888-4899.
34. Galloway CA, Lee H, Nejjar S, et al. Transgenic control of mitochondrial fission induces mitochondrial uncoupling and relieves diabetic oxidative stress. *Diabetes.* 2012;61(8):2093-2104.
35. Zhan M, Usman IM, Sun L, Kanwar YS. Disruption of renal tubular mitochondrial quality control by Myo-inositol oxygenase in diabetic kidney disease. *J Am Soc Nephrol.* 2015;26(6):1304-1321.
36. Hartleben B, Godel M, Meyer-Schwesinger C, et al. Autophagy influences glomerular disease susceptibility and maintains podocyte homeostasis in aging mice. *J Clin Invest.* 2010;120(4):1084-1096.
37. D'Aco KE, Manno M, Clarke C, Ganesh J, Meyers KE, Sondheimer N. Mitochondrial tRNA(Phe) mutation as a cause of end-stage renal disease in childhood. *Pediatr Nephrol.* 2013;28(3):515-519.
38. de Arriba G, Calvino M, Benito S, Parra T. Cyclosporine A-induced apoptosis in renal tubular cells is related to oxidative damage and mitochondrial fission. *Toxicol Lett.* 2013;218(1):30-38.

39. Dinour D, Mini S, Polak-Charcon S, Lotan D, Holtzman EJ. Progressive nephropathy associated with mitochondrial tRNA gene mutation. *Clin Nephrol.* 2004;62(2):149-154.
40. Colom B, Oliver J, Roca P, Garcia-Palmer FJ. Caloric restriction and gender modulate cardiac muscle mitochondrial H2O2 production and oxidative damage. *Cardiovasc Res.* 2007;74(3):456-465.
41. Guevara R, Gianotti M, Oliver J, Roca P. Age and sex-related changes in rat brain mitochondrial oxidative status. *Exp Gerontol.* 2011;46(11):923-928.
42. Gaignard P, Savouroux S, Liere P, et al. Effect of Sex Differences on Brain Mitochondrial Function and Its Suppression by Ovariectomy and in Aged Mice. *Endocrinology.* 2015;156(8):2893-2904.
43. Borras C, Sastre J, Garcia-Sala D, Lloret A, Pallardo FV, Vina J. Mitochondria from females exhibit higher antioxidant gene expression and lower oxidative damage than males. *Free Radic Biol Med.* 2003;34(5):546-552.
44. Vina J, Borras C, Gambini J, Sastre J, Pallardo FV. Why females live longer than males? Importance of the upregulation of longevity-associated genes by oestrogenic compounds. *FEBS Lett.* 2005;579(12):2541-2545.
45. Justo R, Boada J, Frontera M, Oliver J, Bermudez J, Gianotti M. Gender dimorphism in rat liver mitochondrial oxidative metabolism and biogenesis. *Am J Physiol Cell Physiol.* 2005;289(2):C372-378.
46. Colom B, Alcolea MP, Valle A, Oliver J, Roca P, Garcia-Palmer FJ. Skeletal muscle of female rats exhibit higher mitochondrial mass and oxidative-phosphorylative capacities compared to males. *Cell Physiol Biochem.* 2007;19(1-4):205-212.
47. Gomez-Perez Y, Capllonch-Amer G, Gianotti M, Llado I, Proenza AM. Long-term high-fat-diet feeding induces skeletal muscle mitochondrial biogenesis in rats in a sex-dependent and muscle-type specific manner. *Nutr Metab (Lond).* 2012;9:15.
48. Capllonch-Amer G, Llado I, Proenza AM, Garcia-Palmer FJ, Gianotti M. Opposite effects of 17-beta estradiol and testosterone on mitochondrial biogenesis and adiponectin synthesis in white adipocytes. *J Mol Endocrinol.* 2014;52(2):203-214.
49. Rodriguez-Cuenca S, Pujol E, Justo R, et al. Sex-dependent thermogenesis, differences in mitochondrial morphology and function, and adrenergic response in brown adipose tissue. *J Biol Chem.* 2002;277(45):42958-42963.
50. Ventura-Clapier R, Moulin M, Piquereau J, et al. Mitochondria: a central target for sex differences in pathologies. *Clin Sci (Lond).* 2017;131(9):803-822.
51. Ahmad M, Wolberg A, Kahwaji CI. Biochemistry, Electron Transport Chain. *StatPearls*. Treasure Island (FL)2021.
52. Bhargava P, Schnellmann RG. Mitochondrial energetics in the kidney. *Nat Rev Nephrol.* 2017;13(10):629-646.
53. Cipolat S, Martins de Brito O, Dal Zilio B, Scorrano L. OPA1 requires mitofusin 1 to promote mitochondrial fusion. *Proc Natl Acad Sci U S A.* 2004;101(45):15927-15932.
54. Mears JA, Lackner LL, Fang S, Ingerman E, Nunnari J, Hinshaw JE. Conformational changes in Dnm1 support a contractile mechanism for mitochondrial fission. *Nat Struct Mol Biol.* 2011;18(1):20-26.
55. Mishra P, Carelli V, Manfredi G, Chan DC. Proteolytic cleavage of Opa1 stimulates mitochondrial inner membrane fusion and couples fusion to oxidative phosphorylation. *Cell Metab.* 2014;19(4):630-641.
56. Wirthensohn G, Guder WG. Renal substrate metabolism. *Physiol Rev.* 1986;66(2):469-497.
57. Gewin LS. Sugar or Fat? Renal Tubular Metabolism Reviewed in Health and Disease. *Nutrients.* 2021;13(5).

58. Brieger K, Schiavone S, Miller FJ, Jr., Krause KH. Reactive oxygen species: from health to disease. *Swiss Med Wkly.* 2012;142:w13659.
59. Tomsa AM, Alexa AL, Junie ML, Rachisan AL, Ciumarnean L. Oxidative stress as a potential target in acute kidney injury. *PeerJ.* 2019;7:e8046.
60. Granata S, Zaza G, Simone S, et al. Mitochondrial dysregulation and oxidative stress in patients with chronic kidney disease. *BMC Genomics.* 2009;10:388.
61. Aranda-Rivera AK, Cruz-Gregorio A, Aparicio-Trejo OE, Pedraza-Chaverri J. Mitochondrial Redox Signaling and Oxidative Stress in Kidney Diseases. *Biomolecules.* 2021;11(8).
62. Frank M, Duvezin-Caubet S, Koob S, et al. Mitophagy is triggered by mild oxidative stress in a mitochondrial fission dependent manner. *Biochim Biophys Acta.* 2012;1823(12):2297-2310.
63. Frezza C, Cipolat S, Scorrano L. Organelle isolation: functional mitochondria from mouse liver, muscle and cultured fibroblasts. *Nat Protoc.* 2007;2(2):287-295.
64. Calton MA, Beaulieu MO, Benchorin G, Vollrath D. Method for measuring extracellular flux from intact polarized epithelial monolayers. *Mol Vis.* 2018;24:425-433.
65. Yepez VA, Kremer LS, Iuso A, et al. OCR-Stats: Robust estimation and statistical testing of mitochondrial respiration activities using Seahorse XF Analyzer. *PLoS One.* 2018;13(7):e0199938.
66. Zhang J, Zhang Q. Using Seahorse Machine to Measure OCR and ECAR in Cancer Cells. *Methods Mol Biol.* 2019;1928:353-363.
67. Schindelin J, Arganda-Carreras I, Frise E, et al. Fiji: an open-source platform for biological-image analysis. *Nat Methods.* 2012;9(7):676-682.
68. Wang Z, Ying Z, Bosy-Westphal A, et al. Specific metabolic rates of major organs and tissues across adulthood: evaluation by mechanistic model of resting energy expenditure. *Am J Clin Nutr.* 2010;92(6):1369-1377.
69. Nourbakhsh N, Singh P. Role of renal oxygenation and mitochondrial function in the pathophysiology of acute kidney injury. *Nephron Clin Pract.* 2014;127(1-4):149-152.
70. Pagliarini DJ, Calvo SE, Chang B, et al. A mitochondrial protein compendium elucidates complex I disease biology. *Cell.* 2008;134(1):112-123.
71. Palmer LG, Schnermann J. Integrated control of Na transport along the nephron. *Clin J Am Soc Nephrol.* 2015;10(4):676-687.
72. Lee JJ, Tripi LM, Erbe RW, Garimella-Krovi S, Springate JE. A mitochondrial DNA deletion presenting with corneal clouding and severe Fanconi syndrome. *Pediatr Nephrol.* 2012;27(5):869-872.
73. Nishi Y, Satoh M, Nagasu H, et al. Selective estrogen receptor modulation attenuates proteinuria-induced renal tubular damage by modulating mitochondrial oxidative status. *Kidney Int.* 2013;83(4):662-673.
74. Lash LH, Qian W, Putt DA, et al. Renal toxicity of perchloroethylene and S-(1,2,2-trichlorovinyl)glutathione in rats and mice: sex- and species-dependent differences. *Toxicol Appl Pharmacol.* 2002;179(3):163-171.
75. Patil CN, Wallace K, LaMarca BD, et al. Low-dose testosterone protects against renal ischemia-reperfusion injury by increasing renal IL-10-to-TNF-alpha ratio and attenuating T-cell infiltration. *Am J Physiol Renal Physiol.* 2016;311(2):F395-403.
76. Peng Y, Fang Z, Liu M, et al. Testosterone induces renal tubular epithelial cell death through the HIF-1alpha/BNIP3 pathway. *J Transl Med.* 2019;17(1):62.
77. Pronsato L, Boland R, Milanesi L. Non-classical localization of androgen receptor in the C2C12 skeletal muscle cell line. *Arch Biochem Biophys.* 2013;530(1):13-22.

78. Solakidi S, Psarra AM, Nikolaropoulos S, Sekeris CE. Estrogen receptors alpha and beta (ERalpha and ERbeta) and androgen receptor (AR) in human sperm: localization of ERbeta and AR in mitochondria of the midpiece. *Hum Reprod.* 2005;20(12):3481-3487.
79. Karakas B, Aka Y, Giray A, et al. Mitochondrial estrogen receptors alter mitochondrial priming and response to endocrine therapy in breast cancer cells. *Cell Death Discov.* 2021;7(1):189.
80. Friedman JR, Nunnari J. Mitochondrial form and function. *Nature.* 2014;505(7483):335-343.
81. Brand MD, Nicholls DG. Assessing mitochondrial dysfunction in cells. *Biochem J.* 2011;435(2):297-312.
82. Rajeev Dalal ZSB, Jasjit S. Sehdev. Physiology, Renal Blood Flow and Filtration. FL: Treasure Island (FL) : StatPearls Publishing; 2021.
83. Ellam T, Fotheringham J, Kawar B. Differential scaling of glomerular filtration rate and ingested metabolic burden: implications for gender differences in chronic kidney disease outcomes. *Nephrol Dial Transplant.* 2014;29(6):1186-1194.
84. Huang C, Kim Y, Caramori ML, et al. Diabetic nephropathy is associated with gene expression levels of oxidative phosphorylation and related pathways. *Diabetes.* 2006;55(6):1826-1831.
85. Sas KM, Kayampilly P, Byun J, et al. Tissue-specific metabolic reprogramming drives nutrient flux in diabetic complications. *JCI Insight.* 2016;1(15):e86976.
86. Funk JA, Schnellmann RG. Persistent disruption of mitochondrial homeostasis after acute kidney injury. *Am J Physiol Renal Physiol.* 2012;302(7):F853-864.
87. Thome T, Kumar RA, Burke SK, et al. Impaired muscle mitochondrial energetics is associated with uremic metabolite accumulation in chronic kidney disease. *JCI Insight.* 2020;6(1).
88. Gry M, Rimini R, Stromberg S, et al. Correlations between RNA and protein expression profiles in 23 human cell lines. *BMC Genomics.* 2009;10:365.
89. Zager RA, Johnson AC, Hanson SY. Proximal tubular cytochrome c efflux: determinant, and potential marker, of mitochondrial injury. *Kidney Int.* 2004;65(6):2123-2134.
90. Sibarani J, Tjahjodjati T, Atik N, Rachmadi D, Mustafa A. Urinary Cytochrome C and Caspase-3 as Novel Biomarker of Renal Function Impairment in Unilateral Ureteropelvic Junction Obstruction Model of Wistar Rats. *Res Rep Urol.* 2020;12:217-224.
91. Boissan M, Montagnac G, Shen Q, et al. Membrane trafficking. Nucleoside diphosphate kinases fuel dynamin superfamily proteins with GTP for membrane remodeling. *Science.* 2014;344(6191):1510-1515.
92. Miyamoto S, Ochiai A, Boku N, et al. Discrepancies between the gene expression, protein expression, and enzymatic activity of thymidylate synthase and dihydropyrimidine dehydrogenase in human gastrointestinal cancers and adjacent normal mucosa. *Int J Oncol.* 2001;18(4):705-713.
93. Jennifer D Rocca EKH, Jay T Lennon, Sarah E Evans, Mark P Waldrop, James B Cotner, Diana R Nemergut, Emily B Graham & Matthew D Wallenstein Relationships between protein-encoding gene abundance and corresponding process are commonly assumed yet rarely observed. *The ISME Journal.* 2015;9:1693-1699.
94. Taguchi N, Ishihara N, Jofuku A, Oka T, Mihara K. Mitotic phosphorylation of dynamin-related GTPase Drp1 participates in mitochondrial fission. *J Biol Chem.* 2007;282(15):11521-11529.
95. Cho SG, Du Q, Huang S, Dong Z. Drp1 dephosphorylation in ATP depletion-induced mitochondrial injury and tubular cell apoptosis. *Am J Physiol Renal Physiol.* 2010;299(1):F199-206.

96. Wang W, Wang Y, Long J, et al. Mitochondrial fission triggered by hyperglycemia is mediated by ROCK1 activation in podocytes and endothelial cells. *Cell Metab.* 2012;15(2):186-200.
97. Tang WX, Wu WH, Zeng XX, Bo H, Huang SM. Early protective effect of mitofusion 2 overexpression in STZ-induced diabetic rat kidney. *Endocrine.* 2012;41(2):236-247.
98. Guo K, Lu J, Huang Y, et al. Protective role of PGC-1alpha in diabetic nephropathy is associated with the inhibition of ROS through mitochondrial dynamic remodeling. *PLoS One.* 2015;10(4):e0125176.
99. Chen H, Chomyn A, Chan DC. Disruption of fusion results in mitochondrial heterogeneity and dysfunction. *J Biol Chem.* 2005;280(28):26185-26192.
100. Qi W, Keenan HA, Li Q, et al. Pyruvate kinase M2 activation may protect against the progression of diabetic glomerular pathology and mitochondrial dysfunction. *Nat Med.* 2017;23(6):753-762.
101. Xiao X, Hu Y, Quiros PM, Wei Q, Lopez-Otin C, Dong Z. OMA1 mediates OPA1 proteolysis and mitochondrial fragmentation in experimental models of ischemic kidney injury. *Am J Physiol Renal Physiol.* 2014;306(11):F1318-1326.
102. Yoon YS, Yoon DS, Lim IK, et al. Formation of elongated giant mitochondria in DFO-induced cellular senescence: involvement of enhanced fusion process through modulation of Fis1. *J Cell Physiol.* 2006;209(2):468-480.
103. Huang P, Yu T, Yoon Y. Mitochondrial clustering induced by overexpression of the mitochondrial fusion protein Mfn2 causes mitochondrial dysfunction and cell death. *Eur J Cell Biol.* 2007;86(6):289-302.
104. Szabadkai G, Simoni AM, Chami M, Wieckowski MR, Youle RJ, Rizzuto R. Drp-1-dependent division of the mitochondrial network blocks intraorganellar Ca2+ waves and protects against Ca2+-mediated apoptosis. *Mol Cell.* 2004;16(1):59-68.
105. Waterham HR, Koster J, van Roermund CW, Mooyer PA, Wanders RJ, Leonard JV. A lethal defect of mitochondrial and peroxisomal fission. *N Engl J Med.* 2007;356(17):1736-1741.
106. Yoon YM, Go G, Yoon S, et al. Melatonin Treatment Improves Renal Fibrosis via miR-4516/SIAH3/PINK1 Axis. *Cells.* 2021;10(7).
107. Li R, Jia Z, Trush MA. Defining ROS in Biology and Medicine. *React Oxyg Species (Apex).* 2016;1(1):9-21.
108. Lambert AJ, Brand MD. Superoxide production by NADH:ubiquinone oxidoreductase (complex I) depends on the pH gradient across the mitochondrial inner membrane. *Biochem J.* 2004;382(Pt 2):511-517.
109. Wong HS, Dighe PA, Mezera V, Monternier PA, Brand MD. Production of superoxide and hydrogen peroxide from specific mitochondrial sites under different bioenergetic conditions. *J Biol Chem.* 2017;292(41):16804-16809.
110. Davies KJ, Quintanilha AT, Brooks GA, Packer L. Free radicals and tissue damage produced by exercise. *Biochem Biophys Res Commun.* 1982;107(4):1198-1205.
111. Irazabal MV, Torres VE. Reactive Oxygen Species and Redox Signaling in Chronic Kidney Disease. *Cells.* 2020;9(6).
112. Mitchell T, Saba H, Laakman J, Parajuli N, MacMillan-Crow LA. Role of mitochondrial-derived oxidants in renal tubular cell cold-storage injury. *Free Radic Biol Med.* 2010;49(8):1273-1282.
113. Wen Y, Liu YR, Tang TT, et al. mROS-TXNIP axis activates NLRP3 inflammasome to mediate renal injury during ischemic AKI. *Int J Biochem Cell Biol.* 2018;98:43-53.
114. Himmelfarb J, McMonagle E, Freedman S, et al. Oxidative stress is increased in critically ill patients with acute renal failure. *J Am Soc Nephrol.* 2004;15(9):2449-2456.

115. Tanaka S, Tanaka T, Kawakami T, et al. Vascular adhesion protein-1 enhances neutrophil infiltration by generation of hydrogen peroxide in renal ischemia/reperfusion injury. *Kidney Int.* 2017;92(1):154-164.
116. Bayorh MA, Ganafa AA, Socci RR, Silvestrov N, Abukhalaf IK. The role of oxidative stress in salt-induced hypertension. *Am J Hypertens.* 2004;17(1):31-36.
117. Banday AA, Muhammad AB, Fazili FR, Lokhandwala M. Mechanisms of oxidative stress-induced increase in salt sensitivity and development of hypertension in Sprague-Dawley rats. *Hypertension.* 2007;49(3):664-671.
118. Granatiero V, De Stefani D, Rizzuto R. Mitochondrial Calcium Handling in Physiology and Disease. *Adv Exp Med Biol.* 2017;982:25-47.
119. Santulli G, Marks AR. Essential Roles of Intracellular Calcium Release Channels in Muscle, Brain, Metabolism, and Aging. *Curr Mol Pharmacol.* 2015;8(2):206-222.
120. Peng TI, Jou MJ. Oxidative stress caused by mitochondrial calcium overload. *Ann N Y Acad Sci.* 2010;1201:183-188.
121. Korge P, Langer GA. Mitochondrial Ca2+ uptake, efflux, and sarcolemmal damage in Ca2+-overloaded cultured rat cardiomyocytes. *Am J Physiol.* 1998;274(6):H2085-2093.
122. Votyakova TV, Reynolds IJ. Ca2+-induced permeabilization promotes free radical release from rat brain mitochondria with partially inhibited complex I. *J Neurochem.* 2005;93(3):526-537.
123. Duan Y, Gross RA, Sheu SS. Ca2+-dependent generation of mitochondrial reactive oxygen species serves as a signal for poly(ADP-ribose) polymerase-1 activation during glutamate excitotoxicity. *J Physiol.* 2007;585(Pt 3):741-758.
124. Halestrap AP. What is the mitochondrial permeability transition pore? *J Mol Cell Cardiol.* 2009;46(6):821-831.
125. Niimi K, Yasui T, Hirose M, et al. Mitochondrial permeability transition pore opening induces the initial process of renal calcium crystallization. *Free Radic Biol Med.* 2012;52(7):1207-1217.
126. Crompton M, Ellinger H, Costi A. Inhibition by cyclosporin A of a Ca2+-dependent pore in heart mitochondria activated by inorganic phosphate and oxidative stress. *Biochem J.* 1988;255(1):357-360.
127. Halestrap AP, Davidson AM. Inhibition of Ca2(+)-induced large-amplitude swelling of liver and heart mitochondria by cyclosporin is probably caused by the inhibitor binding to mitochondrial-matrix peptidyl-prolyl cis-trans isomerase and preventing it interacting with the adenine nucleotide translocase. *Biochem J.* 1990;268(1):153-160.
128. Szabo I, De Pinto V, Zoratti M. The mitochondrial permeability transition pore may comprise VDAC molecules. II. The electrophysiological properties of VDAC are compatible with those of the mitochondrial megachannel. *FEBS Lett.* 1993;330(2):206-210.
129. Kokoszka JE, Waymire KG, Levy SE, et al. The ADP/ATP translocator is not essential for the mitochondrial permeability transition pore. *Nature.* 2004;427(6973):461-465.
130. Briston T, Roberts M, Lewis S, et al. Mitochondrial permeability transition pore: sensitivity to opening and mechanistic dependence on substrate availability. *Sci Rep.* 2017;7(1):10492.
131. Che R, Yuan Y, Huang S, Zhang A. Mitochondrial dysfunction in the pathophysiology of renal diseases. *Am J Physiol Renal Physiol.* 2014;306(4):F367-378.
132. Lagranha CJ, Deschamps A, Aponte A, Steenbergen C, Murphy E. Sex differences in the phosphorylation of mitochondrial proteins result in reduced production of reactive oxygen species and cardioprotection in females. *Circ Res.* 2010;106(11):1681-1691.

133. Manning RD, Jr., Meng S, Tian N. Renal and vascular oxidative stress and salt-sensitivity of arterial pressure. *Acta Physiol Scand.* 2003;179(3):243-250.
134. Mitchell T, De Miguel C, Gohar EY. Sex differences in redox homeostasis in renal disease. *Redox Biol.* 2020;31:101489.
135. Nordstrom A, Hadrevi J, Olsson T, Franks PW, Nordstrom P. Higher Prevalence of Type 2 Diabetes in Men Than in Women Is Associated With Differences in Visceral Fat Mass. *J Clin Endocrinol Metab.* 2016;101(10):3740-3746.
136. Ricardo AC, Yang W, Sha D, et al. Sex-Related Disparities in CKD Progression. *J Am Soc Nephrol.* 2019;30(1):137-146.
137. Li C, Deng X, Xie X, Liu Y, Friedmann Angeli JP, Lai L. Activation of Glutathione Peroxidase 4 as a Novel Anti-inflammatory Strategy. *Front Pharmacol.* 2018;9:1120.
138. Bell EL, Klimova TA, Eisenbart J, et al. The Qo site of the mitochondrial complex III is required for the transduction of hypoxic signaling via reactive oxygen species production. *J Cell Biol.* 2007;177(6):1029-1036.
139. Chandel NS, McClintock DS, Feliciano CE, et al. Reactive oxygen species generated at mitochondrial complex III stabilize hypoxia-inducible factor-1alpha during hypoxia: a mechanism of O2 sensing. *J Biol Chem.* 2000;275(33):25130-25138.
140. Connor KM, Subbaram S, Regan KJ, et al. Mitochondrial H2O2 regulates the angiogenic phenotype via PTEN oxidation. *J Biol Chem.* 2005;280(17):16916-16924.
141. Meng TC, Fukada T, Tonks NK. Reversible oxidation and inactivation of protein tyrosine phosphatases in vivo. *Mol Cell.* 2002;9(2):387-399.
142. DeNicola GM, Karreth FA, Humpton TJ, et al. Oncogene-induced Nrf2 transcription promotes ROS detoxification and tumorigenesis. *Nature.* 2011;475(7354):106-109.
143. Acehan D, Jiang X, Morgan DG, Heuser JE, Wang X, Akey CW. Three-dimensional structure of the apoptosome: implications for assembly, procaspase-9 binding, and activation. *Mol Cell.* 2002;9(2):423-432.
144. Zermati Y, Garrido C, Amsellem S, et al. Caspase activation is required for terminal erythroid differentiation. *J Exp Med.* 2001;193(2):247-254.
145. Arama E, Agapite J, Steller H. Caspase activity and a specific cytochrome C are required for sperm differentiation in Drosophila. *Dev Cell.* 2003;4(5):687-697.
146. Sordet O, Rebe C, Plenchette S, et al. Specific involvement of caspases in the differentiation of monocytes into macrophages. *Blood.* 2002;100(13):4446-4453.
147. De Botton S, Sabri S, Daugas E, et al. Platelet formation is the consequence of caspase activation within megakaryocytes. *Blood.* 2002;100(4):1310-1317.
148. Woo M, Hakem R, Furlonger C, et al. Caspase-3 regulates cell cycle in B cells: a consequence of substrate specificity. *Nat Immunol.* 2003;4(10):1016-1022.
149. Jang HS, Noh MR, Kim J, Padanilam BJ. Defective Mitochondrial Fatty Acid Oxidation and Lipotoxicity in Kidney Diseases. *Front Med (Lausanne).* 2020;7:65.
150. Gadkari TV, Cortes N, Madrasi K, Tsoukias NM, Joshi MS. Agmatine induced NO dependent rat mesenteric artery relaxation and its impairment in salt-sensitive hypertension. *Nitric Oxide.* 2013;35:65-71.
151. Szabo AJ, Wagner L, Erdely A, Lau K, Baylis C. Renal neuronal nitric oxide synthase protein expression as a marker of renal injury. *Kidney Int.* 2003;64(5):1765-1771.
152. Seddon MD, Chowienczyk PJ, Brett SE, Casadei B, Shah AM. Neuronal nitric oxide synthase regulates basal microvascular tone in humans in vivo. *Circulation.* 2008;117(15):1991-1996.
153. Yoneyama H, Yamamoto A, Kosaka H. Neuronal nitric oxide synthase generates superoxide from the oxygenase domain. *Biochem J.* 2001;360(Pt 1):247-253.

154. Salabei JK, Gibb AA, Hill BG. Comprehensive measurement of respiratory activity in permeabilized cells using extracellular flux analysis. *Nat Protoc.* 2014;9(2):421-438.
155. Martinez-Reyes I, Chandel NS. Mitochondrial TCA cycle metabolites control physiology and disease. *Nat Commun.* 2020;11(1):102.
156. Martinez-Reyes I, Diebold LP, Kong H, et al. TCA Cycle and Mitochondrial Membrane Potential Are Necessary for Diverse Biological Functions. *Mol Cell.* 2016;61(2):199-209.
157. Patten DA, Lafleur VN, Robitaille GA, Chan DA, Giaccia AJ, Richard DE. Hypoxia-inducible factor-1 activation in nonhypoxic conditions: the essential role of mitochondrial-derived reactive oxygen species. *Mol Biol Cell.* 2010;21(18):3247-3257.
158. Selak MA, Armour SM, MacKenzie ED, et al. Succinate links TCA cycle dysfunction to oncogenesis by inhibiting HIF-alpha prolyl hydroxylase. *Cancer Cell.* 2005;7(1):77-85.
159. Arts RJ, Novakovic B, Ter Horst R, et al. Glutaminolysis and Fumarate Accumulation Integrate Immunometabolic and Epigenetic Programs in Trained Immunity. *Cell Metab.* 2016;24(6):807-819.
160. Yang H, van der Stel W, Lee R, et al. Dynamic Modeling of Mitochondrial Membrane Potential Upon Exposure to Mitochondrial Inhibitors. *Front Pharmacol.* 2021;12:679407.
161. Ribeiro RF, Jr., Ronconi KS, Morra EA, et al. Sex differences in the regulation of spatially distinct cardiac mitochondrial subpopulations. *Mol Cell Biochem.* 2016;419(1-2):41-51.
162. Yao CH, Wang R, Wang Y, Kung CP, Weber JD, Patti GJ. Mitochondrial fusion supports increased oxidative phosphorylation during cell proliferation. *Elife.* 2019;8.
163. Wenzel P, Mollnau H, Oelze M, et al. First evidence for a crosstalk between mitochondrial and NADPH oxidase-derived reactive oxygen species in nitroglycerin-triggered vascular dysfunction. *Antioxid Redox Signal.* 2008;10(8):1435-1447.
164. Kitada M, Xu J, Ogura Y, Monno I, Koya D. Manganese Superoxide Dismutase Dysfunction and the Pathogenesis of Kidney Disease. *Front Physiol.* 2020;11:755.
165. Fukui M, Zhu BT. Mitochondrial superoxide dismutase SOD2, but not cytosolic SOD1, plays a critical role in protection against glutamate-induced oxidative stress and cell death in HT22 neuronal cells. *Free Radic Biol Med.* 2010;48(6):821-830.
166. Kim S, Kang SW, Joo J, et al. Correction: Characterization of ferroptosis in kidney tubular cell death under diabetic conditions. *Cell Death Dis.* 2021;12(4):382.
167. Wortmann M, Schneider M, Pircher J, et al. Combined deficiency in glutathione peroxidase 4 and vitamin E causes multiorgan thrombus formation and early death in mice. *Circ Res.* 2013;113(4):408-417.
168. Zhang J, Bi J, Ren Y, et al. Involvement of GPX4 in irisin's protection against ischemia reperfusion-induced acute kidney injury. *J Cell Physiol.* 2021;236(2):931-945.
169. C. ZLXXHQaD. Targeting Ferroptosis Attenuates Interstitial Inflammation and Kidney Fibrosis. *Karger.*
170. Gal-Oz ST, Maier B, Yoshida H, et al. ImmGen report: sexual dimorphism in the immune system transcriptome. *Nat Commun.* 2019;10(1):4295.
171. Fisher DW, Bennett DA, Dong H. Sexual dimorphism in predisposition to Alzheimer's disease. *Neurobiol Aging.* 2018;70:308-324.
172. Leinwand LA. Sex is a potent modifier of the cardiovascular system. *J Clin Invest.* 2003;112(3):302-307.
173. Brie B, Ramirez MC, De Winne C, et al. Brain Control of Sexually Dimorphic Liver Function and Disease: The Endocrine Connection. *Cell Mol Neurobiol.* 2019;39(2):169-180.
174. Garcia-Carrizo F, Priego T, Szostaczuk N, Palou A, Pico C. Sexual Dimorphism in the Age-Induced Insulin Resistance, Liver Steatosis, and Adipose Tissue Function in Rats. *Front Physiol.* 2017;8:445.

175. Posa A, Kupai K, Menesi R, et al. Sexual dimorphism of cardiovascular ischemia susceptibility is mediated by heme oxygenase. *Oxid Med Cell Longev.* 2013;2013:521563.

1. Hall JE, Guyton AC. *Guyton and Hall textbook of medical physiology.* 12th ed. Philadelphia, Pa.: Saunders/Elsevier; 2011.
2. The top 10 causes of death. 2020; https://www.who.int/news-room/fact-sheets/detail/the-top-10-causes-of-death. Accessed 3 October 2021, 2021.
3. Leading Causes of Death. https://www.cdc.gov/nchs/fastats/leading-causes-of-death.htm.
4. Chronic Kidney Disease. https://www.worldkidneyday.org/facts/chronic-kidney-disease/, 2021.
5. Stenvinkel P, Wanner C, Metzger T, et al. Inflammation and outcome in end-stage renal failure: does female gender constitute a survival advantage? *Kidney Int.* 2002;62(5):1791-1798.
6. Neugarten J, Golestaneh L. Female sex reduces the risk of hospital-associated acute kidney injury: a meta-analysis. *BMC Nephrol.* 2018;19(1):314.
7. Zhang J, Zhu J, Wei J, et al. New Mechanism for the Sex Differences in Salt-Sensitive Hypertension: The Role of Macula Densa NOS1beta-Mediated Tubuloglomerular Feedback. *Hypertension.* 2020;75(2):449-457.
8. Neugarten J, Acharya A, Silbiger SR. Effect of gender on the progression of nondiabetic renal disease: a meta-analysis. *J Am Soc Nephrol.* 2000;11(2):319-329.
9. Tejpal A, Gianos E, Cerise J, et al. Sex-Based Differences in COVID-19 Outcomes. *J Womens Health (Larchmt).* 2021;30(4):492-501.
10. Baylis C. Sexual dimorphism in the aging kidney: differences in the nitric oxide system. *Nat Rev Nephrol.* 2009;5(7):384-396.
11. Veiras LC, Girardi ACC, Curry J, et al. Sexual Dimorphic Pattern of Renal Transporters and Electrolyte Homeostasis. *J Am Soc Nephrol.* 2017;28(12):3504-3517.
12. Mirabito KM, Hilliard LM, Kett MM, et al. Sex- and age-related differences in the chronic pressure-natriuresis relationship: role of the angiotensin type 2 receptor. *Am J Physiol Renal Physiol.* 2014;307(8):F901-907.
13. Yu MK, Lyles CR, Bent-Shaw LA, Young BA, Pathways A. Risk factor, age and sex differences in chronic kidney disease prevalence in a diabetic cohort: the pathways study. *Am J Nephrol.* 2012;36(3):245-251.
14. Garovic VD, August P. Sex Differences and Renal Protection: Keeping in Touch with Your Feminine Side. *J Am Soc Nephrol.* 2016;27(10):2921-2924.
15. Lee CJ, Gardiner BS, Evans RG, Smith DW. Analysis of the critical determinants of renal medullary oxygenation. *Am J Physiol Renal Physiol.* 2019;317(6):F1483-F1502.
16. Zhang W, Edwards A. Oxygen transport across vasa recta in the renal medulla. *Am J Physiol Heart Circ Physiol.* 2002;283(3):H1042-1055.
17. Scholz H, Boivin FJ, Schmidt-Ott KM, et al. Kidney physiology and susceptibility to acute kidney injury: implications for renoprotection. *Nat Rev Nephrol.* 2021;17(5):335-349.
18. Pruijm M, Milani B, Pivin E, et al. Reduced cortical oxygenation predicts a progressive decline of renal function in patients with chronic kidney disease. *Kidney Int.* 2018;93(4):932-940.

19. Sugiyama K, Inoue T, Kozawa E, et al. Reduced oxygenation but not fibrosis defined by functional magnetic resonance imaging predicts the long-term progression of chronic kidney disease. *Nephrol Dial Transplant.* 2020;35(6):964-970.
20. Zhou H, Yang M, Jiang Z, Ding J, Di J, Cui L. Renal Hypoxia: An Important Prognostic Marker in Patients with Chronic Kidney Disease. *Am J Nephrol.* 2018;48(1):46-55.
21. Bleyer AJ, Chen R, D'Agostino RB, Jr., Appel RG. Clinical correlates of hypertensive end-stage renal disease. *Am J Kidney Dis.* 1998;31(1):28-34.
22. Palm F. Intrarenal oxygen in diabetes and a possible link to diabetic nephropathy. *Clin Exp Pharmacol Physiol.* 2006;33(10):997-1001.
23. Munger K, Baylis C. Sex differences in renal hemodynamics in rats. *Am J Physiol.* 1988;254(2 Pt 2):F223-231.
24. Tiede LM, Cook EA, Morsey B, Fox HS. Oxygen matters: tissue culture oxygen levels affect mitochondrial function and structure as well as responses to HIV viroproteins. *Cell Death Dis.* 2011;2:e246.
25. Serebrovskaya TV, Nosar VI, Bratus LV, Gavenauskas BL, Mankovska IM. Tissue oxygenation and mitochondrial respiration under different modes of intermittent hypoxia. *High Alt Med Biol.* 2013;14(3):280-288.
26. Daehn I, Casalena G, Zhang T, et al. Endothelial mitochondrial oxidative stress determines podocyte depletion in segmental glomerulosclerosis. *J Clin Invest.* 2014;124(4):1608-1621.
27. Corcoran JB, McCarthy S, Griffin B, et al. IHG-1 must be localised to mitochondria to decrease Smad7 expression and amplify TGF-beta1-induced fibrotic responses. *Biochim Biophys Acta.* 2013;1833(8):1969-1978.
28. Long J, Badal SS, Ye Z, et al. Long noncoding RNA Tug1 regulates mitochondrial bioenergetics in diabetic nephropathy. *J Clin Invest.* 2016;126(11):4205-4218.
29. Qi H, Casalena G, Shi S, et al. Glomerular Endothelial Mitochondrial Dysfunction Is Essential and Characteristic of Diabetic Kidney Disease Susceptibility. *Diabetes.* 2017;66(3):763-778.
30. Casalena G, Krick S, Daehn I, et al. Mpv17 in mitochondria protects podocytes against mitochondrial dysfunction and apoptosis in vivo and in vitro. *Am J Physiol Renal Physiol.* 2014;306(11):F1372-1380.
31. Wang Z, Sun Q, Sun N, Liang M, Tian Z. Mitochondrial Dysfunction and Altered Renal Metabolism in Dahl Salt-Sensitive Rats. *Kidney Blood Press Res.* 2017;42(3):587-597.
32. Domondon M, Polina I, Nikiforova AB, et al. Renal Glomerular Mitochondria Function in Salt-Sensitive Hypertension. *Front Physiol.* 2019;10:1588.
33. Dugan LL, You YH, Ali SS, et al. AMPK dysregulation promotes diabetes-related reduction of superoxide and mitochondrial function. *J Clin Invest.* 2013;123(11):4888-4899.
34. Galloway CA, Lee H, Nejjar S, et al. Transgenic control of mitochondrial fission induces mitochondrial uncoupling and relieves diabetic oxidative stress. *Diabetes.* 2012;61(8):2093-2104.
35. Zhan M, Usman IM, Sun L, Kanwar YS. Disruption of renal tubular mitochondrial quality control by Myo-inositol oxygenase in diabetic kidney disease. *J Am Soc Nephrol.* 2015;26(6):1304-1321.
36. Hartleben B, Godel M, Meyer-Schwesinger C, et al. Autophagy influences glomerular disease susceptibility and maintains podocyte homeostasis in aging mice. *J Clin Invest.* 2010;120(4):1084-1096.
37. D'Aco KE, Manno M, Clarke C, Ganesh J, Meyers KE, Sondheimer N. Mitochondrial tRNA(Phe) mutation as a cause of end-stage renal disease in childhood. *Pediatr Nephrol.* 2013;28(3):515-519.

38. de Arriba G, Calvino M, Benito S, Parra T. Cyclosporine A-induced apoptosis in renal tubular cells is related to oxidative damage and mitochondrial fission. *Toxicol Lett.* 2013;218(1):30-38.
39. Dinour D, Mini S, Polak-Charcon S, Lotan D, Holtzman EJ. Progressive nephropathy associated with mitochondrial tRNA gene mutation. *Clin Nephrol.* 2004;62(2):149-154.
40. Colom B, Oliver J, Roca P, Garcia-Palmer FJ. Caloric restriction and gender modulate cardiac muscle mitochondrial H2O2 production and oxidative damage. *Cardiovasc Res.* 2007;74(3):456-465.
41. Guevara R, Gianotti M, Oliver J, Roca P. Age and sex-related changes in rat brain mitochondrial oxidative status. *Exp Gerontol.* 2011;46(11):923-928.
42. Gaignard P, Savouroux S, Liere P, et al. Effect of Sex Differences on Brain Mitochondrial Function and Its Suppression by Ovariectomy and in Aged Mice. *Endocrinology.* 2015;156(8):2893-2904.
43. Borras C, Sastre J, Garcia-Sala D, Lloret A, Pallardo FV, Vina J. Mitochondria from females exhibit higher antioxidant gene expression and lower oxidative damage than males. *Free Radic Biol Med.* 2003;34(5):546-552.
44. Vina J, Borras C, Gambini J, Sastre J, Pallardo FV. Why females live longer than males? Importance of the upregulation of longevity-associated genes by oestrogenic compounds. *FEBS Lett.* 2005;579(12):2541-2545.
45. Justo R, Boada J, Frontera M, Oliver J, Bermudez J, Gianotti M. Gender dimorphism in rat liver mitochondrial oxidative metabolism and biogenesis. *Am J Physiol Cell Physiol.* 2005;289(2):C372-378.
46. Colom B, Alcolea MP, Valle A, Oliver J, Roca P, Garcia-Palmer FJ. Skeletal muscle of female rats exhibit higher mitochondrial mass and oxidative-phosphorylative capacities compared to males. *Cell Physiol Biochem.* 2007;19(1-4):205-212.
47. Gomez-Perez Y, Capllonch-Amer G, Gianotti M, Llado I, Proenza AM. Long-term high-fat-diet feeding induces skeletal muscle mitochondrial biogenesis in rats in a sex-dependent and muscle-type specific manner. *Nutr Metab (Lond).* 2012;9:15.
48. Capllonch-Amer G, Llado I, Proenza AM, Garcia-Palmer FJ, Gianotti M. Opposite effects of 17-beta estradiol and testosterone on mitochondrial biogenesis and adiponectin synthesis in white adipocytes. *J Mol Endocrinol.* 2014;52(2):203-214.
49. Rodriguez-Cuenca S, Pujol E, Justo R, et al. Sex-dependent thermogenesis, differences in mitochondrial morphology and function, and adrenergic response in brown adipose tissue. *J Biol Chem.* 2002;277(45):42958-42963.
50. Ventura-Clapier R, Moulin M, Piquereau J, et al. Mitochondria: a central target for sex differences in pathologies. *Clin Sci (Lond).* 2017;131(9):803-822.
51. Ahmad M, Wolberg A, Kahwaji CI. Biochemistry, Electron Transport Chain. *StatPearls*. Treasure Island (FL)2021.
52. Bhargava P, Schnellmann RG. Mitochondrial energetics in the kidney. *Nat Rev Nephrol.* 2017;13(10):629-646.
53. Cipolat S, Martins de Brito O, Dal Zilio B, Scorrano L. OPA1 requires mitofusin 1 to promote mitochondrial fusion. *Proc Natl Acad Sci U S A.* 2004;101(45):15927-15932.
54. Mears JA, Lackner LL, Fang S, Ingerman E, Nunnari J, Hinshaw JE. Conformational changes in Dnm1 support a contractile mechanism for mitochondrial fission. *Nat Struct Mol Biol.* 2011;18(1):20-26.
55. Mishra P, Carelli V, Manfredi G, Chan DC. Proteolytic cleavage of Opa1 stimulates mitochondrial inner membrane fusion and couples fusion to oxidative phosphorylation. *Cell Metab.* 2014;19(4):630-641.

56. Wirthensohn G, Guder WG. Renal substrate metabolism. *Physiol Rev.* 1986;66(2):469-497.
57. Gewin LS. Sugar or Fat? Renal Tubular Metabolism Reviewed in Health and Disease. *Nutrients.* 2021;13(5).
58. Brieger K, Schiavone S, Miller FJ, Jr., Krause KH. Reactive oxygen species: from health to disease. *Swiss Med Wkly.* 2012;142:w13659.
59. Tomsa AM, Alexa AL, Junie ML, Rachisan AL, Ciumarnean L. Oxidative stress as a potential target in acute kidney injury. *PeerJ.* 2019;7:e8046.
60. Granata S, Zaza G, Simone S, et al. Mitochondrial dysregulation and oxidative stress in patients with chronic kidney disease. *BMC Genomics.* 2009;10:388.
61. Aranda-Rivera AK, Cruz-Gregorio A, Aparicio-Trejo OE, Pedraza-Chaverri J. Mitochondrial Redox Signaling and Oxidative Stress in Kidney Diseases. *Biomolecules.* 2021;11(8).
62. Frank M, Duvezin-Caubet S, Koob S, et al. Mitophagy is triggered by mild oxidative stress in a mitochondrial fission dependent manner. *Biochim Biophys Acta.* 2012;1823(12):2297-2310.
63. Frezza C, Cipolat S, Scorrano L. Organelle isolation: functional mitochondria from mouse liver, muscle and cultured fibroblasts. *Nat Protoc.* 2007;2(2):287-295.
64. Calton MA, Beaulieu MO, Benchorin G, Vollrath D. Method for measuring extracellular flux from intact polarized epithelial monolayers. *Mol Vis.* 2018;24:425-433.
65. Yepez VA, Kremer LS, Iuso A, et al. OCR-Stats: Robust estimation and statistical testing of mitochondrial respiration activities using Seahorse XF Analyzer. *PLoS One.* 2018;13(7):e0199938.
66. Zhang J, Zhang Q. Using Seahorse Machine to Measure OCR and ECAR in Cancer Cells. *Methods Mol Biol.* 2019;1928:353-363.
67. Schindelin J, Arganda-Carreras I, Frise E, et al. Fiji: an open-source platform for biological-image analysis. *Nat Methods.* 2012;9(7):676-682.
68. Wang Z, Ying Z, Bosy-Westphal A, et al. Specific metabolic rates of major organs and tissues across adulthood: evaluation by mechanistic model of resting energy expenditure. *Am J Clin Nutr.* 2010;92(6):1369-1377.
69. Nourbakhsh N, Singh P. Role of renal oxygenation and mitochondrial function in the pathophysiology of acute kidney injury. *Nephron Clin Pract.* 2014;127(1-4):149-152.
70. Pagliarini DJ, Calvo SE, Chang B, et al. A mitochondrial protein compendium elucidates complex I disease biology. *Cell.* 2008;134(1):112-123.
71. Palmer LG, Schnermann J. Integrated control of Na transport along the nephron. *Clin J Am Soc Nephrol.* 2015;10(4):676-687.
72. Lee JJ, Tripi LM, Erbe RW, Garimella-Krovi S, Springate JE. A mitochondrial DNA deletion presenting with corneal clouding and severe Fanconi syndrome. *Pediatr Nephrol.* 2012;27(5):869-872.
73. Nishi Y, Satoh M, Nagasu H, et al. Selective estrogen receptor modulation attenuates proteinuria-induced renal tubular damage by modulating mitochondrial oxidative status. *Kidney Int.* 2013;83(4):662-673.
74. Lash LH, Qian W, Putt DA, et al. Renal toxicity of perchloroethylene and S-(1,2,2-trichlorovinyl)glutathione in rats and mice: sex- and species-dependent differences. *Toxicol Appl Pharmacol.* 2002;179(3):163-171.
75. Patil CN, Wallace K, LaMarca BD, et al. Low-dose testosterone protects against renal ischemia-reperfusion injury by increasing renal IL-10-to-TNF-alpha ratio and attenuating T-cell infiltration. *Am J Physiol Renal Physiol.* 2016;311(2):F395-403.

76. Peng Y, Fang Z, Liu M, et al. Testosterone induces renal tubular epithelial cell death through the HIF-1alpha/BNIP3 pathway. *J Transl Med.* 2019;17(1):62.
77. Pronsato L, Boland R, Milanesi L. Non-classical localization of androgen receptor in the C2C12 skeletal muscle cell line. *Arch Biochem Biophys.* 2013;530(1):13-22.
78. Solakidi S, Psarra AM, Nikolaropoulos S, Sekeris CE. Estrogen receptors alpha and beta (ERalpha and ERbeta) and androgen receptor (AR) in human sperm: localization of ERbeta and AR in mitochondria of the midpiece. *Hum Reprod.* 2005;20(12):3481-3487.
79. Karakas B, Aka Y, Giray A, et al. Mitochondrial estrogen receptors alter mitochondrial priming and response to endocrine therapy in breast cancer cells. *Cell Death Discov.* 2021;7(1):189.
80. Friedman JR, Nunnari J. Mitochondrial form and function. *Nature.* 2014;505(7483):335-343.
81. Brand MD, Nicholls DG. Assessing mitochondrial dysfunction in cells. *Biochem J.* 2011;435(2):297-312.
82. Rajeev Dalal ZSB, Jasjit S. Sehdev. Physiology, Renal Blood Flow and Filtration. FL: Treasure Island (FL) : StatPearls Publishing; 2021.
83. Ellam T, Fotheringham J, Kawar B. Differential scaling of glomerular filtration rate and ingested metabolic burden: implications for gender differences in chronic kidney disease outcomes. *Nephrol Dial Transplant.* 2014;29(6):1186-1194.
84. Huang C, Kim Y, Caramori ML, et al. Diabetic nephropathy is associated with gene expression levels of oxidative phosphorylation and related pathways. *Diabetes.* 2006;55(6):1826-1831.
85. Sas KM, Kayampilly P, Byun J, et al. Tissue-specific metabolic reprogramming drives nutrient flux in diabetic complications. *JCI Insight.* 2016;1(15):e86976.
86. Funk JA, Schnellmann RG. Persistent disruption of mitochondrial homeostasis after acute kidney injury. *Am J Physiol Renal Physiol.* 2012;302(7):F853-864.
87. Thome T, Kumar RA, Burke SK, et al. Impaired muscle mitochondrial energetics is associated with uremic metabolite accumulation in chronic kidney disease. *JCI Insight.* 2020;6(1).
88. Gry M, Rimini R, Stromberg S, et al. Correlations between RNA and protein expression profiles in 23 human cell lines. *BMC Genomics.* 2009;10:365.
89. Zager RA, Johnson AC, Hanson SY. Proximal tubular cytochrome c efflux: determinant, and potential marker, of mitochondrial injury. *Kidney Int.* 2004;65(6):2123-2134.
90. Sibarani J, Tjahjodjati T, Atik N, Rachmadi D, Mustafa A. Urinary Cytochrome C and Caspase-3 as Novel Biomarker of Renal Function Impairment in Unilateral Ureteropelvic Junction Obstruction Model of Wistar Rats. *Res Rep Urol.* 2020;12:217-224.
91. Boissan M, Montagnac G, Shen Q, et al. Membrane trafficking. Nucleoside diphosphate kinases fuel dynamin superfamily proteins with GTP for membrane remodeling. *Science.* 2014;344(6191):1510-1515.
92. Miyamoto S, Ochiai A, Boku N, et al. Discrepancies between the gene expression, protein expression, and enzymatic activity of thymidylate synthase and dihydropyrimidine dehydrogenase in human gastrointestinal cancers and adjacent normal mucosa. *Int J Oncol.* 2001;18(4):705-713.
93. Jennifer D Rocca EKH, Jay T Lennon, Sarah E Evans, Mark P Waldrop, James B Cotner, Diana R Nemergut, Emily B Graham & Matthew D Wallenstein Relationships between protein-encoding gene abundance and corresponding process are commonly assumed yet rarely observed. *The ISME Journal.* 2015;9:1693-1699.

94. Taguchi N, Ishihara N, Jofuku A, Oka T, Mihara K. Mitotic phosphorylation of dynamin-related GTPase Drp1 participates in mitochondrial fission. *J Biol Chem.* 2007;282(15):11521-11529.
95. Cho SG, Du Q, Huang S, Dong Z. Drp1 dephosphorylation in ATP depletion-induced mitochondrial injury and tubular cell apoptosis. *Am J Physiol Renal Physiol.* 2010;299(1):F199-206.
96. Wang W, Wang Y, Long J, et al. Mitochondrial fission triggered by hyperglycemia is mediated by ROCK1 activation in podocytes and endothelial cells. *Cell Metab.* 2012;15(2):186-200.
97. Tang WX, Wu WH, Zeng XX, Bo H, Huang SM. Early protective effect of mitofusion 2 overexpression in STZ-induced diabetic rat kidney. *Endocrine.* 2012;41(2):236-247.
98. Guo K, Lu J, Huang Y, et al. Protective role of PGC-1alpha in diabetic nephropathy is associated with the inhibition of ROS through mitochondrial dynamic remodeling. *PLoS One.* 2015;10(4):e0125176.
99. Chen H, Chomyn A, Chan DC. Disruption of fusion results in mitochondrial heterogeneity and dysfunction. *J Biol Chem.* 2005;280(28):26185-26192.
100. Qi W, Keenan HA, Li Q, et al. Pyruvate kinase M2 activation may protect against the progression of diabetic glomerular pathology and mitochondrial dysfunction. *Nat Med.* 2017;23(6):753-762.
101. Xiao X, Hu Y, Quiros PM, Wei Q, Lopez-Otin C, Dong Z. OMA1 mediates OPA1 proteolysis and mitochondrial fragmentation in experimental models of ischemic kidney injury. *Am J Physiol Renal Physiol.* 2014;306(11):F1318-1326.
102. Yoon YS, Yoon DS, Lim IK, et al. Formation of elongated giant mitochondria in DFO-induced cellular senescence: involvement of enhanced fusion process through modulation of Fis1. *J Cell Physiol.* 2006;209(2):468-480.
103. Huang P, Yu T, Yoon Y. Mitochondrial clustering induced by overexpression of the mitochondrial fusion protein Mfn2 causes mitochondrial dysfunction and cell death. *Eur J Cell Biol.* 2007;86(6):289-302.
104. Szabadkai G, Simoni AM, Chami M, Wieckowski MR, Youle RJ, Rizzuto R. Drp-1-dependent division of the mitochondrial network blocks intraorganellar Ca2+ waves and protects against Ca2+-mediated apoptosis. *Mol Cell.* 2004;16(1):59-68.
105. Waterham HR, Koster J, van Roermund CW, Mooyer PA, Wanders RJ, Leonard JV. A lethal defect of mitochondrial and peroxisomal fission. *N Engl J Med.* 2007;356(17):1736-1741.
106. Yoon YM, Go G, Yoon S, et al. Melatonin Treatment Improves Renal Fibrosis via miR-4516/SIAH3/PINK1 Axis. *Cells.* 2021;10(7).
107. Li R, Jia Z, Trush MA. Defining ROS in Biology and Medicine. *React Oxyg Species (Apex).* 2016;1(1):9-21.
108. Lambert AJ, Brand MD. Superoxide production by NADH:ubiquinone oxidoreductase (complex I) depends on the pH gradient across the mitochondrial inner membrane. *Biochem J.* 2004;382(Pt 2):511-517.
109. Wong HS, Dighe PA, Mezera V, Monternier PA, Brand MD. Production of superoxide and hydrogen peroxide from specific mitochondrial sites under different bioenergetic conditions. *J Biol Chem.* 2017;292(41):16804-16809.
110. Davies KJ, Quintanilha AT, Brooks GA, Packer L. Free radicals and tissue damage produced by exercise. *Biochem Biophys Res Commun.* 1982;107(4):1198-1205.
111. Irazabal MV, Torres VE. Reactive Oxygen Species and Redox Signaling in Chronic Kidney Disease. *Cells.* 2020;9(6).

112. Mitchell T, Saba H, Laakman J, Parajuli N, MacMillan-Crow LA. Role of mitochondrial-derived oxidants in renal tubular cell cold-storage injury. *Free Radic Biol Med.* 2010;49(8):1273-1282.
113. Wen Y, Liu YR, Tang TT, et al. mROS-TXNIP axis activates NLRP3 inflammasome to mediate renal injury during ischemic AKI. *Int J Biochem Cell Biol.* 2018;98:43-53.
114. Himmelfarb J, McMonagle E, Freedman S, et al. Oxidative stress is increased in critically ill patients with acute renal failure. *J Am Soc Nephrol.* 2004;15(9):2449-2456.
115. Tanaka S, Tanaka T, Kawakami T, et al. Vascular adhesion protein-1 enhances neutrophil infiltration by generation of hydrogen peroxide in renal ischemia/reperfusion injury. *Kidney Int.* 2017;92(1):154-164.
116. Bayorh MA, Ganafa AA, Socci RR, Silvestrov N, Abukhalaf IK. The role of oxidative stress in salt-induced hypertension. *Am J Hypertens.* 2004;17(1):31-36.
117. Banday AA, Muhammad AB, Fazili FR, Lokhandwala M. Mechanisms of oxidative stress-induced increase in salt sensitivity and development of hypertension in Sprague-Dawley rats. *Hypertension.* 2007;49(3):664-671.
118. Granatiero V, De Stefani D, Rizzuto R. Mitochondrial Calcium Handling in Physiology and Disease. *Adv Exp Med Biol.* 2017;982:25-47.
119. Santulli G, Marks AR. Essential Roles of Intracellular Calcium Release Channels in Muscle, Brain, Metabolism, and Aging. *Curr Mol Pharmacol.* 2015;8(2):206-222.
120. Peng TI, Jou MJ. Oxidative stress caused by mitochondrial calcium overload. *Ann N Y Acad Sci.* 2010;1201:183-188.
121. Korge P, Langer GA. Mitochondrial Ca2+ uptake, efflux, and sarcolemmal damage in Ca2+-overloaded cultured rat cardiomyocytes. *Am J Physiol.* 1998;274(6):H2085-2093.
122. Votyakova TV, Reynolds IJ. Ca2+-induced permeabilization promotes free radical release from rat brain mitochondria with partially inhibited complex I. *J Neurochem.* 2005;93(3):526-537.
123. Duan Y, Gross RA, Sheu SS. Ca2+-dependent generation of mitochondrial reactive oxygen species serves as a signal for poly(ADP-ribose) polymerase-1 activation during glutamate excitotoxicity. *J Physiol.* 2007;585(Pt 3):741-758.
124. Halestrap AP. What is the mitochondrial permeability transition pore? *J Mol Cell Cardiol.* 2009;46(6):821-831.
125. Niimi K, Yasui T, Hirose M, et al. Mitochondrial permeability transition pore opening induces the initial process of renal calcium crystallization. *Free Radic Biol Med.* 2012;52(7):1207-1217.
126. Crompton M, Ellinger H, Costi A. Inhibition by cyclosporin A of a Ca2+-dependent pore in heart mitochondria activated by inorganic phosphate and oxidative stress. *Biochem J.* 1988;255(1):357-360.
127. Halestrap AP, Davidson AM. Inhibition of Ca2(+)-induced large-amplitude swelling of liver and heart mitochondria by cyclosporin is probably caused by the inhibitor binding to mitochondrial-matrix peptidyl-prolyl cis-trans isomerase and preventing it interacting with the adenine nucleotide translocase. *Biochem J.* 1990;268(1):153-160.
128. Szabo I, De Pinto V, Zoratti M. The mitochondrial permeability transition pore may comprise VDAC molecules. II. The electrophysiological properties of VDAC are compatible with those of the mitochondrial megachannel. *FEBS Lett.* 1993;330(2):206-210.
129. Kokoszka JE, Waymire KG, Levy SE, et al. The ADP/ATP translocator is not essential for the mitochondrial permeability transition pore. *Nature.* 2004;427(6973):461-465.

130. Briston T, Roberts M, Lewis S, et al. Mitochondrial permeability transition pore: sensitivity to opening and mechanistic dependence on substrate availability. *Sci Rep.* 2017;7(1):10492.
131. Che R, Yuan Y, Huang S, Zhang A. Mitochondrial dysfunction in the pathophysiology of renal diseases. *Am J Physiol Renal Physiol.* 2014;306(4):F367-378.
132. Lagranha CJ, Deschamps A, Aponte A, Steenbergen C, Murphy E. Sex differences in the phosphorylation of mitochondrial proteins result in reduced production of reactive oxygen species and cardioprotection in females. *Circ Res.* 2010;106(11):1681-1691.
133. Manning RD, Jr., Meng S, Tian N. Renal and vascular oxidative stress and salt-sensitivity of arterial pressure. *Acta Physiol Scand.* 2003;179(3):243-250.
134. Mitchell T, De Miguel C, Gohar EY. Sex differences in redox homeostasis in renal disease. *Redox Biol.* 2020;31:101489.
135. Nordstrom A, Hadrevi J, Olsson T, Franks PW, Nordstrom P. Higher Prevalence of Type 2 Diabetes in Men Than in Women Is Associated With Differences in Visceral Fat Mass. *J Clin Endocrinol Metab.* 2016;101(10):3740-3746.
136. Ricardo AC, Yang W, Sha D, et al. Sex-Related Disparities in CKD Progression. *J Am Soc Nephrol.* 2019;30(1):137-146.
137. Li C, Deng X, Xie X, Liu Y, Friedmann Angeli JP, Lai L. Activation of Glutathione Peroxidase 4 as a Novel Anti-inflammatory Strategy. *Front Pharmacol.* 2018;9:1120.
138. Bell EL, Klimova TA, Eisenbart J, et al. The Qo site of the mitochondrial complex III is required for the transduction of hypoxic signaling via reactive oxygen species production. *J Cell Biol.* 2007;177(6):1029-1036.
139. Chandel NS, McClintock DS, Feliciano CE, et al. Reactive oxygen species generated at mitochondrial complex III stabilize hypoxia-inducible factor-1alpha during hypoxia: a mechanism of O2 sensing. *J Biol Chem.* 2000;275(33):25130-25138.
140. Connor KM, Subbaram S, Regan KJ, et al. Mitochondrial H2O2 regulates the angiogenic phenotype via PTEN oxidation. *J Biol Chem.* 2005;280(17):16916-16924.
141. Meng TC, Fukada T, Tonks NK. Reversible oxidation and inactivation of protein tyrosine phosphatases in vivo. *Mol Cell.* 2002;9(2):387-399.
142. DeNicola GM, Karreth FA, Humpton TJ, et al. Oncogene-induced Nrf2 transcription promotes ROS detoxification and tumorigenesis. *Nature.* 2011;475(7354):106-109.
143. Acehan D, Jiang X, Morgan DG, Heuser JE, Wang X, Akey CW. Three-dimensional structure of the apoptosome: implications for assembly, procaspase-9 binding, and activation. *Mol Cell.* 2002;9(2):423-432.
144. Zermati Y, Garrido C, Amsellem S, et al. Caspase activation is required for terminal erythroid differentiation. *J Exp Med.* 2001;193(2):247-254.
145. Arama E, Agapite J, Steller H. Caspase activity and a specific cytochrome C are required for sperm differentiation in Drosophila. *Dev Cell.* 2003;4(5):687-697.
146. Sordet O, Rebe C, Plenchette S, et al. Specific involvement of caspases in the differentiation of monocytes into macrophages. *Blood.* 2002;100(13):4446-4453.
147. De Botton S, Sabri S, Daugas E, et al. Platelet formation is the consequence of caspase activation within megakaryocytes. *Blood.* 2002;100(4):1310-1317.
148. Woo M, Hakem R, Furlonger C, et al. Caspase-3 regulates cell cycle in B cells: a consequence of substrate specificity. *Nat Immunol.* 2003;4(10):1016-1022.
149. Jang HS, Noh MR, Kim J, Padanilam BJ. Defective Mitochondrial Fatty Acid Oxidation and Lipotoxicity in Kidney Diseases. *Front Med (Lausanne).* 2020;7:65.
150. Gadkari TV, Cortes N, Madrasi K, Tsoukias NM, Joshi MS. Agmatine induced NO dependent rat mesenteric artery relaxation and its impairment in salt-sensitive hypertension. *Nitric Oxide.* 2013;35:65-71.

151. Szabo AJ, Wagner L, Erdely A, Lau K, Baylis C. Renal neuronal nitric oxide synthase protein expression as a marker of renal injury. *Kidney Int.* 2003;64(5):1765-1771.
152. Seddon MD, Chowienczyk PJ, Brett SE, Casadei B, Shah AM. Neuronal nitric oxide synthase regulates basal microvascular tone in humans in vivo. *Circulation.* 2008;117(15):1991-1996.
153. Yoneyama H, Yamamoto A, Kosaka H. Neuronal nitric oxide synthase generates superoxide from the oxygenase domain. *Biochem J.* 2001;360(Pt 1):247-253.
154. Salabei JK, Gibb AA, Hill BG. Comprehensive measurement of respiratory activity in permeabilized cells using extracellular flux analysis. *Nat Protoc.* 2014;9(2):421-438.
155. Martinez-Reyes I, Chandel NS. Mitochondrial TCA cycle metabolites control physiology and disease. *Nat Commun.* 2020;11(1):102.
156. Martinez-Reyes I, Diebold LP, Kong H, et al. TCA Cycle and Mitochondrial Membrane Potential Are Necessary for Diverse Biological Functions. *Mol Cell.* 2016;61(2):199-209.
157. Patten DA, Lafleur VN, Robitaille GA, Chan DA, Giaccia AJ, Richard DE. Hypoxia-inducible factor-1 activation in nonhypoxic conditions: the essential role of mitochondrial-derived reactive oxygen species. *Mol Biol Cell.* 2010;21(18):3247-3257.
158. Selak MA, Armour SM, MacKenzie ED, et al. Succinate links TCA cycle dysfunction to oncogenesis by inhibiting HIF-alpha prolyl hydroxylase. *Cancer Cell.* 2005;7(1):77-85.
159. Arts RJ, Novakovic B, Ter Horst R, et al. Glutaminolysis and Fumarate Accumulation Integrate Immunometabolic and Epigenetic Programs in Trained Immunity. *Cell Metab.* 2016;24(6):807-819.
160. Yang H, van der Stel W, Lee R, et al. Dynamic Modeling of Mitochondrial Membrane Potential Upon Exposure to Mitochondrial Inhibitors. *Front Pharmacol.* 2021;12:679407.
161. Ribeiro RF, Jr., Ronconi KS, Morra EA, et al. Sex differences in the regulation of spatially distinct cardiac mitochondrial subpopulations. *Mol Cell Biochem.* 2016;419(1-2):41-51.
162. Yao CH, Wang R, Wang Y, Kung CP, Weber JD, Patti GJ. Mitochondrial fusion supports increased oxidative phosphorylation during cell proliferation. *Elife.* 2019;8.
163. Wenzel P, Mollnau H, Oelze M, et al. First evidence for a crosstalk between mitochondrial and NADPH oxidase-derived reactive oxygen species in nitroglycerin-triggered vascular dysfunction. *Antioxid Redox Signal.* 2008;10(8):1435-1447.
164. Kitada M, Xu J, Ogura Y, Monno I, Koya D. Manganese Superoxide Dismutase Dysfunction and the Pathogenesis of Kidney Disease. *Front Physiol.* 2020;11:755.
165. Fukui M, Zhu BT. Mitochondrial superoxide dismutase SOD2, but not cytosolic SOD1, plays a critical role in protection against glutamate-induced oxidative stress and cell death in HT22 neuronal cells. *Free Radic Biol Med.* 2010;48(6):821-830.
166. Kim S, Kang SW, Joo J, et al. Correction: Characterization of ferroptosis in kidney tubular cell death under diabetic conditions. *Cell Death Dis.* 2021;12(4):382.
167. Wortmann M, Schneider M, Pircher J, et al. Combined deficiency in glutathione peroxidase 4 and vitamin E causes multiorgan thrombus formation and early death in mice. *Circ Res.* 2013;113(4):408-417.
168. Zhang J, Bi J, Ren Y, et al. Involvement of GPX4 in irisin's protection against ischemia reperfusion-induced acute kidney injury. *J Cell Physiol.* 2021;236(2):931-945.
169. C. ZLXXHQaD. Targeting Ferroptosis Attenuates Interstitial Inflammation and Kidney Fibrosis. *Karger.*
170. Gal-Oz ST, Maier B, Yoshida H, et al. ImmGen report: sexual dimorphism in the immune system transcriptome. *Nat Commun.* 2019;10(1):4295.
171. Fisher DW, Bennett DA, Dong H. Sexual dimorphism in predisposition to Alzheimer's disease. *Neurobiol Aging.* 2018;70:308-324.

172. Leinwand LA. Sex is a potent modifier of the cardiovascular system. *J Clin Invest.* 2003;112(3):302-307.
173. Brie B, Ramirez MC, De Winne C, et al. Brain Control of Sexually Dimorphic Liver Function and Disease: The Endocrine Connection. *Cell Mol Neurobiol.* 2019;39(2):169-180.
174. Garcia-Carrizo F, Priego T, Szostaczuk N, Palou A, Pico C. Sexual Dimorphism in the Age-Induced Insulin Resistance, Liver Steatosis, and Adipose Tissue Function in Rats. *Front Physiol.* 2017;8:445.
175. Posa A, Kupai K, Menesi R, et al. Sexual dimorphism of cardiovascular ischemia susceptibility is mediated by heme oxygenase. *Oxid Med Cell Longev.* 2013;2013:521563.
176. Gessner A, Mieth M, Auge D, et al. Establishment of reference values for the lysine acetylation marker N(varepsilon)-acetyllysine in small volume human plasma samples by a multi-target LC-MS/MS method. *Amino Acids.* 2019;51(9):1259-1271.
177. Izquierdo-Garcia JL, Nin N, Cardinal-Fernandez P, et al. Identification of novel metabolomic biomarkers in an experimental model of septic acute kidney injury. *Am J Physiol Renal Physiol.* 2019;316(1):F54-F62.
178. Rebholz CM, Surapaneni A, Levey AS, et al. The Serum Metabolome Identifies Biomarkers of Dietary Acid Load in 2 Studies of Adults with Chronic Kidney Disease. *J Nutr.* 2019;149(4):578-585.
179. Petrosillo G, Ruggiero FM, Pistolese M, Paradies G. Ca2+-induced reactive oxygen species production promotes cytochrome c release from rat liver mitochondria via mitochondrial permeability transition (MPT)-dependent and MPT-independent mechanisms: role of cardiolipin. *J Biol Chem.* 2004;279(51):53103-53108.
180. Chance B, Hollunger G. The interaction of energy and electron transfer reactions in mitochondria. I. General properties and nature of the products of succinate-linked reduction of pyridine nucleotide. *J Biol Chem.* 1961;236:1534-1543.
181. Hinkle PC, Butow RA, Racker E, Chance B. Partial resolution of the enzymes catalyzing oxidative phosphorylation. XV. Reverse electron transfer in the flavin-cytochrome beta region of the respiratory chain of beef heart submitochondrial particles. *J Biol Chem.* 1967;242(22):5169-5173.
182. Zorov DB, Juhaszova M, Sollott SJ. Mitochondrial reactive oxygen species (ROS) and ROS-induced ROS release. *Physiol Rev.* 2014;94(3):909-950.
183. Hoffman DL, Salter JD, Brookes PS. Response of mitochondrial reactive oxygen species generation to steady-state oxygen tension: implications for hypoxic cell signaling. *Am J Physiol Heart Circ Physiol.* 2007;292(1):H101-108.
184. Bonnet S, Michelakis ED, Porter CJ, et al. An abnormal mitochondrial-hypoxia inducible factor-1alpha-Kv channel pathway disrupts oxygen sensing and triggers pulmonary arterial hypertension in fawn hooded rats: similarities to human pulmonary arterial hypertension. *Circulation.* 2006;113(22):2630-2641.
185. Sanjuan-Pla A, Cervera AM, Apostolova N, et al. A targeted antioxidant reveals the importance of mitochondrial reactive oxygen species in the hypoxic signaling of HIF-1alpha. *FEBS Lett.* 2005;579(12):2669-2674.
186. Weissmann N, Ebert N, Ahrens M, et al. Effects of mitochondrial inhibitors and uncouplers on hypoxic vasoconstriction in rabbit lungs. *Am J Respir Cell Mol Biol.* 2003;29(6):721-732.
187. Scialo F, Sriram A, Fernandez-Ayala D, et al. Mitochondrial ROS Produced via Reverse Electron Transport Extend Animal Lifespan. *Cell Metab.* 2016;23(4):725-734.
188. Noh MR, Kim KY, Han SJ, Kim JI, Kim HY, Park KM. Methionine Sulfoxide Reductase A Deficiency Exacerbates Cisplatin-Induced Nephrotoxicity via Increased Mitochondrial Damage and Renal Cell Death. *Antioxid Redox Signal.* 2017;27(11):727-741.

189. Arieli Y, Gursahani H, Eaton MM, Hernandez LA, Schaefer S. Gender modulation of Ca(2+) uptake in cardiac mitochondria. *J Mol Cell Cardiol.* 2004;37(2):507-513.
190. HJH F. The oxidation of tartaric acid in presence of iron. *J Chem Soc Proc.* 1893;9:113.
191. Michael M Gaschler BRS. Lipid peroxidation in cell death. *Biochem Biophys Res Commun.* 2017;3(482):419-425.
192. Schreiber R, Buchholz B, Kraus A, et al. Lipid Peroxidation Drives Renal Cyst Growth In Vitro through Activation of TMEM16A. *J Am Soc Nephrol.* 2019;30(2):228-242.
193. Ongajooth L, Ongajyooth S, Likidlilid A, Chantachum Y, Shayakul C, Nilwarangkur S. Role of lipid peroxidation, trace elements and anti-oxidant enzymes in chronic renal disease patients. *J Med Assoc Thai.* 1996;79(12):791-800.
194. Liao TL, Tzeng CR, Yu CL, Wang YP, Kao SH. Estrogen receptor-beta in mitochondria: implications for mitochondrial bioenergetics and tumorigenesis. *Ann N Y Acad Sci.* 2015;1350:52-60.